

Assessment of Passive Safety Injection Systems of ALWRs

Final report of the European Commission 4th Framework Programme Project FI4I-CT95-0004 (APSI)

Jari Tuunanen

VTT Energy, Finland

Juhani Vihavainen

Lappeenranta University of Technology (LTKK), Finland

Francesco D'Auria

University of Pisa, Italy

George Kimber

AEA Technology, UK



ISBN 951-38-5436-1 (soft back ed.)

ISSN 1235-0605 (soft back ed.)

ISBN 951-38-5437-X (URL: <http://www.inf.vtt.fi/pdf/>)

ISSN 1455-0865 (URL: <http://www.inf.vtt.fi/pdf/>)

ISBN 951-38-5445-0 (CD-ROM)

Copyright © Valtion teknillinen tutkimuskeskus (VTT) 1999

JULKAISIJA – UTGIVARE – PUBLISHER

Valtion teknillinen tutkimuskeskus (VTT), Vuorimiehentie 5, PL 2000, 02044 VTT
puh. vaihde (09) 4561, faksi (09) 456 4374

Statens tekniska forskningscentral (VTT), Bergsmansvägen 5, PB 2000, 02044 VTT
tel. växel (09) 4561, fax (09) 456 4374

Technical Research Centre of Finland (VTT), Vuorimiehentie 5, P.O.Box 2000, FIN-02044 VTT,
Finland
phone internat. + 358 9 4561, fax + 358 9 456 4374

VTT Energia, Ydinenergia, Tekniikantie 4 C, PL 1604, 02044 VTT
puh. vaihde (09) 4561, faksi (09) 456 5000

VTT Energi, Kärnkraft, Teknikvägen 4 C, PB 1604, 02044 VTT
tel. växel (09) 4561, fax (09) 456 5000

VTT Energy, Nuclear Energy, Tekniikantie 4 C, P.O.Box 1604, FIN-02044 VTT, Finland
phone internat. + 358 9 4561, fax + 358 9 456 5000

CONTRIBUTORS:

M. Puustinen, H. Purhonen, J. Kouhia and V. Riikonen
VTT Energy, Lappeenranta, Finland

S. Semken, H. Partanen, H. Pylkkö and I. Saure
Lappeenranta University of Technology, Lappeenranta, Finland

M. Frogheri and G. M. Galassi
University of Pisa, Pisa, Italy

J. N. Lillington, E. J. Allen and T. G. Williams
AEA Technology, UK

Technical editing Kerttu Tirronen

Libella Painopalvelu Oy, Espoo 1999

Tuunanen, Jari, Vihavainen, Juhani, D'Auria, Francesco & Kimber, George. Assessment of Passive Safety Injection Systems of ALWRs. Final report of the European Commission 4th Framework Programme Project FI4I-CT95-0004 (APSI). Espoo 1999, Technical Research Centre of Finland, VTT Tiedotteita – Meddelanden – Research Notes 1957. 77 p. + app. 2 p.

Keywords nuclear power plants, nuclear reactors, simulation, injection, safety

ABSTRACT

The European Commission 4th Framework Programme project “*Assessment of Passive Safety Injection Systems of Advanced Light Water Reactors Reactors (FI4I-CT95-0004)*” involved experiments on the PACTEL test facility and computer simulations of selected experiments. The experiments focused on the performance of Passive Safety Injection Systems (PSIS) of Advanced Light Water Reactors (ALWRs) in Small Break Loss-Of-Coolant Accident (SBLOCA) conditions. The PSIS consisted of a Core Make-up Tank (CMT) and two pipelines. A pressure balancing line (PBL) connected the CMT to one cold leg. The injection line (IL) connected it to the downcomer. The project involved 15 experiments in three series. The experiments provided valuable information about condensation and heat transfer processes in the CMT, thermal stratification of water in the CMT, and natural circulation flow through the PSIS lines. The experiments showed the examined PSIS works efficiently in SBLOCAs although the flow through the PSIS may stop in very small SBLOCAs, when the hot water fills the CMT. The experiments also demonstrated the importance of flow distributor (sparger) in the CMT to limit rapid condensation.

The project included validation of three thermal-hydraulic computer codes (APROS, CATHARE and RELAP5). The analyses showed the codes are capable of simulating the overall behaviour of the transients. The codes predicted accurately the core heatup, which occurred when the primary coolant inventory was reduced so much that the core top became free of water. The detailed analyses of the calculation results showed that some models in the codes still need improvements. Especially, further development of models for thermal stratification, condensation and natural circulation flow with small driving forces would be necessary for accurate simulation of phenomena in the PSIS.

ABBREVIATIONS

ALWR	Advanced Light Water Reactor
APROS	Computer code, <u>A</u> dvanced <u>P</u> rocess <u>S</u> imulator
APWR	Advanced Pressurized Water Reactor
CATHARE	Computer code, <u>C</u> ode <u>A</u> vançè de <u>T</u> hermo- <u>H</u> draulic pour les <u>A</u> ccidents des <u>R</u> ecteurs a' <u>E</u> au
CHF	Critical Heat Flux
CMT	Core Makeup Tank
ECCS	Emergency Core Cooling System
GRINAP	Graphical User Interface of APROS
IL	Injection Line
LOCA	Loss off Coolant Accident
LTKK	Lappeenranta University of Technology
NFS	Nuclear Fission Safety
PACTEL	Parallel Channel Test Loop
PBL	Pressure Balancing Line
PSIS	Passive Safety Injection System
RELAP	Computer code, <u>R</u> ector <u>L</u> eak and <u>A</u> nalyses <u>P</u> rogramme
SBLOCA	Small Break Loss off Coolant Accident
VTT	Technical Research Centre of Finland
WP	Work Package

TABLE OF CONTENTS

ABSTRACT	3
ABBREVIATIONS	4
TABLE OF CONTENTS	5
1. INTRODUCTION	7
2. REVIEW OF ALWR THERMAL-HYDRAULIC PHENOMENA OF INTEREST AND EVALUATION OF CURRENT SYSTEM CODE CAPABILITIES IN THEIR MODELLING	9
3. PACTEL EXPERIMENTS	10
3.1 EXPERIMENT PARAMETERS AND PROCEDURE.....	10
3.1.1 PSIS configurations.....	12
3.2 RESULTS	15
3.2.1 PSIS operation modes	15
3.2.2 Parametric studies	17
Break size	17
Break location	19
CMT size and position	19
Flow distributor (sparger)	20
Initial temperature in the PSIS	21
PBL connection position	21
IL flow resistance	22
3.2.3 Heat transfer to the CMT wall.....	22
3.2.4 Thermal stratification in the CMT	25
3.2.5 Reproducibility of the phenomena.....	27
3.3 STEAM GENERATOR PERFORMANCE	27
3.4 LIMITATIONS OF THE MEASUREMENT INSTRUMENTATION.....	28
3.5 UNCERTAINTIES IN BOUNDARY CONDITIONS	30
3.6 CONCLUSIONS FROM THE EXPERIMENTS	30
4. COMPUTER CODE SIMULATIONS	32
4.1 CODE DESCRIPTION.....	32
4.1.1 APROS.....	32
4.1.2 CATHARE.....	33
4.1.3 RELAP	35
4.2 NODALIZATION.....	36
4.2.1 APROS	36
Secondary side pressure control in APROS code	37
Pressure losses.....	37
Calculation of the steady state condition	38
4.2.2 CATHARE.....	39
Nodalization qualification.....	40

4.2.3 RELAP5	44
4.3 COMPARISON OF DIFFERENT CODE PREDICTIONS AGAINST EXPERIMENTS	46
4.3.1 GDE-24	46
Experiment description	46
Code calculation results	47
4.3.2 GDE-34	53
Experiment description	53
Code calculation results	53
4.3.3 GDE-43	59
Experiment description	59
Code calculation results	60
4.4 CONCLUSIONS FROM THE CALCULATIONS	66
4.4.1 APROS	66
Conclusions	66
4.4.2 CATHARE	66
4.4.3 RELAP5	67
GDE-24 experiment	67
GDE-34 experiment	68
GDE-43 experiment	69
Overall conclusions	70
5. CONCLUSIONS.....	71
6. RECOMMENDATIONS	72
REFERENCES	74

1. INTRODUCTION

An important aspect of ALWR decay heat removal concerns the plant response under Loss of Coolant Accident (LOCA) conditions. In many ALWRs, e.g. Westinghouse AP600, gravity driven passive safety injection systems replace active pump driven Emergency Core Cooling Systems (ECCS). It is therefore important, that in such accidents, the ALWR coolant system pressure can be controlled to allow gravity fed injection to take place. The safety issue here is whether undesirable system responses could occur in any circumstances. Additionally, it is necessary to prove that the plant always depressurizes sufficiently for the ECCS to operate efficiently.

The European Commission Nuclear Fission Safety (NFS2) program project "*Assessment Of Passive Safety Injection Systems Of Advanced Light Water Reactors (FI4I-CT95-0004)*" involved experiments with the PACTEL test facility [1] on the performance of a passive CMT in SBLOCAs. Of particular interest were the phenomena occurring in the CMT, such as condensation and temperature stratification of water. The project also included validation of thermal-hydraulic computer codes, such as APROS [2], CATHARE [3] and RELAP5 [4]. The use of PACTEL had an advantage of being independent of reactor manufacturers and designers. Hence, these tests contributed to an independent public data base on the performance of PSISs. Most of the experiment data in the world is proprietary, due to the commercial interests of reactor manufacturers and designers. The shared-cost type project started in January 1st, 1996 and ended September 30th, 1998.

The main objectives of the project were

- to provide new and independent information about PSIS performance,
- to contribute to a public data base for users and developers of thermal-hydraulic computer codes on the phenomenological behaviour of PSISs in SBLOCAs, and
- to identify the accuracy, uncertainties and limitations of thermal-hydraulic computer codes in the modelling of PSIS behaviour.

The CMT used in the experiments followed the proposed design of the Westinghouse AP600 Advanced Pressurized Water Reactor (APWR) concept. The PACTEL facility, however, differs substantially from the AP600 reactor since it has been designed for simulation of VVER440 type PWRs. The CMT used in the experiments was one of the two normal accumulators of PACTEL. The experiment team modified the accumulators to better simulate the CMT tanks. Some modifications to the original loop geometry and the installation of additional instrumentation were also necessary. The geometry of the tank and the tank internals still differed from the geometry of the CMT tanks of the AP600 reactor. For these reasons, the purpose of the experiments was to provide information about the phenomena in the PSIS, not to simulate accurately the AP600 reactor.

The project partners used the experiment data for the validation of thermal-hydraulic system codes. The main interest in the analyses was in the simulation of the PSIS behaviour. Of special interest were the condensation and thermal stratification processes in the CMT, and the PSIS behaviour in situations where the driving head for flow through the system was small. It is very important to test the current safety codes capabilities to simulate PSISs and to identify the possible areas where the codes need further development.

The project involved the following *four work packages (WP)*:

- WP1. Review of ALWR thermal-hydraulic phenomena of interest and the evaluation of current system code capabilities in their modelling,
- WP2. PACTEL experiments with gravity driven core cooling, analysis of the experiment data, and preparation of qualified experiment reports,
- WP3. computer code validation, including feedback from code users to experimenters, and
- WP4. preparation of the final report of the project.

VTT Energy (VTT) and the Lappeenranta University of Technology (LTKK) from Finland were responsible for the PACTEL experiments (WP 2). VTT, the University of Pisa from Italy, and the AEA Technology from the UK were responsible for the WP 1, WP 3 and WP 4. VTT Energy co-ordinated the project.

The first part of the report (Chapter 2) presents an overview to the Work Package 1. Chapter 3 presents a summary of the main experiment results. Chapter 4 summarises the computer calculation results and presents a comparison of different code calculations. The last part of the report presents the conclusions (Chapter 5), recommendations (Chapter 6) and lists references and publications prepared in the project (Appendix 1).

2. REVIEW OF ALWR THERMAL-HYDRAULIC PHENOMENA OF INTEREST AND EVALUATION OF CURRENT SYSTEM CODE CAPABILITIES IN THEIR MODELLING

The first work package of the project included a review of ALWR thermal-hydraulic phenomena of interest and evaluation of current system code capabilities in their modelling. The project team decided to expand the task to gather information about the available experimental data on the passive safety injection systems of advanced PWRs. The project team went through the available public data and wrote a status report [6].

The phenomenological description of the AP600 reactor CMT behaviour in SBLOCAs in the status report, which was based on the SPES [7] and ROSA [8] experimental data, well covered the phenomena observed in this experiment programme. So, the report formed a good basis for the current experiments.

During the project, more results of APWR's have been published in international conferences and papers. The project team also received more information about the AP600 experiments (SPES and APEX [9] -experiments) through the visits to the test sites. The results of the visits have been reported [10] and [11]. The project team has prepared an addendum [12] to the WP1 report, based on the available new data.

The reference concept of the current experiments was the AP600 CMT system. Other APWR designs, such as Korean CP-1000 and Russian VVER-640, include passive safety system which are partly similar to the AP 600 CMT design, and where similar phenomena would occur. The data prepared in the current program is partially applicable also for the other APWRs. These other concepts have been described in WP1 report.

3. PACTEL EXPERIMENTS

3.1 EXPERIMENT PARAMETERS AND PROCEDURE

The PACTEL experimental programme included three series with altogether fifteen experiments. See Table 1. In the experiments, all three loops of the PACTEL rig were in operation. See Figure 1 for a view of PACTEL with the PSIS. The first series focused on break size effects on the PSIS behaviour. The second series concentrated on studying the influence of break location on the PSIS performance. The third series studied the influences of the CMT position on the PSIS behaviour. For the third series experiments, the PACTEL operators moved the CMT to 1 metre higher elevation than in the second experiment series to increase the driving head for PSIS flow. The main interest in all experiments was in the PSIS behaviour. The main phenomena of interest were the PSIS flow rate, heat transfer to the CMT walls and thermal stratification and condensation in the CMT. See the experimental data reports for detailed experiment parameters, procedures and PSIS instrumentation and configuration [13], [14], [15], [16], [17] and [18]. All experiments studied SBLOCA transients. The CMT was the only safety injection system in use. The experiments did not include accident management procedures, such as depressurization of the primary or secondary circuits, which are an important part of the AP600 accident management procedures.

Table 1. Main parameters in PACTEL experiments.

EXPERIMENT	BREAK DIAMETER (mm)	BREAK LOCATION	CORE POWER (kW)	OBJECTIVES
<i>First series</i>				
GDE-21	1	cold leg close to DC	160	break size effects
GDE-22	2,5	cold leg close to DC	160	break size effects
GDE-23	5	cold leg close to DC	160	break size effects
GDE-24	3,5	cold leg close to DC	160	break size effects
GDE-25	3,5	cold leg close to DC	160	reproducibility of the phenomena
<i>Second series</i>				
GDE-31	3,5	cold leg close to DC	160	small CMT
GDE-32	3,5	hot leg loop seal	160	break location, flow reversal in cold leg
GDE-33	3,5	cold leg between steam generator and pressure balancing line	160	break location, flow reversal in cold leg
GDE-34	3,5	cold leg close to DC	160	hot CMT; no recirculation flow
GDE-35	3,5	cold leg close to DC	160	no sparger; condensation in the CMT
<i>Third series</i>				
GDE-41	3,5	cold leg close to DC	160	CMT position; increased driving force for CMT flow
GDE-42	3,5	cold leg close to DC	160	additional IL flow orifice
GDE-43	1	cold leg close to DC	160	long recirculation phase; disappearance of driving force for injection
GDE-44	3,5	cold leg close to DC	160	cold CMT; PBL heating
GDE-45	3,5	cold leg close to DC	160	PBL connected to PRZ

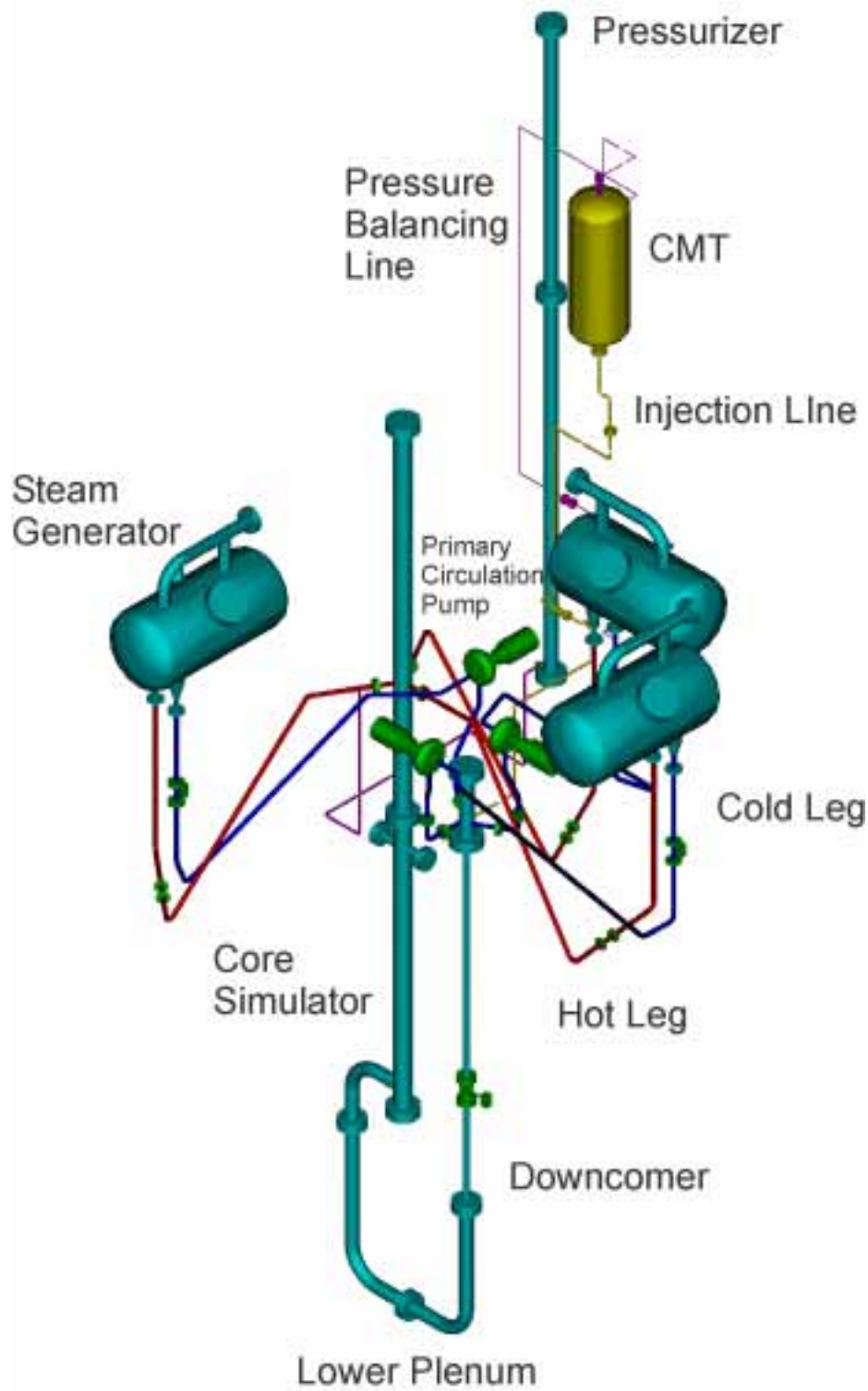


Figure 1. PACTEL-rig with a Core Make-up Tank.

The experimental procedure was similar in all experiments. To prepare for the experiments, the PACTEL operators filled the primary and secondary systems

with water, and heated the loop to the desired initial conditions. In all experiments except GDE-34, GDE-44 and GDE-45, the PACTEL operators filled the PBL with hot water, and the CMT and the IL with cold water. In GDE-34, the PSIS was initially full of hot water. In the GDE-44 experiment, the CMT and the lines were initially full of cold water. In the GDE-45 experiment, the PBL was initially full of steam since the PBL connected the CMT to the top of pressurizer.

After reaching the desired initial conditions, the PACTEL operators maintained them for one hour before beginning the experiment. The initial conditions included a steady-state single-phase forced circulation in the primary loops. The initial primary and secondary pressures were about 4.3 and 2.0 MPa. The pressurizer heaters controlled the primary pressure and the secondary side controller maintained the secondary pressure. The core power set point was about 3,6% (160 kW) of the scale nominal power of the reference plant. The operators used the feed water pumps manually to keep the secondary side liquid inventory constant. The level set point was 72 cm, which is 4 cm above the horizontal heat-exchange tube bundle in the steam generators. In the PSIS, all the valves in the PBL were open all the time. The IL check valve was closed during the heat-up and steady state phases of the experiments.

The first 1000 seconds of the experiments included steady-state measurements. Before opening the break, the operators opened the PBL drain valve to fill the line with hot water. The transient began at 1000 seconds when the operators opened the valve downstream the break orifice. Simultaneously they stopped the primary circulation pumps. The operators opened the isolation valve in the IL and switched off the pressurizer heaters when the pressurizer level dropped below 3,5 metres. The operators finished the experiments when the primary loop liquid inventory reached the point where the surface temperatures of the fuel rod simulators at the core exit region exceeded 300 °C, or when the experiment had lasted 15 000 seconds.

3.1.1 PSIS configurations

The PSIS configuration varied in different experiment series. Figure 2 presents PSIS configuration in the second and third experiment series. The first series used a similar PSIS configuration to the second series but with a larger CMT. The CMTs used in the experiments were equipped with a flow distributor (sparger). The purpose of the sparger was to reduce condensation in the tank. See Figure 3 for details of the sparger geometry.

The CMT instrumentation included thermocouples in different elevations for water and wall temperature measurements. Differential pressure transducers measured the levels in the CMT. See Figure 4. Flow meters in the PBL and IL measured the single-phase liquid flow in the PSIS pipelines. The PBL flowmeter measured accurately small flow rates, such as typical for PSIS recirculation phase. The IL flow meter measured accurately the flow during CMT injection phase, but was inaccurate during the recirculation phase.

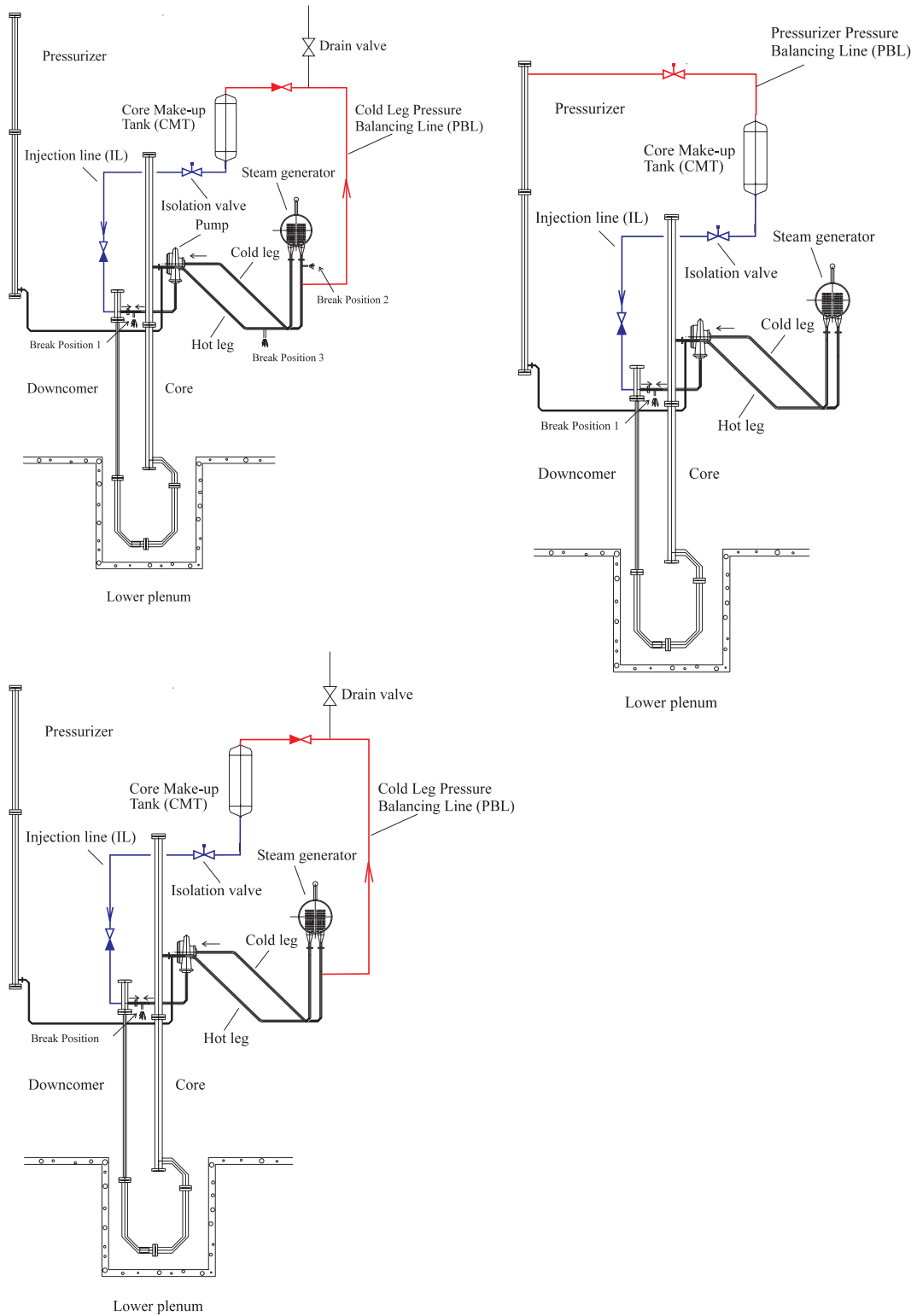


Figure 2. Different PSIS configurations (first series (top left), second series (bottom left) and third series experiment GDE-45 (top right)).

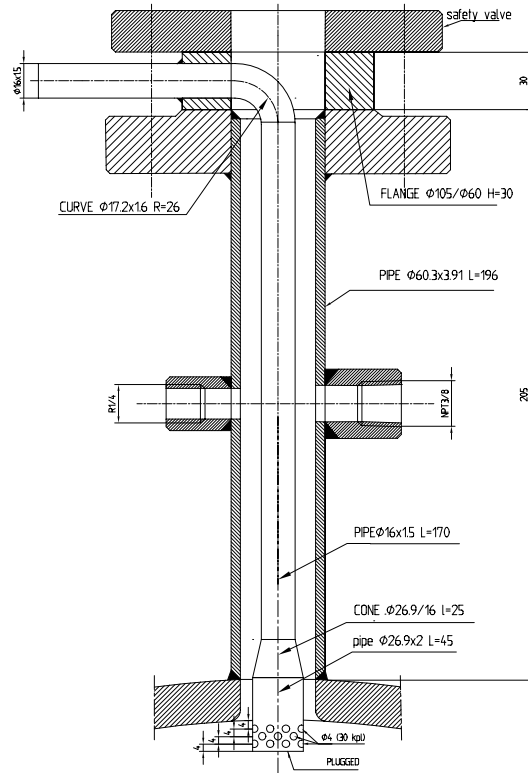


Figure 3. Sparger.

INSTRUMENTATION OF THE CORE MAKE-UP TANK (CMTφ660)

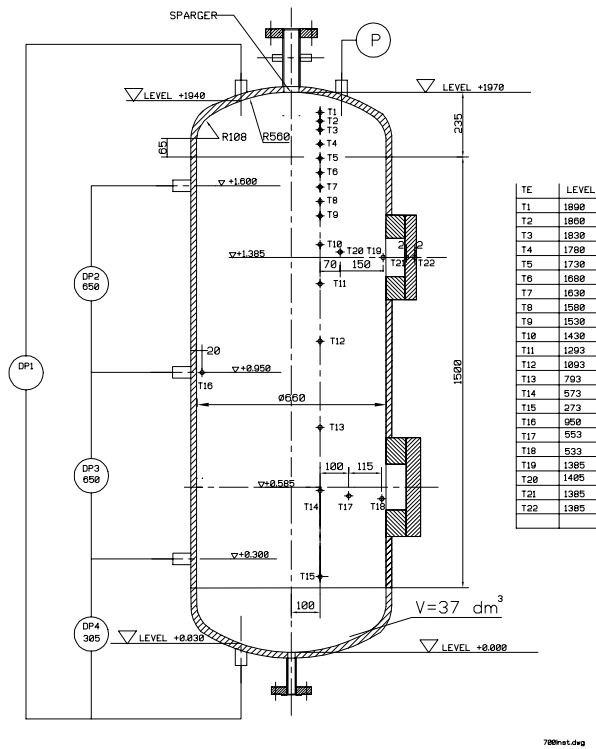


Figure 4. CMT instrumentation in the third series.

3.2 RESULTS

3.2.1 PSIS operation modes

Figure 5 shows the principle configuration of the PSIS in the experiments. The PSIS consisted of PBL, CMT and IL. The PBL connected the CMT to the cold leg. The IL connected the bottom of the CMT to the downcomer. The IL isolation valve was closed during normal operation of the loop. The PBL was open all the time and the CMT was at same pressure as the primary circuit.

During normal operation of the loop, there was no flow through the PSIS. The flow began when the operators opened the IL isolation valve, usually from the low pressurizer level. The first PSIS operation mode, **recirculation phase**, included single-phase water circulation through the system. The density difference between the hot water in the PBL and the cold in the CMT and IL created the driving force for the flow. The second mode, **oscillating phase**, included two-phase flow in the PBL. The density difference which drove the flow was larger since the PBL was now full of two-phase mixture. The flow rate during this phase was larger than during recirculation phase. The third operation mode was called **injection phase**. During this phase, steam flowed to the CMT and level in the tank dropped. The driving force for flow was large and the flow through the PSIS was at its maximum

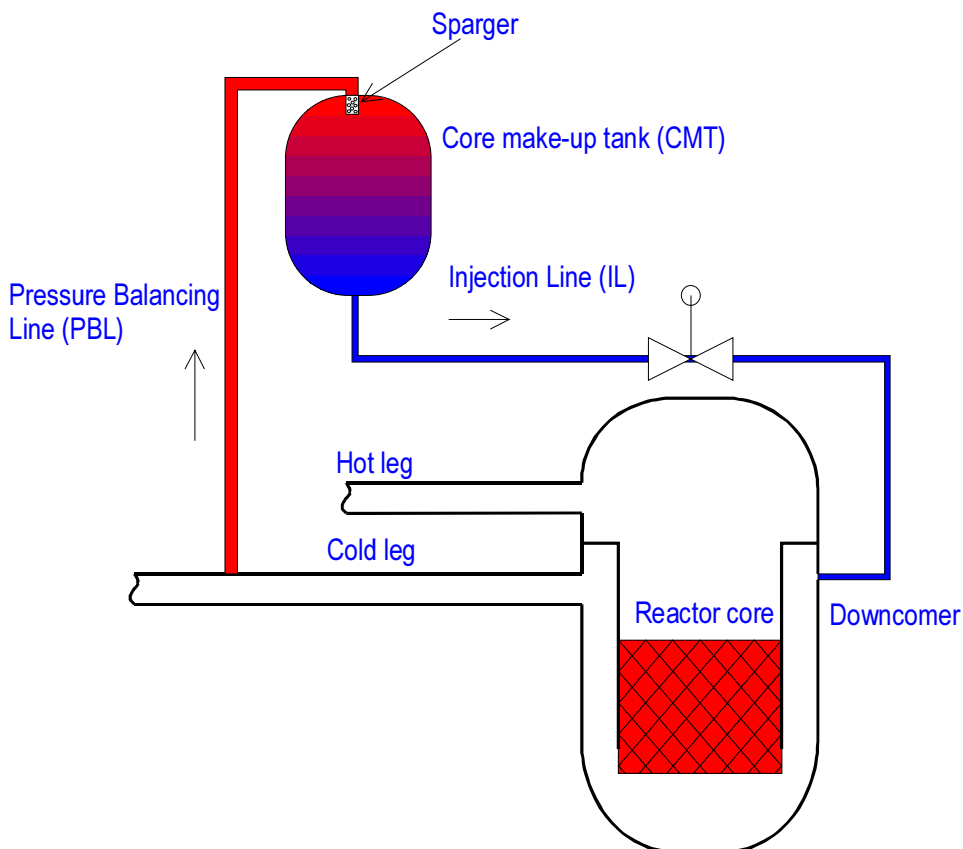


Figure 5. Principle PSIS configuration.

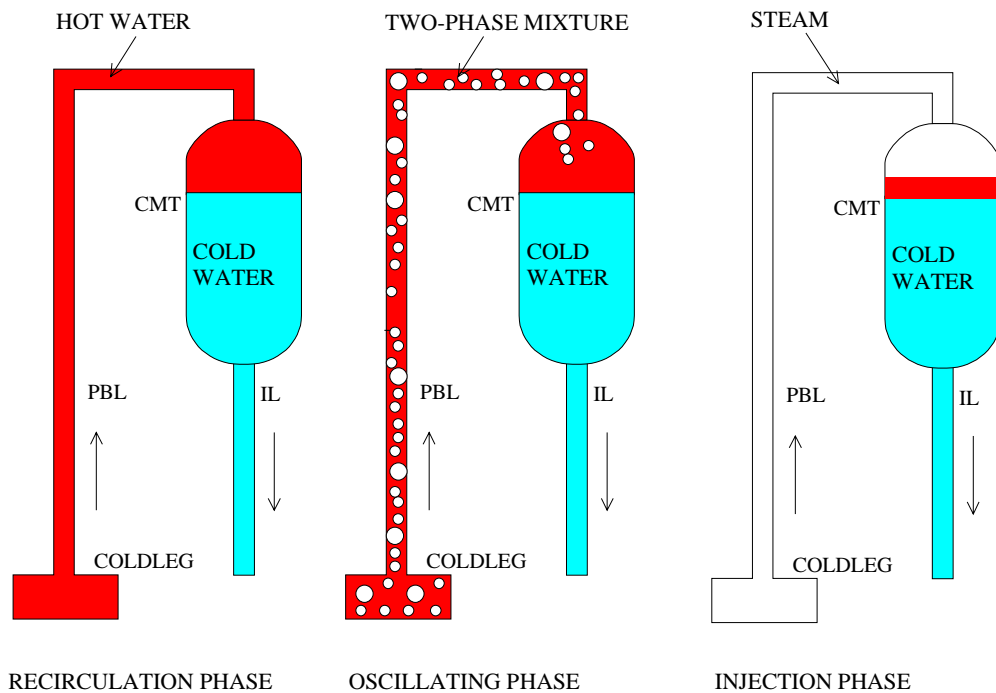


Figure 6. PSIS operation modes.

Figure 6 illustrates the different PSIS operation modes. The recirculation phase was important, because the hot water flowing to the CMT formed an isolating layer in the tank between the cold water and the steam. This reduced possibilities for rapid condensation in the CMT. Condensation may disturb PSIS operation if the hot liquid layer breaks down. This may happen, for example, during oscillating phase when two-phase mixture flows to the CMT.

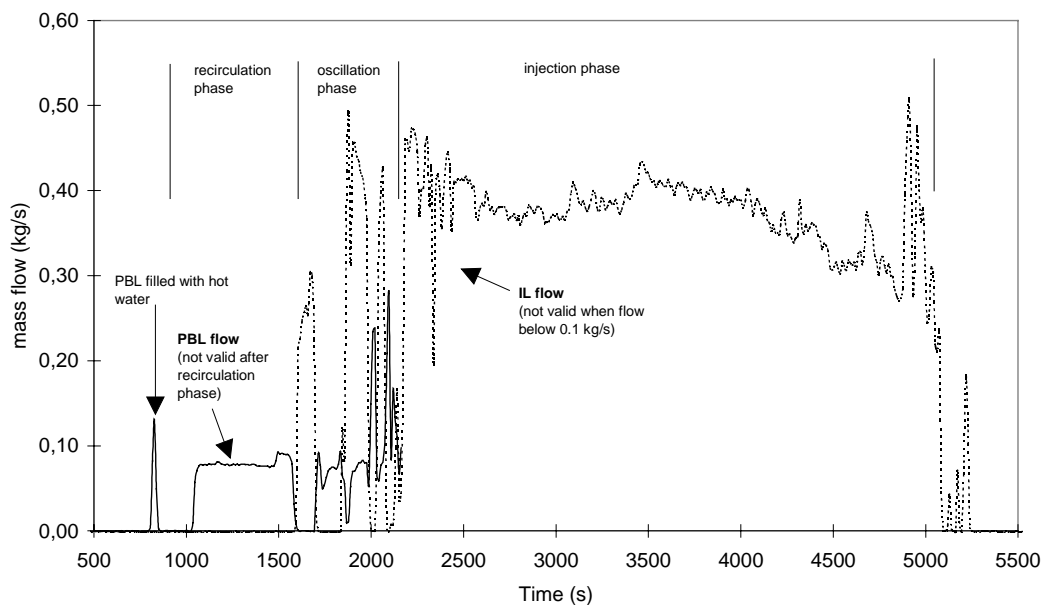


Figure 7. Mass flow rate through the PSIS in the GDE-24 experiment.

Mass flow rate through the PSIS varied as the driving force changed during different PSIS operation modes. The mass flow was low during the recirculation phase and high during the injection phase. Between these two phases, mass flow rate oscillated. See Figure 7.

3.2.2 Parametric studies

The experiments studied the effects of

- the break size and location,
- the CMT size and position,
- the removal of the flow distributor (sparger),
- the initial water temperature in the CMT and PBL,
- the PBL connection position and
- the injection line flow resistance

on the PSIS behavior during SBLOCA's.

Break size

During the recirculation phase, hot water flowed through the PBL to the CMT and replaced cold water there. The average recirculation phase mass flow rate varied between 0.074 and 0.083 kg/s and decreased slightly with decreasing break size and Loop 2 flow rate. See Table 2 for a summary of the PSIS flow rates in the experiments. The break size had large influence on the duration of the recirculation phase. The recirculation phase began when the operators opened the IL isolation valve, and ended when the water level in the Cold Leg 2 dropped below the PBL connection. The length of the recirculation phase increased as the break size decreased. This was important because the driving head for recirculation flow, the density difference between the PBL and IL, reduced when hot water filled the CMT. In an extreme case, the whole CMT and the IL became full of hot water, and the driving head for recirculation flow disappeared. This happened in the experiment GDE-43. The whole CMT became full of hot water and the flow through it stopped for 2000 seconds after about 9000 seconds of recirculation flow. In the PACTEL loop, only one CMT was in operation. In the real plant, flow through the all CMTs would stop if the break is small enough. In PACTEL, the fact that the flow through the PSIS stopped did not effect the main function of the PSIS: the CMT began to inject water normally as the level in the cold leg of the Loop 2 dropped below the PBL connection.

The maximum break diameter in the experiments was 5 mm. In the 5 mm break experiment, there were condensation problems (water hammer) near the ECC water injection position in the downcomer. Problems occurred when water-plugs moving in the horizontal part of the Loop 2 cold leg between the break and downcomer hit the downcomer diffuser. See Figure 8 for the geometry of PACTEL near the break position. The reason for the water plug movement was condensation, which occurred when steam coming from the cold leg met cold water near the break position. The cold water flow rate from the downcomer was

not large enough to fill the cold leg pipe completely, when it flowed into the break. This led to condensation induced water hammer in the horizontal section of the Loop 2 cold leg.

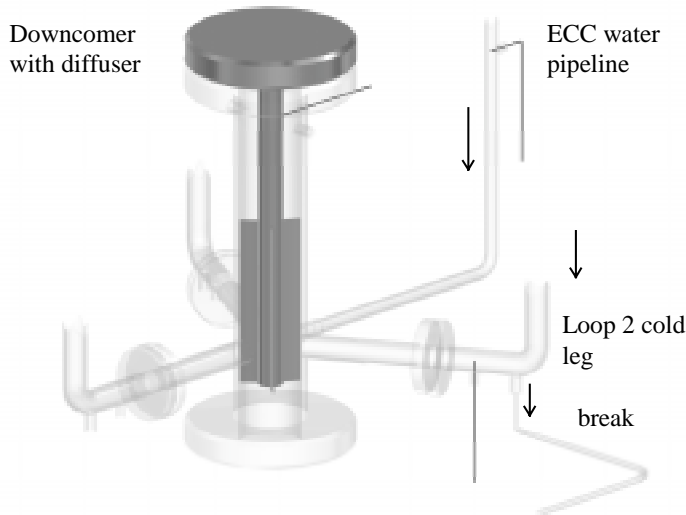


Figure 8. Cold leg connections to the downcomer in the PACTEL. Break locates in the bottom of the Loop 2 cold leg pipe in the lower right corner of the figure.

Table 2. Overview of the PSIS flow rates in the PACTEL CMT experiments.

Experiment	Break size (mm)	Recirculation phase			Injection and oscillating phases	
		Average flow rate through the PSIS (kg/s)	Average Loop 2 flow rate (kg/s)	Duration (s)	Average flow rate from the CMT (kg/s)	Time needed to empty the CMT (s)
First series (large CMT)						
GDE-21	1	0,074	0,33	8820	0,02	over 4500 s
GDE-22	2,5	0,079	0,46	1145	0,21	5675
GDE-23	5	0,083	0,61	380	0,34	3300
GDE-24	3,5	0,080	0,49	540	0,33	3650
GDE-25	3,5	0,080	0,50	530	0,33	3570
Second series (small CMT)						
GDE-31	3,5	0,078	0,50	550	0,30	2215
GDE-32	3,5	0,075	0,18	960	0,08	9470
GDE-33	3,5	0,072	0,27	685	0,07	11740
GDE-34	3,5	0	0,57	-	0,31	1780
GDE-35	3,5	0,080	0,50	540	not started	experiment terminated before the CMT begun to inject
Third series (small CMT at high position)						
GDE-41	3,5	0,085	0,51	565	0,33	2115
GDE-42	3,5	<0,02	0,50	1000	0,15	3800
GDE-43	1	0,077	0,26	8265	0,07	over 5200 s
GDE-44	3,5	0,087	0,47	560	0,32	2125
GDE-45	3,5	not measured	-	35	0,30	2290

Between the recirculation phase and the injection phase the flow through the PSIS oscillated. The oscillations took place when the cold leg water-level was close to the PBL connection. During this phase, the level in the CMT dropped, but the PBL was only partially full of steam. Flow of water to the CMT was possible. In the experiments with the smallest break size, the flow through the PSIS was in this oscillating region until the end of the experiments and the injection phase never really started. The injection phase of CMT operation began when the level near the PBL connection dropped so much that only steam could enter the PBL. The CMT became empty more quickly in the experiments with larger break size.

Break location

In loss-of-coolant accidents, the flow through the broken cold leg may reverse. If the loop flow reverses in the AP600 type reactor in the loop which has a PBL connection, water below the saturation temperature may flow from the downcomer through the broken cold leg to the PBL and, finally, back to the CMT. This may lead to condensation in the CMT. The PACTEL experiments GDE-32 and GDE-33 demonstrated that the flow reversal and the flow of cold water from the downcomer through the cold leg towards the PBL could occur. The temperature of water flowing through the cold leg was so high that no significant condensation in the CMT occurred. Flow reversal in the broken cold leg will affect only one CMT and the CMT's connected to the intact loops of the reactor would remain unaffected.

When the break was located in the hot leg or close to the steam generator outlet in the cold leg, the water level stabilized near the PBL connection and the PSIS operated in the oscillating mode for an extended time. The injection flow rate from the CMT never reached the full value since the PBL did not become completely empty of water.

CMT size and position

The experiments used two different CMT tanks. The first series, experiments GDE-21 through GDE-25, used the large CMT (2,06m high; 0,85/0,90m inside/outside diameter). Experiments GDE-31 through GDE-45 used a taller CMT with a smaller volume (1,95m high; 0,66/0,70m inside/outside diameter). The experiments also studied effects of the CMT position on the PSIS behaviour. For the GDE-41 through GDE-45 experiments, the PACTEL operators moved the CMT to a 1 metre higher elevation than in the previous experiments. This increased the driving head for PSIS flow from about 6.6 to 7.6 metres.

As expected, the core heatup occurred later in the experiments with the larger CMT. The time needed to empty the CMT was directly proportional to the CMT water volume. The ratio of the initial water volume in the small and large CMT was about 0,58 ($\approx 632\text{dm}^3/1088\text{dm}^3$). The ratio of draining time in the identical experiments with the small and large CMT was about 0,61 ($\approx 2215\text{s}/3650\text{s}$). This means that the difference between the wall mass of the CMT's, about 50 % more

in the larger CMT due to thicker walls and larger diameter, did not have a significant influence on the condensation rate in the tank or the draining time.

The elevated CMT position increased the recirculation phase flow rate. The flow through the PSIS was about 10 % higher when the CMT was at the 1 m higher position. The flow rate increased since the PSIS pipeline pressure losses had to compensate for the increased driving head because of the higher CMT position. During the CMT injection phase, the flow through the PSIS was more unstable. The flow stagnated and oscillated, which made comparison of the flow rates between the experiments more difficult. Some increase of IL flow was obvious in the experiments with CMT at higher position, but the increase was not as large as during the recirculation phase.

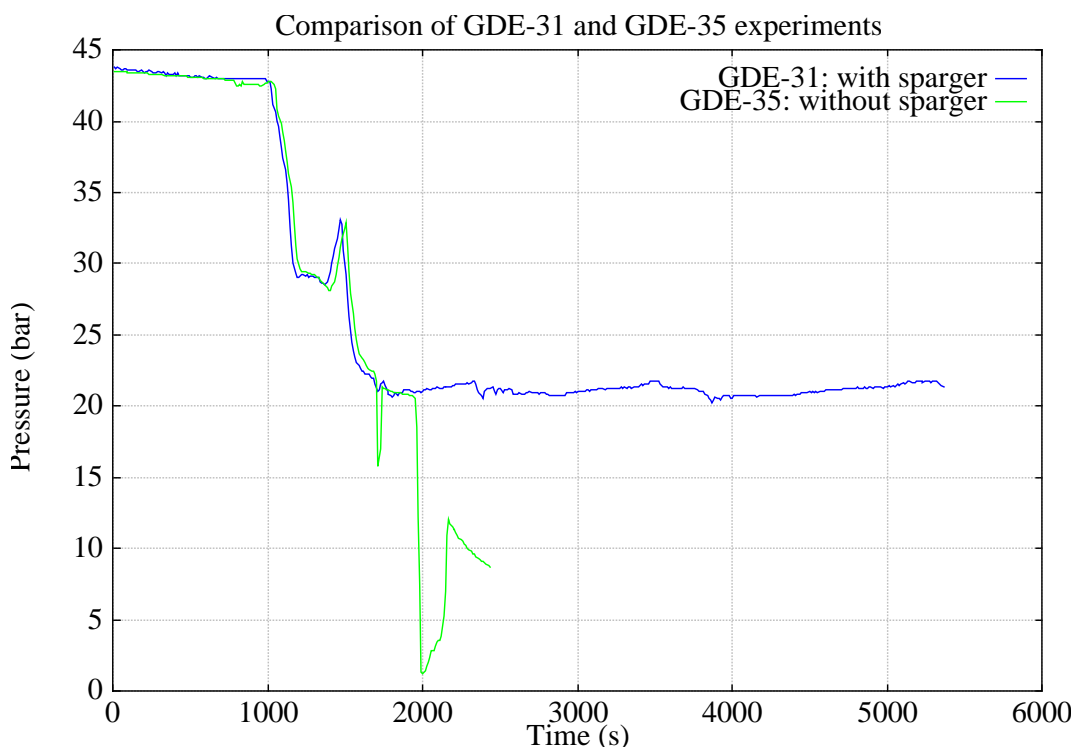


Figure 9. Pressure in the CMT. Experiments with (GDE-31) and without (GDE-35) sparger in the CMT.

Flow distributor (sparger)

The purpose of the flow distributor (sparger) in the CMT was to diminish the possibility of rapid condensation in the CMT, such as was observed in the earlier passive safety injection experiments in PACTEL [19]. In the current experiments, the sparger was in use in the CMT and there were no problems with rapid condensation. Some condensation occurred in the CMT when steam began to flow there after the recirculation phase. In some experiments, the injection flowrate stopped temporarily during the injection phase when the steam condensation in the tank reduced the pressure there. Condensation occurred when water (possibly condensate flowing from the steam generator to the cold leg loop seal) temporarily filled the cold leg near the PBL connection and the water flowed to the CMT. The

injection flow resumed soon after the PBL connection position in the cold leg became free of water again. The flow stagnations lasted typically no longer than 2-3 minutes.

The removal of sparger had significant influence on the PSIS behavior. In the experiment without a sparger, intensive condensation in the CMT occurred and the CMT pressure dropped when steam began to flow to the CMT i.e. when the PSIS injection phase began. The rapid condensation in the CMT led to strong mixing of the hot and cold water layers in the tank, and the temperature profile in the CMT became almost uniform. The pressure in the CMT dropped close to atmospheric whereas the pressure in the other primary loop remained unchanged. The CMT pressure history from experiments with and without sparger is presented in Figure 9. When the CMT pressure collapsed the PACTEL operators terminated the experiment to avoid damage to the rig.

Initial temperature in the PSIS

The AP600 reactor PSIS design includes initially hot water in the PBL and cold water in the CMT and IL. The PBL configuration is such that hot water from the primary circuit fills the line through natural convection without any heating equipments or operator actions. The PSIS may, however, become full of hot water during normal operation of the plant if the IL check valve leaks. As an extreme case, the PACTEL experiment programme also studied the situation where the PBL was initially full of cold water.

The fact that the CMT becomes full of hot water during normal operation of the plant eliminates the PSIS recirculation phase, since the driving force for the PSIS flow disappears. In the PACTEL experiment, the fact that the PSIS was initially full of hot water eliminated the PSIS recirculation phase, but did not affect the main function of the PSIS. The PSIS injection phase began as planned when the water level in the cold leg dropped below the PBL connection position. The PSIS worked as planned also in the experiment where the PBL was initially full of cold water. In this experiment there was no initial driving force for flow through the PSIS due to the temperature difference between the PSIS lines. The flow through the PSIS started when the operators opened the IL check valve. Also, in this case, the PSIS fulfilled its main function of providing water to the primary circuit.

The initial water temperature in the CMT affected the water level in the reactor pressure vessel and the timing of core heatup at the end of the experiments. The core heated up earlier in the experiments where the PSIS was initially full of hot water. When the water was hot a lower water level in the core side was enough to balance the downcomer water column.

PBL connection position

In the Westinghouse AP600 reactor, the PBL connects the top of the CMT to the cold leg of the primary circuit. In the Korean (CARR) CP-1300 Reactor [20], the PBL connects the top of the pressurizer to the CMT top. The experimental programme included one SBLOCA test with the PBL connection to the top of the

pressurizer. The CMT worked as planned also in this experiment. There were no problems with condensation in the CMT, although there was practically no water circulation through the PBL before the CMT started to inject water. The injection mass flow rate oscillated, but this was a consequence of the PACTEL primary loop geometry with loop seals in the hot legs. The change of PBL connection position affected the primary coolant distribution and, hence, timing of core heat-up at the end of the experiment. Core heat-up occurred earlier in the experiment with the PBL connection to the top of pressurizer than in the similar experiment with the cold leg PBL connection. The reason was the accumulation of water in the pressurizer and PSIS injection line.

IL flow resistance

For one experiment, the PACTEL operators installed an extra flow orifice in the IL, to reduce the flow through the PSIS. The reduced flow from the CMT had an influence on the water-level behaviour in the core section. The water-level in the core section was lower when the extra orifice was in use. The core water-level settled to the hot leg loop seal bottom elevation, and remained there as long as there was water in the CMT. The fact the level was at the hot leg loop seal bottom elevation led to pressure fluctuations, when the hot leg loop seals opened and closed. The pressure oscillations started simultaneously with the beginning of the CMT injection phase. The higher flow resistance in the PSIS injection line did not change the principle behaviour of the PSIS system. All three PSIS operation modes were present, with lower flow rates only. During the injection phase, because of the higher flow resistance, the injection mass flow rate was not oscillating as much as earlier.

3.2.3 Heat transfer to the CMT wall

As the CMT recirculated, hot liquid flowed to the top and created a hot liquid layer. Since the flows in the CMT were small, there was very little mixing of this layer with the colder water and a thermally stratified hot liquid layer formed. Above this thermally stratified layer there was a layer of saturated liquid. The thickness of the layers depended on the break size, as discussed earlier in this report. Since the CMT walls were initially cold, the hot liquid layer transferred heat to the walls.

PACTEL CMT instrumentation did not include thermocouples directly in the CMT walls, but in the manhole cover. See Figure 4. The thickness of the cover was 40 mm, and the thermocouples located 2 millimeters from the both surfaces of the cover. The same cover was in use in both CMT's. Using the temperature measurement data it was possible to estimate the heat flux to the cover as the hot liquid layer passed the thermocouples and as the steam began to condense. The measured wall heat flux profile depended on the thickness of the hot liquid layer. In the smallest break experiments, the hot liquid layer was thick and the maximum heat flux occurred when the hot water layer passed the thermocouple position. In medium size break experiments, the heat flux showed two peaks. The first peak

occurred when the hot liquid layer passed the thermocouple. The second peak corresponded to the time when the top of the liquid layer passed the thermocouple and condensation began. In the large break experiment, the hot liquid layer was very thin and the two peaks coincided.

When the wall thermocouples were underwater, the heat transfer mechanism was natural convection from liquid to the wall. During this phase the heat transfer coefficient varied between 1 and 4 kW/m²K. As the water surface passed the thermocouple, condensation began. The change in the heat transfer mode increased local heat transfer coefficient. During this phase, the temperature difference between the wall and steam was small and close to the lower measurement limit of the thermocouples.

During the natural convection heat transfer period, an appropriate correlation is the McAdams natural convection correlation, as suggested by Cunningham *et. al.* [21]. During the condensation phase Cunningham *et. al.* suggested the Nusselt film condensation model. Figure 10 and Figure 11 present a comparison of the PACTEL experiment data from the first experiment series and the values calculated from the McAdams and Nusselt correlations. A separate report presents the heat flux and heat transfer coefficient values for the second and third experiment series [22].

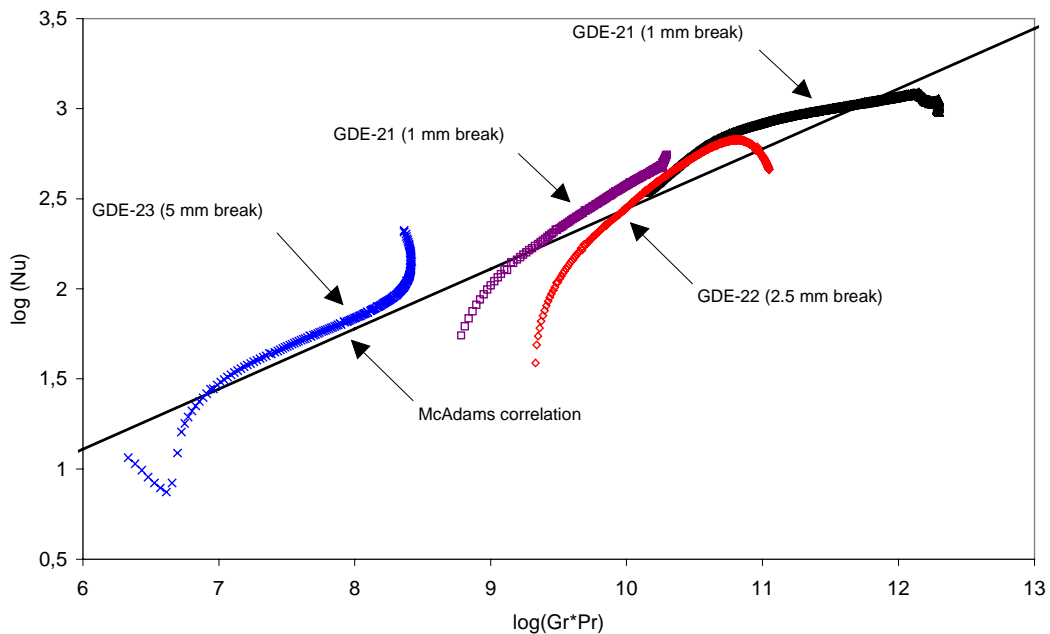


Figure 10. Comparison of the measured heat transfer coefficient from hot liquid layer to the CMT wall and the McAdams natural convection correlation. Results from the first experiment series.

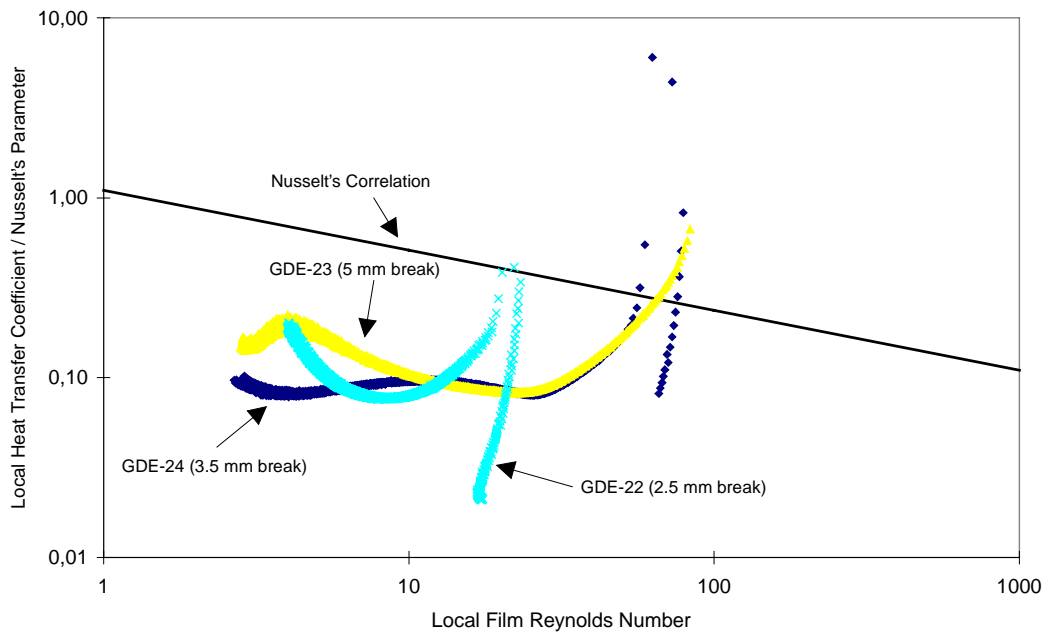


Figure 11. Comparison of measured condensation heat transfer coefficient with the Nusselt correlation. Results from the first experiment series.

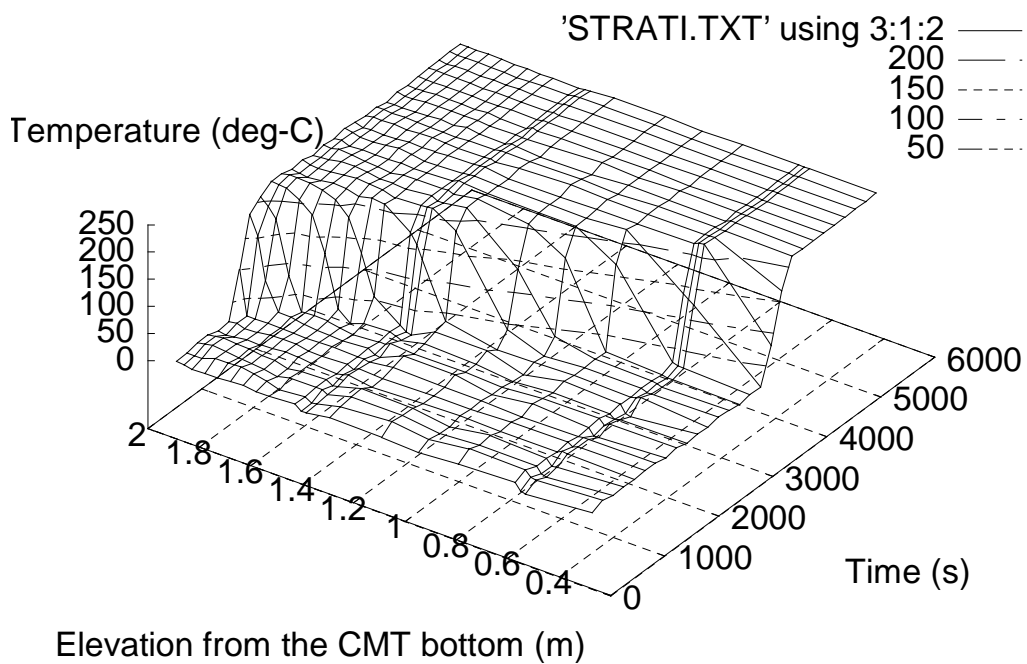


Figure 12. Temperature profile in the CMT in the GDE-31 experiment.

3.2.4 Thermal stratification in the CMT

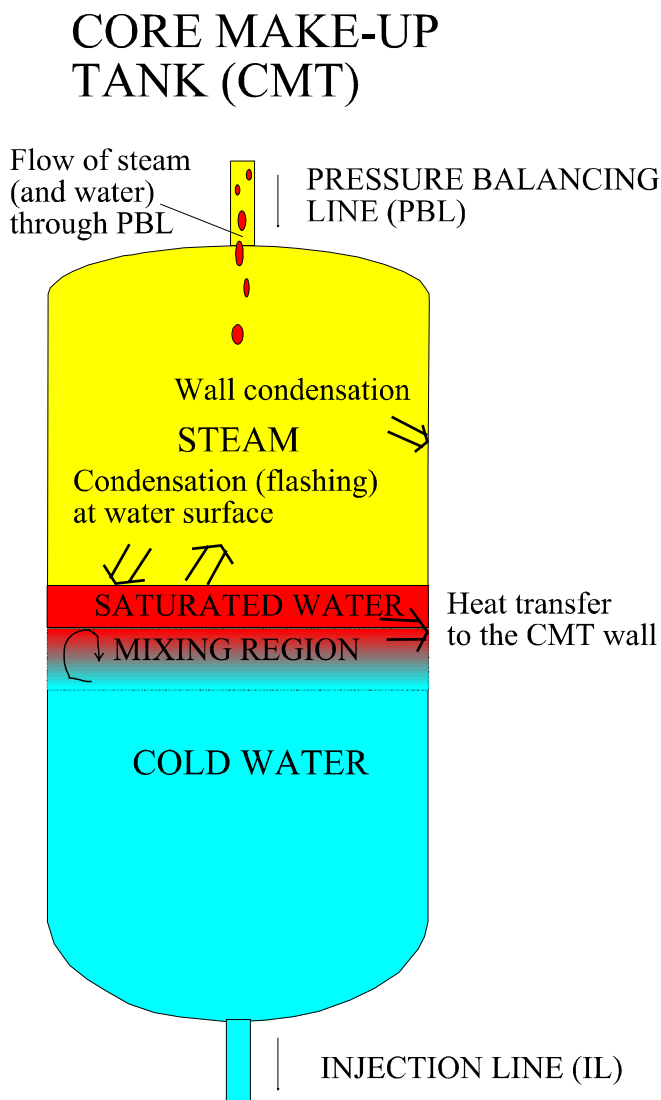


Figure 13. Phenomena in the CMT during ECC water injection.

larger break or when the break was at the outlet part of the cold leg, the saturated liquid layer was very thin and the water temperature in the CMT reached saturation only close to the water surface. The thickness of saturated layer increased as the break size decreased or when the break position was changed to the inlet part of the cold leg or to the hot leg. See Figure 14 and Figure 15 for the positions of actual water level and the top and bottom of the thermally stratified layer in two PACTEL experiments. Information about the thickness of the hot liquid layers in the CMT in the second and third experiment series can be found in reference [22].

During the recirculation phase of the PSIS operation, hot water filled the upper part of the CMT. Since the walls of the CMT were initially cold, hot water transferred heat to the walls and a thermally stratified layer formed in the CMT. The temperature profile in the CMT was steep in the beginning of the transient but became less steep as the water level in the tank lowered. See Figure 11. Condensation of steam and flow of water to the tank brought more hot water to the CMT and increased the hot liquid layer thickness. Flashing of hot liquid layer may also have happened when the pressure in the tank dropped due to steam condensation. See Figure 12 for the phenomena in the CMT during the experiments.

The thickness of the thermally stratified and saturated liquid layers varied in the experiments. In the experiments with

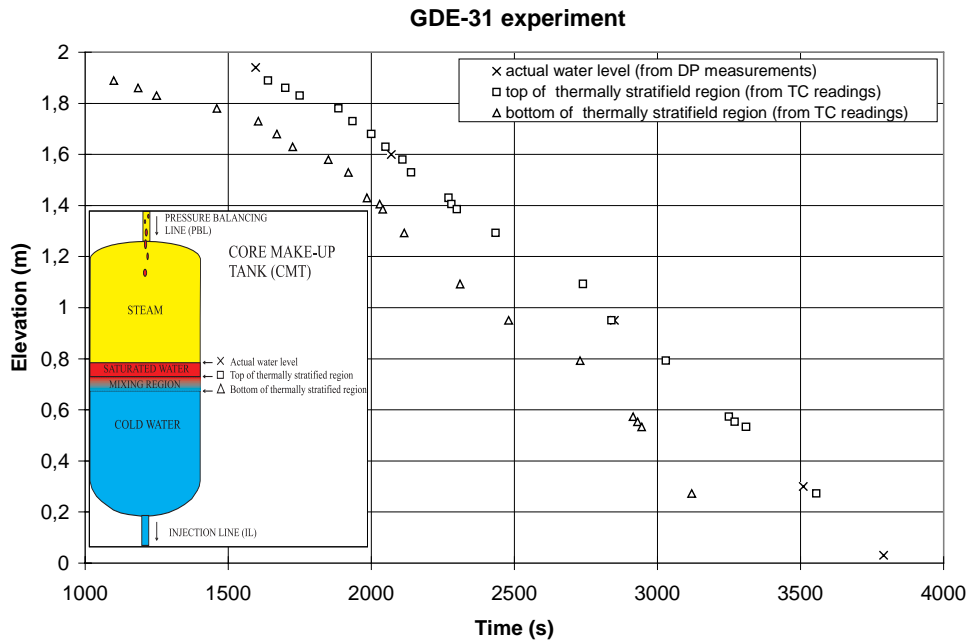


Figure 14. Water level behaviour in the GDE-31 experiments. Position of thermally stratified region detected using the temperature and differential pressure measurement data.

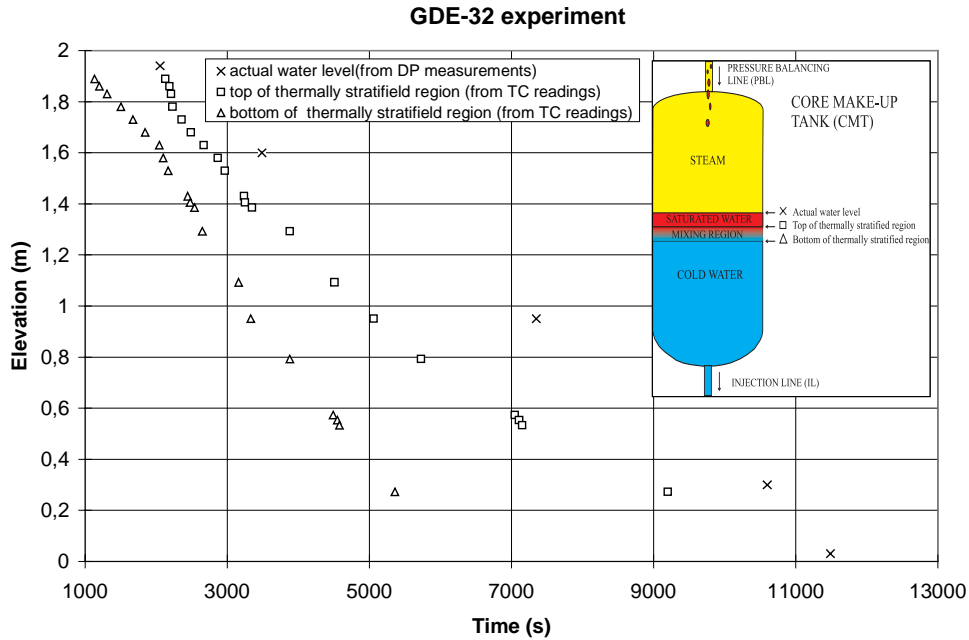


Figure 15. Water level behaviour in the GDE-32 experiments. Position of thermally stratified region detected using the temperature and differential pressure measurement data.

3.2.5 Reproducibility of the phenomena

To study the reproducibility of the phenomena in the CMT, the experimental team repeated one experiment with identical parameters. The overall behavior of the primary and secondary systems was similar in both experiments. The later phase of the experiments showed some differences in the primary and secondary pressures and in the pressurizer level behavior. The pressure in the CMT dropped due to condensation in the both experiments when the injection phase of CMT operation started. The CMT draining times were about 100 seconds different in the experiments. Consequently, the core heat-up was delayed by about 170 seconds. See Figure 16 for comparison of the primary pressure and core water level in the repeated experiments.

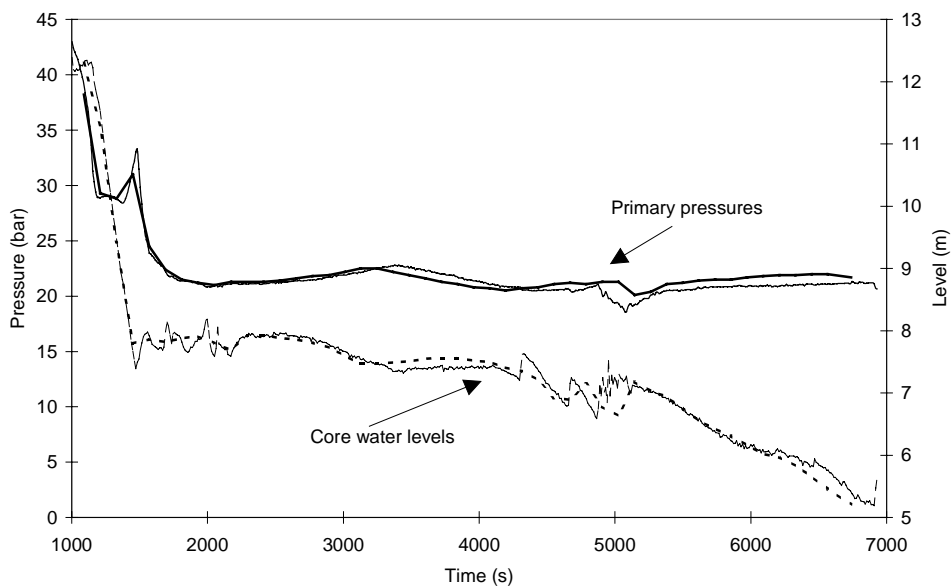


Figure 16. Primary pressure and core water level in the experiments studying reproducibility of the PSIS phenomena.

3.3 STEAM GENERATOR PERFORMANCE

The PACTEL experiment loop has three horizontal steam generators. In the passive safety injection experiments, the secondary side pressure and water level were kept constant during the experiments. Separate feed water injection to each steam generator kept water level in the steam generator secondary side above the heat exchange tubes. The level variations in the experiments were slow and the operators controlled the levels manually. Feed water temperature and flow rate were about 50°C and 1-2 l/min, respectively. The feed water temperature measurement position was such that the measurement did not show the correct value when the feed water pumps were off. When the feed water pumps were off, hot water from the steam generator secondary side filled the measurement position and the temperature rose.

Table 3 Information about the secondary side control valve.

Flow area in fully open position = 0,000794 m ²		
Valve position	Normalized area	Flow area
(-)	(-)	(m ²)
0,0	0,0	0,0
0,21	0,0	0,0
0,25	0,02	0,00001588
0,30	0,05	0,0000397
0,40	0,12	0,00009528
0,50	0,22	0,00017468
0,60	0,33	0,00026202
0,70	0,47	0,00037318
0,80	0,62	0,00049228
0,90	0,80	0,0006352
1,00	1,00	0,000794

A standard PI-controller of Loop 1 steam generator controlled the pressure in all steam generators through the common steam line. The control valve is a normal servo valve and all steam produced in the secondary side flows through this single valve. The valve flow area follows a parabolic curve after the dimensionless valve position value exceeds 0,21. Below that value, the valve is closed.

Table 3 gives basic information about the valve. The valve position is controlled using the measured steam line pressure as a control value. This value is then compared with the secondary pressure setpoint, and a new value for the valve position is determined.

The controller uses the following formulas to calculate the valve position $O(t)$:

$$O(t) = C * DEV(t) + INT(t)$$

$$INT(t) = INT(t-TS) + C * TS / TI * DEV(t)$$

$$DEV(t) = p - p_a$$

C = amplification factor = 1

TS = measurement frequency 1 (s)

TI = integration time = 30 s

p_a = pressure setpoint (bar)

p = measured pressure (bar)

t = time

$$0 \leq O(t) \leq 1$$

3.4 LIMITATIONS OF THE MEASUREMENT INSTRUMENTATION

PACTEL instrumentation consists of temperature, pressure, differential pressure and single phase flow measurements. Since the flow in the primary circuit was sometimes two phase flow, some measurement instrumentation did not show

correct values all the time. Also the operation of the main circulation pumps in the steady phase of the experiments, and the break flow affected some measurements. The users of the experiment data should take into account the following:

- **PBL flow measurement:**

Flow meter in the PBL could only measure **single phase liquid flow**. The measurement value was correct only when the PBL was full of water i.e. during the PSIS recirculation phase.

- **IL flow measurement:**

Flow meter in the IL could only measure **single phase liquid flow**. The measurement value was correct only when the IL was full of water. The minimum detected mass flow rate was 0.1 kg/s. The IL flow meter did not measure as low flow rates as the flow meter in the PBL, because of the larger pipe diameter of the IL.

- **Level measurements:**

The operation of the main circulation pumps during the first 1000 seconds of the experiments affected all level measurements in the primary circuits and the reactor pressure vessel simulator. The level measurements were based on differential pressure measurements, and during high mass flow rate of forced convection, the effect of friction pressure loss is significant to most differential pressure measurements. That is why some differential pressure measurements were out of range in forced convection. Furthermore, the level values did not correspond to the actual level in the loop while pumps were running. However, the measured levels agreed well with the real levels after the operators stopped the main circulation pumps and the loop flow changed to natural circulation.

- **Downcomer mass flow rate measurement:**

The measurement range of the downcomer flow meter was 0.3-3.0 kg/s. When the primary circulation pumps were running, the downcomer flow rate exceeded the upper limit of the meter. The downcomer flow rate measurement detected only single phase liquid flow to the downward direction i.e. it couldn't measure steam flow or reversed flow.

- **Loop mass flow rate measurements:**

The primary loop flow rate measurement were valid as long as there was water in the measurement position. During the steady state period of the experiments when the primary pumps were running, sum of the three loop flow rate measurements gives the total flow rate through the PACTEL core simulator.

- **Secondary side feed water temperature measurements:**

These measurements were valid only when the feed water pumps were running, as described in the previous chapter.

- **Differential pressure measurements near the break position:**

The break line was connected to a differential pressure measurement tap. The flow of water and steam to the break affected the two differential pressure measurements connected to the same tap.

3.5 UNCERTAINTIES IN BOUNDARY CONDITIONS

Heat losses to the environment and the flow resistance of the primary circulation loops and PSIS lines form an important boundary condition for the code calculations. Separate measurements have provided data for code user for determining these boundary conditions. The boundary conditions include some uncertainties, which should be taken into account when making code calculations:

- **Heat losses distribution and size**

Measurement data available at the moment gives the total heat losses and an estimate of their distribution in the PACTEL rig [23] and [24]. The heat losses from the main circulation pumps are the most important contributor to the total losses and they can be determined using the measured pump cooling water temperatures and flow rates. At the maximum operation pressure and temperature of the primary loop, the total heat losses of the three main circulation pumps is 28 ± 5 kW. Linear interpolation to the initial temperature of the experiments gives heat losses of about 20 kW, which is of the same order of magnitude as the value calculated from the measured cooling water temperature and flow (15 kW).

- **Pressure losses in the primary loops and PSIS pipes**

Differential pressure measurements in the primary circuits give data about the pressure losses of the PACTEL loops. Separate measurements gave data about the PSIS pipelines pressure losses [25], [26] and [27]. More measurements have been conducted recently to determine more accurately the pressure losses in the nominal and reversed loop flow conditions [28]. Reversed flow was observed in the experiments in the broken loop between the break position and downcomer.

- **Core power**

Two different methods were used to measure core heating power in the PACTEL experiments. The first one uses the measurement of the power control system and the second measures the total energy used during the experiments. The accuracy of these measurements is $\pm 6\%$ and $\pm 1\%$ of the measured value, respectively.

- **Steam generator control valve position**

Measurement data does not include secondary side valve position information. The initial valve position may have affects on the secondary side pressure behavior in the beginning of the transients i.e. when the operators open the break in the primary circuit.

3.6 CONCLUSIONS FROM THE EXPERIMENTS

The purpose of the examined PSIS is to provide an alternative to the HPI pumps of the current PWRs in APWR plant. In the PACTEL experiments, the PSIS fulfilled its function and provided water to the primary circuit as planned in all experiments where the CMT sparger was in operation. The PSIS did not work as

planned in the experiment where the sparger was removed, due to rapid condensation in the CMT.

The experiments demonstrated the importance of the CMT flow distributor (sparger) on the PSIS behavior. The removal of sparger led to strong condensation in the CMT, which stopped safety injection. Due to the condensation, the operators of the PACTEL loop had to terminate the experiment to avoid damage to the loop.

The experiments showed that the CMT could become full of hot water during the PSIS recirculation phase and the flow through the PSIS could stop, if the recirculation phase is long enough. In the PACTEL experiments this did not affect the main function of the system: the PSIS began to inject water as planned when the cold leg level dropped below the PBL connection.

Moving the CMT to a higher elevation increased the flow through the PSIS. The increasing flow rate through the PSIS increases the thickness of hot liquid layer in the CMT, which separates cold water from steam when the safety injection begins. Hence, the possibilities for condensation problems decrease as the CMT is moved to a higher position.

The CMT worked as planned with all different break positions. The flow in the broken cold leg was reversed in some experiments, but this did not cause problems for the CMT operation.

The experiments provided data about the heat transfer mechanisms to the CMT walls and thermal stratification in the tank. The comparison of the data with the McAdams natural convection correlation and Nusselt condensation correlation showed that the McAdams natural convection correlation is suitable for calculating heat transfer from the hot liquid layer to the CMT walls. The Nusselt correlation gave somewhat higher values than the measurement data.

"Water hammer" occurred in one experiment in which steam condensation near the ECC water injection position led to movements of water plugs. The water plugs accelerated in the horizontal part of the cold leg near the downcomer and hit the downcomer diffuser. This was possible since the ECC water flow rate was small enough for stratified flow to occur in the horizontal part of the cold leg.

4. COMPUTER CODE SIMULATIONS

The project partners selected one experiment from each series for computer simulations. The first experiment selected was GDE-24, which was a 3,5 mm cold leg break case with the break close to the downcomer. The computer simulations focused on the CMT phenomena, such as thermal stratification and condensation. The second one selected was GDE-34, which was similar to the GDE-24 but with a smaller CMT and with the CMT initially full of hot water. The main interest was the PSIS recirculation phase: the recirculation phase did not exist in the experiment since the driving force for starting the flow was too small. The third simulation case, called GDE-43, focused on natural circulation flow through the PSIS when the driving force for flow slowly disappears. The following chapters describe briefly the three computer codes used in the analyses, compare the results of different code calculations and draw conclusions about code calculations.

4.1 CODE DESCRIPTION

4.1.1 APROS

APROS is a multifunctional code which has been widely used for analyzing and simulating conventional and nuclear power plants [2]. The code is capable for feasibility studies, design, operating instructions, accident analysis, optimization and training. The graphical interface called GRINAP (Graphical User Interface of APROS) can be used for model construction, on-line modifications and control and monitoring of the simulation process. The code user can work in three different levels: process, process component and calculation levels. Creation of a simulation process starts usually with the definition of the necessary connections points. Between these points the user can add desired process components, such as pipes, tanks, valves, to build up the simulation model. The APROS code creates automatically the necessary nodalization and calculation level modules according to the given data.

APROS user can choose between three different thermal hydraulic models:

- Homogenous 3-equation model,
- 5-equation drift-flux model or
- 6-equation two-fluid model

The 5-equation model is designed for fast running simulations and it can be used, for example, in the training simulators. The 6-equation model contains two fluid model and it is usually used as a tool for detailed engineering and safety analysis. It is also possible to use the different models within the simulation e.g. more accurate six equation model in the primary circuit and more simple three equation model in the secondary side. APROS uses an iterative solution method when solving the equations.

Constitutive models for six-equation model

The APROS code uses following models in calculation of the phenomena important in the calculations of the PSIS behavior in SBLOCAs:

Interfacial condensation:

- Shah correlation for the liquid phase
- Lee-Ryley correlation for the gas phase

Interfacial flashing:

- Exponential function of void fraction

Interfacial friction:

- Interfacial friction is obtained from a weight function, which describes different flow types: bubbly, annular, droplet and stratified flow

Wall friction:

- Blasius equation for both phases

Wall heat transfer

- There are three separate heat transfer zones where the wall heat transfer is calculated from different correlations: wetted wall, dry wall and a transition between wetted and dry wall. If the wall temperature is lower than the saturation of the fluid, only water is assumed to be in contact with the wall. When the wall temperature rises, the heat flux increases. After the heat flux has exceeded the critical heat flux, the wall begins to dry out and the heat transfer decreases.

4.1.2 CATHARE

The CATHARE code has been extensively used at the DCMN of Pisa University since 1986 [29], [30], [31] and [32]. In particular, the CATHARE code has been applied to the OECD/CSNI ISP 33 based on the original PACTEL facility [33] and [34].

The CATHARE (Code Avancè de Thermo-Hydraulic pour les Accidents des Reacteurs a' Eau) [3] has been developed for best estimate calculations of PWR accidents. It includes several independent modules that take into account mechanical and thermal non-equilibrium which can occur during PWR LOCAs. CATHARE is based on a six partial differential equation (mass, energy and momentum balance equations) model which is solved by a completely implicit method. The definition of further models concerning mass, energy and momentum exchanges between liquid and vapor and each phase with the wall has to be added to the main system. In order to obtain the model correlation, the classic correlation and experimental data derived from so called "separate effects" experiments performed in several facilities, have been extensively used [35]. In the following,

two particular models relevant to the scenarios of the considered experiment are described in some detail.

Three types of thermal exchanges are considered in the code: wall-fluid, liquid-interface and vapor-interface.

1) Wall to fluid heat transfer

According to the general boiling curve three main regions can be distinguished:

1a) Wet wall zone: this region is characterized by the presence of liquid in contact with the wall. The model takes into account forced convection and nucleate boiling. The first one is described by classical laminar and turbulent heat transfer correlation (Colburn); the second one is described by the Thom correlation (applied when $T_w > T_{sat}$). Moreover, in accordance to the model of net vapor generation of Zuber and Saha, a distribution of the heat flux between liquid and interface is proposed.

1b) Transition zone: it corresponds to the region between wet wall and dry wall and is delimited by the Critical Heat Flux (CHF) value and the Minimum stable film boiling temperature (T_{MIN}). The CHF is based on the Zuber-Griffith and Biasi correlation (with some correction factors applied by Groeneveld). For the T_{MIN} the Groeneveld-Sterward correlation has been introduced in the code.

1c) Dry wall zone: it is characterized by the contact of the vapor with the wall. Four kinds of heat transfer regime are assumed: pool boiling (Berenson correlation modified by Groeneveld), forced convection (Hadaller correlation), natural convection and radiative heat transfer (Deruaz model).

2) Liquid interface heat transfer

Two main regions are taken into account:

2a) Boiling region (where $H_L > H_{L,sat}$): the used correlation is derived from the analysis of data of the Moby-Dick and Super Moby-Dick experiments.

2b) Condensation region (where $H_L < H_{L,sat}$): in this region a flow with separated phases (in which the Saha correlation is used) and a droplet flow (in which is introduced a rate of entrainment in analogy with Stee-Wallis model) are considered.

3) Vapor interface heat transfer

Both for boiling and condensation situation, the vapor heat transfer is provided by classical correlation which express the conductive and convective heat exchange on droplets for dispersed flows and laminar or turbulent heat exchange with the liquid core for inverted annular flows.

4) Wall shear

The pressure gradient due to the wall shear stress is expressed by a relation in which single phase conditions are assumed and the usual friction factors for liquid and vapor are chosen as the maximum value between laminar and turbulent shear coefficient. For the vapor phase the flow regime factor is equal to the void fraction; for the liquid phase the coefficient is equal to the value of the fraction of perimeter in contact with the liquid (stratified flow) and it is based on the analysis of separate effect experiments in case of non stratified flow.

5) Interfacial friction

A distinction among different flow regimes is carried out. For each flow regime a specific correlation has been developed, taking into account experimental data.

a) Non stratified flow

- i) Slug flow: the Zuber and Findlay model has been used for a tube geometry, while for the rod bundle geometry the correlation used is derived from G2 and Pericles experiments.
- ii) Annular flow-mist flow: a correlation has been obtained taking into account the Wallis correlation for annular flow, the Steen-Wallis model of entrainment and the data from the Rebeca experiment.

b) Stratified flow

c) Transition flow

The interfacial shear in this flow regime is evaluated as a weighting between stratified and non-stratified regime, using the degree of stratification as weighting factor.

4.1.3 RELAP

The RELAP5 code has been developed over many years as a best estimate system thermal-hydraulics code for PWR accident conditions. The mass, momentum and energy equations are solved for the steam and water phases. The model allows for thermal-disequilibrium between the phases and also for heat transfer between the fluid phases and heat structures. Current generation PWRs utilize powered ECCS for SBLOCA. Hence the code models have been exercised and validated under flow conditions rather different from those encountered in these applications.

In general the key phenomena modeled by the code, including the wall, fluid heat transfer and shear require empirical correlations. These are flow regime and, therefore, applications dependent. A key consideration in the RELAP5 modeling concerns the behavior of the CMT. The phenomena of interest and which it is crucial to model correctly include thermal stratification, condensation and the liquid and wall heat transfer. The performance of the code models is considered in more detail in the analysis results from the individual tests.

4.2 NODALIZATION

4.2.1 APROS

For the APSI project, the APROS code calculations were made at the Lappeenranta University of Technology through a subcontract from VTT [36], [37] and [38]. The original APROS input deck of the PACTEL facility was prepared for small break LOCA simulations using 6-equation model. To calculate the GDE-24 experiment the input deck was modified by adding necessary PSIS components. For the calculation of GDE-34 and GDE-43, the deck had to be modified but only with minor changes. The basic nodalization scheme is presented in Figure 17. The number of different modules used in the deck in different calculations is presented in Table 4.

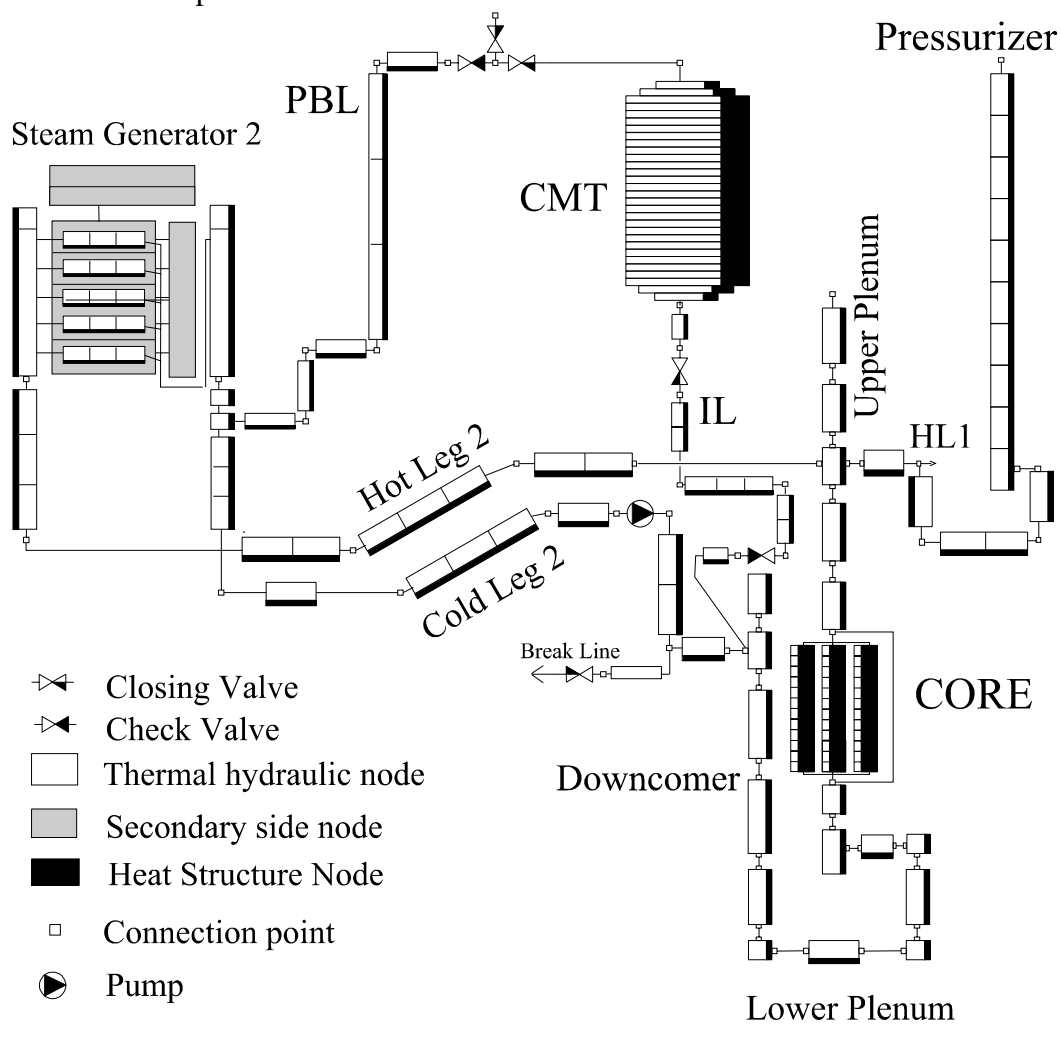


Figure 17. APROS nodalization of the PACTEL facility for calculation of GDE-24. Only loop 2 is shown.

Table 4. Number of nodes and modules in the APROS model of PACTEL

	GDE-24	GDE-34	GDE-43
Thermal hydraulic nodes	390	391	396
Heat structure nodes	1347	1347	1368
PBL nodes	14	14	18
CMT nodes	30	30	30
IL nodes	16	16	17

In all base case calculations, the CMT was modeled with 30 nodes with equal length. APROS created automatically the nodalization according to given data. So the node length of the CMT was approximately 0.065 m. The flow area of two top and two bottom nodes were diminished in order to simulate the rounded ends of the CMT.

Secondary side pressure control in APROS code

In the APROS model of PACTEL, the secondary pressure was controlled also with one control-valve only. The PI-controller took care of the controlling of the valve. The control scheme is shown in Figure 18. The transfer function of the controller is:

$$O(s) = K_p * (1 + \frac{1}{T_i * s}) * E(s) + K_{ff} * F(s),$$

where the symbols and their values are shown in Table 5.

Table 5. Transfer function symbols and values in PI-controller of APROS model

Symbol	Explanation	APROS model value
O(s)	Output of the controller	calculated value
E(s)	Control deviation of the controller	set point - measurement
F(s)	Feed forward signal of the controller	0
K _p	Controller gain	-1
T _i	Integration time (sec)	30
K _{ff}	Feed forward coefficient	0

To make the APROS pressure control valve to correspond to the PACTEL valve, an extra function module was included between the PI-controller output signal and the valve control device. The function modified the output value of the controller according to the data in Table 3.

Pressure losses

Pressure losses in the PBL and in the IL play important role in the operation of PSIS. Before simulation of each case, the pressure losses of the lines were validated against measured data [25], [26] and [27].

Calculation of the steady state condition

Each calculated experiment case needed pre-transient simulation to reach a proper initial state. After a few thousands seconds of simulation the steady state was reached. The comparison of main parameters between calculated and measured values is presented in following tables.

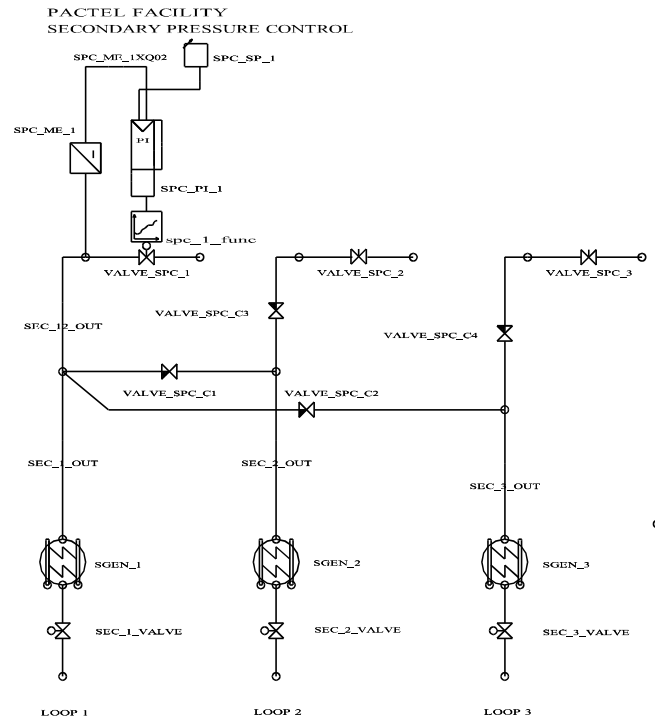


Figure 18. The secondary side pressure control scheme of APROS

Table 6. Measured and calculated initial conditions ($t = 1000$ s, before break opening) in GDE-24

PARAMETER	Experiment	APROS
Primary pressure [MPa]	4.33	4.35
Secondary pressure [MPa]	2.06/2.07/2.08	2.07
CMT pressure [MPa]	4.31	4.3
Loop1/2/3 flows [kg/s]	2.20/2.16/2.11	2.16/2.16/2.16
Core inlet temperature [C]	215.4	214.8
Core outlet temperature [C]	217.7	220.1
CMT water temperature [C]	11.8	12.4
PBL water temperature [C]	157.2	189.8
IL water temperature [C]	15.3	17.4
SG1/2/3 levels [cm]	74.1/73.0/74.4	74.2/72.6/74.3
Pressurizer level [m]	4.35	4.22
Core power [kW]	163	163

Table 7. Measured and calculated initial conditions ($t = 1000$ s, before break opening) in GDE-34

PARAMETER	Experiment	APROS
Primary pressure [MPa]	4.33	4.32
Secondary pressure [MPa]	2.09/2.10/2.12	2.10
CMT pressure [MPa]	4.32	4.31
Loop1/2/3 flows [kg/s]	2.16/2.09/1.97	2.16/2.09/1.97
SG Feed water flows [l/min.]	1.53/1.18/1.15	1.53/1.18/1.15
Core inlet temperature [°C]	213.3	215.5
Core outlet temperature [°C]	217.4	220.6
CMT water temperature [°C]	194.8	194.9
PBL water temperature [°C]	182.2	170.4
IL water temperature [°C]	71.3/141.4	65.3***
SG1/2/3 levels [cm]	71.8/71.2/71.3	72.6/72.2/71.6
Pressurizer level [m]	4.92	4.97

*** In the calculation the IL temperature was set equal throughout the line.

Table 8. Measured and calculated initial conditions ($t = 1000$ s, before break opening) in GDE-43.

PARAMETER	Experiment	APROS
Primary pressure [MPa]	4.38	4.38
Secondary pressure [MPa]	2.05/2.07/2.10	2.10
CMT pressure [MPa]	4.38	4.32
Loop1/2/3 flows [kg/s]	2.15/2.05/2.13	2.15/2.06/2.13
SG Feed water flows [l/min.]	1.42/1.41/1.41	1.42/1.41/1.41
Core inlet temperature [°C]	207.5	215.1
Core outlet temperature [°C]	218.3	220.3
CMT water temperature [°C]	18.4	18.8
PBL water temperature [°C]	173.1	184.0
IL water temperature [°C]	31.3	24.1
SG1/2/3 levels [cm]	72.5/72.1/72.1	75.5/74.8/74.0
Pressurizer level [m]	4.85	4.78
Core power [kW]	152	151.9

4.2.2 CATHARE

Starting from the nodalization developed and qualified adopting the ISP 33 data base (this is related to the 'original' PACTEL facility), a new nodalization has been set up in order to analyze the transient GDE-24 [39]. For the tests GDE-34 and GDE-43 only some minor nodalization changes have been done. The sketch

of the initial version of such nodalization is given in Figure 19. Details about the CMT line are reported in Figure 18. Significant details related to the adopted code resources are given in Table 9. It should be noted that around 700 hydraulic nodes are part of the nodalization. The most significant noding approximation, commensurate with the 1-D capability of the adopted code version, is constituted by the secondary side of the steam generators; only a vertical riser has been considered: the recirculation flow path has been neglected. This may cause poor prediction in transients where the heat transfer to secondary side plays a significant role including the cases of draining of the low pressure side of the steam generators.

Table 9. Adopted code resources for the CATHARE 2 v1.3U PACTEL 'initial' nodalization.

	PRIMARY SIDE	SECONDARY SIDE	TOTAL
VOLUME elements	11	3	14
AXIAL elements	35	3	38
TEE elements	2	0	2
BCONDIT elements	1	6	7
Junctions	62	9	71
Heat structures	26	6	32
Active structures	3	0	3
Hydraulic meshes	700	21	721

Nodalization qualification

A procedure has been proposed to demonstrate the qualification level of a facility or of NPP nodalization [40]. This consists of two main steps dealing with the 'steady state' and the 'on-transient' levels, respectively. Quantitative criteria have been defined for both the steps. The 'steady state' criteria are summarized in Table 10 (the 'on-transient' qualification needs the use of the Fast Fourier Transform based method [41] and has not been completed in the present frame).

The results obtained in relation to the steady state calculation are summarized in Table 11 and are compared with the experimental data. These essentially comply with the limits reported in Table 10.

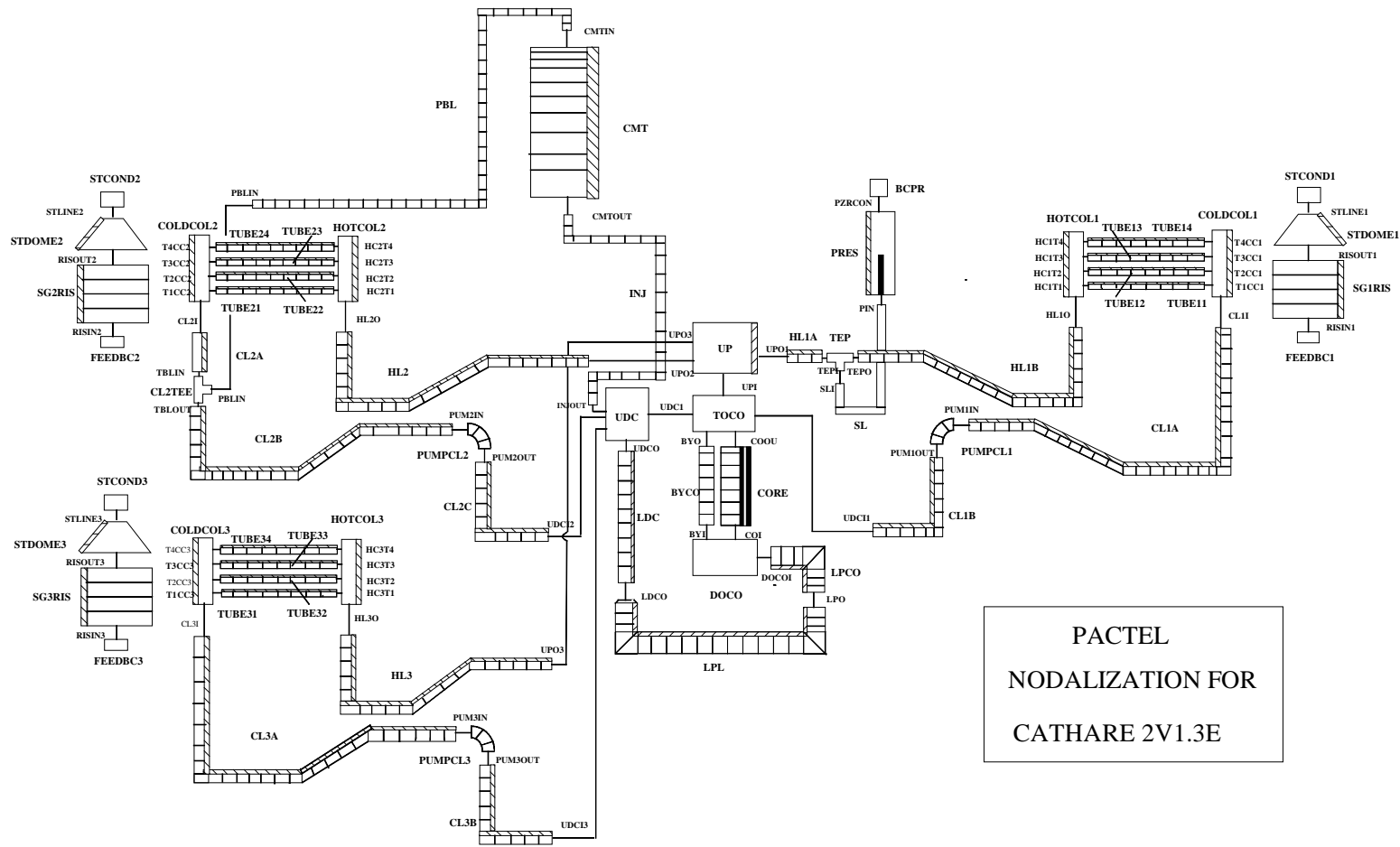


Figure 19. Sketch of the 'initial' PACTEL nodalization for CATHARE 2 v1.3U code, adopted in the analysis of the CMT related experiments.

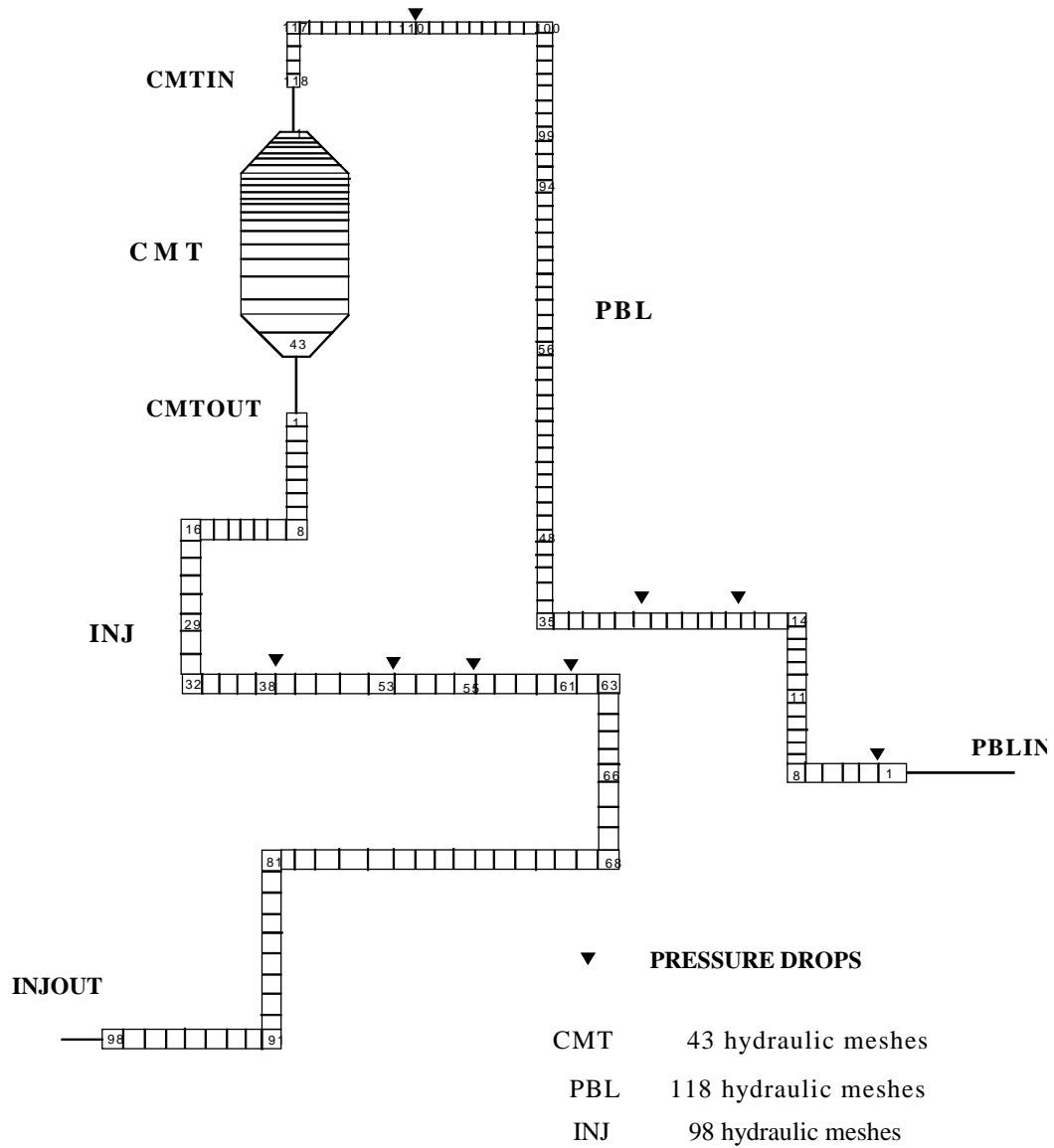


Figure 20. Details related to the CMT loop nodalization ('initial nodalization', see also Figure 19).

Table 10. List of acceptability criteria defined for the qualification at 'steady state' level of a nodalization.

	Quantity	Acceptable error (+)
1	Primary circuit volume	1%
2	Secondary circuit volume	2%
3	Non-active structures heat transfer area (overall)	10%
4	Active structures heat transfer area (overall)	0.1%
5	Non-active structures heat transfer volume (overall)	14%
6	Active structures heat transfer volume (volume)	0.2%
7	Volume vs. height curve (i.e. « local » primary and secondary circuit volume)	10%
8	Component relative elevation	0.01 m
9	Axial and radial power distr. (++)	1%
10	Flow area of components like valves, pumps, orifices	1%
11	Generic flow areas (*)	10%
12	Primary circuit power balance	2%
13	Secondary circuit power balance	2%
14	Absolute press. (PRZ, SG, ACC)	0.1%
15	Fluid temperature	0.5% (**)
16	Rod surface temperature	10 K
17	Pumps velocity	1%
18	Heat losses	10%
19	Local pressure drops	10% (^)
20	Mass inventory in primary circuit	2% (^^)
21	Mass in secondary circuit	5% (^^)
22	Flowrates (prim. and sec. circuit)	2%
23	Bypass mass flowrates	10%
24	Pressurizer level (collapsed)	0.05 m
25	Sec. side or downcomer level	0.1 m (^^)

(+) The % error is defined as the ratio $|\text{reference or measured value} - \text{calculated value}| / |\text{reference or measured value}|$; it is to be added to the experimental uncertainty. The « dimensional » error is the numerator of the above expression.

(++) Additional consideration needed.

(*) With reference to each of the quantities below, following a 100 s « transient-steady state » calculation, the solution must be stable with an inherent drift $< 1\%/100$ s.

(**) And consistent with power error

(^) Of the difference between maximum and minimum pressure in the loop.

(^^) And consistent with other errors

Table 11. PACTEL test GDE-34: comparison between predicted and measured initial conditions.

Parameter	Unit	PACTEL Test GDE-34	CATHARE2 V1.3U Calculation
Primary system:			
Core power	kW	147	147
Pressurizer pressure	MPa	4.33	4.36
Core inlet temperature/CL temperature	°C	213.3	214.6
HL temperature	°C	217.4	222.5
Loop total flow	kg/s	6.22	5.52
Pressurizer level	m	4.92	4.92
Pump speed	rpm	675/667/640	692
Secondary system:			
SD pressure	MPa	2.09/2.10/2.12	2.06
FW flowrates	-	1.53/1.18/1.15 (°)	0.0097 (*)
FW temperatures	°C	-	200.8
SG levels	m	0.718/0.712/0.713	1.507 (**)

(°) l/min

(*) kg/s

(**) The SG were not correctly modeled

4.2.3 RELAP5

The original deck for the analysis was supplied by VTT and was compatible with RELAP5 MOD/3.2. AEA Technology undertook a thorough review of the deck, making modifications to the pressurizer model and adding a model for the CMT and associated pipework.

A critical factor in this work was the nodalisation chosen to ensure appropriate representation of the physics and numerical stability for the solution scheme. More details are given in the RELAP5 analyses reports [42], [43] and [44]. The basic nodalisation is shown in Figure 21. The same version of the code, RELAP5/MOD 3.2.1.2 was used for all the tests. The analyses are presented for three experiments GDE-24, GDE-34 and GDE-43.

The model represented all the main components for the PACTEL rig with the appropriate volumes and their associated heat structures. Active pumps were also included and used in establishing the steady state conditions. The break was modeled as an orifice/valve with the appropriate off-take orientation to the cold leg. Attempts to model the full break tank system led to slow running of the code. It was found to be difficult in the early stages of the project to obtain steady conditions in the pressurizer which was modeled in the original deck with a central core and an annulus. The latter offers a better means of modeling the

recirculation in the pressurizer due to heat losses from the walls. It is now believed that this problem arose because of coding errors which have recently been corrected [45]. For the analyses presented here the pressurizer was modeled as a single pipe. The original model may now be satisfactory and may overcome some of the discrepancy found in modeling test GDE43.

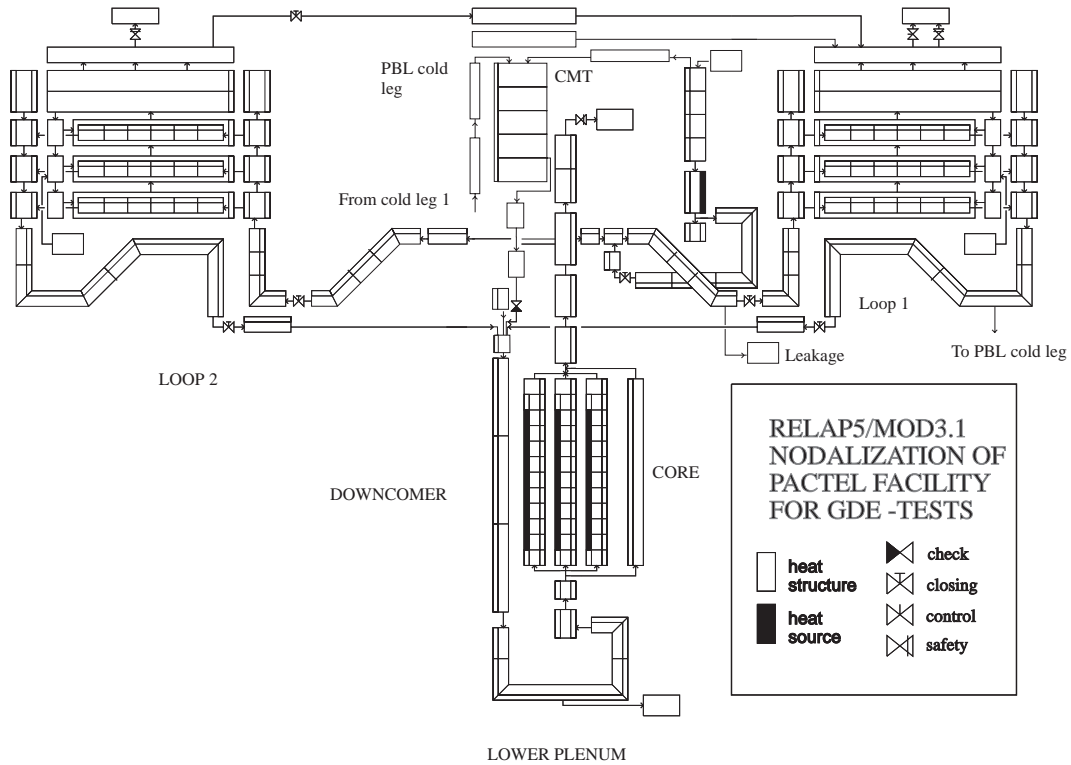


Figure 21. Principle nodalization of the PACTEL rig for GDE analyses (before modifications at the AEA).

Renoding of the hot leg connections to the upper head also proved necessary in the calculation of test GDE43. The downward facing junction with the top of the upper plenum connection allowed vapor to become trapped in the hot leg, between the vessel and the loop seal, which did not occur in the test. The use of cross-flow connections in the mid-level of a revised upper plenum node overcame this problem and gave a much better prediction of the natural circulation flow.

It was also found for test GDE43 that the rate of steam generation in the steam generators was significantly under-predicted and that it was not possible to maintain the secondary side pressure. The source of the problem was found to be a very low prediction of the secondary side heat transfer coefficient, particularly under conditions of natural circulation in the primary side. The code manual indicates that there is a difficulty establishing correct correlations for this and the low coefficient is not inconsistent with figures provided in the manual. Fortunately, the course of the transient is not sensitive to the precise value of the secondary side coefficient so a constant value taken from [46] was set via the input deck.

Additional modeling for this project included adding nodding for the CMT, the pressure balance line and the injection line. As the project progressed the number of hydraulic volumes employed in the modeling of the CMT was increased from 15 to 20. Separate investigations, particularly of the effects of condensation, were performed with the CMT and the associated pipe work being used in a separate deck on a standalone basis.

4.3 COMPARISON OF DIFFERENT CODE PREDICTIONS AGAINST EXPERIMENTS

4.3.1 GDE-24

Experiment description

The GDE-24 experiment was a 3.5 mm cold leg SBLOCA transient with the break located close to the downcomer. The main results of the GDE-24 experiment are presented in the Figure 22 through Figure 30. The main events in the GDE-24 experiment are summarized in Table 12.

The primary pressure dropped rapidly to the hot leg saturation pressure after the break was opened at 1000 seconds. The flow stagnated and the pressure rose when the water level in the upper plenum reached the hot leg elevation. The primary flow resumed after the hot leg loop seals in Loops 1 and 2 were opened and the primary pressure dropped. The pressure in the CMT dropped due to condensation when the injection phase started and steam began to flow to the CMT. Condensation in the downcomer, close to the ECC water injection position, took place when the injection phase ended. Due to this, the primary pressure dropped below the secondary pressure for about 300 seconds.

The first flow peak in the PBL flow measurement occurred when the operators filled the PBL with hot water slightly before they opened the break. When the IL valve was opened, the flow through the PBL was single phase liquid, and the CMT was operating in recirculation mode for about 540 seconds. The injection phase of CMT operation started at about 1570 seconds and ended after 5220 seconds when the CMT became empty.

Water level in the upper plenum remained close to the hot leg connections as long as there was water in the CMT. When the injection from the CMT ended, the upper plenum water level started to drop. Core heat-up took place when the level reached about 5.2 meters. The downcomer remained full of liquid until about 5000 seconds. At that moment, condensation in the downcomer took place, which can be observed as level oscillations in the downcomer.

The water level in the pressurizer dropped slightly when the operators drained water from the PBL. When the operators opened the break, the pressurizer emptied. During the primary flow stagnation, water flowed to the pressurizer but the pressurizer emptied again after the loop seals opened. After about 2100 seconds, water started to fill the pressurizer. Some water stayed in the pressurizer until the end of the experiment.

Code calculation results

APROS and CATHARE simulated the general primary pressure behavior well. APROS pressure oscillated, due to condensation in the CMT. CATHARE pressure rose higher than the measured pressure during the pressure peak. Pressure in the RELAP5 calculation followed the measured pressure until the CMT started to empty and strong condensation in the tank lowered the pressure. In the RELAP5 sensitivity calculations, the condensation rate was artificially reduced which corrected the pressure behavior. The core water level behavior followed the experiment behavior well in the APROS simulation, but dropped too fast in the later phases of the experiment in the CATHARE simulation. The main reasons for this were too high break mass flow rate and the accumulation of water in the pressurizer in the CATHARE calculation. Consequently, the core heat-up began 1200 seconds too early in CATHARE calculation. The core heat-up started 300 seconds too late in APROS simulations. The core water level behavior in the RELAP5 calculation was correct during the first 5000 seconds but the level remained too high after that. The break flow rate was too low. In the RELAP5 calculation, no core heat-up was observed. When the condensation rate was artificially reduced, core water level behavior was correct and the core heat-up occurred after 6000 seconds of transient. The pressurizer level behavior was similar in all calculations. At the end of the simulations, there was about 0,5 m too much water in the pressurizer in the APROS and CATHARE calculations. The pressurizer was almost empty at the end of the transient in RELAP5 simulation and in the experiment. Downcomer flow rate was well simulated during the first 1000 seconds of natural circulation flow after the operators stopped the main circulation pumps. After that, the codes calculated too low a downcomer flow rate. The CMT became empty too late in the APROS and RELAP5 calculations, but the timing was correct in the CATHARE calculation. The levels dropped too slowly due to the fact that the CMT injection flow oscillated strongly, and never reached the full value. The injection flow rate was more stable in the CATHARE calculation, although the injection flow stagnated periodically for some hundreds of seconds. The reduction of the CMT exit nozzle flow area to about 17% of the nominal value was enough to stabilize injection flow in the CATHARE calculation. The calculated water temperature profile in the CMT was not as steep as in the experiment, due to numerical diffusion. APROS and CATHARE calculated the general trend of the CMT pressure well, but the APROS calculations oscillated when the steam condensed in the CMT. The CMT pressure in the RELAP5 calculation followed the experimental behavior nicely during the first 2500 seconds, but the pressure dropped clearly below the measured value after that as too much steam condensed in the CMT. Reduction

of condensation artificially in the CMT corrected the pressure behavior in RELAP5 sensitivity calculations, indicating that the condensation modeling in the code is inadequate.

Table 12. Timing of main events in the GDE-24 experiment and code calculations.

EVENT	TIME (s)			
	EXPERIMENT	APROS	CATHARE	RELAP5
PBL filled with hot water	820-840	805-825	1000	-
Blowdown initiated	1000	1000	1000	1000
Pumps switched off	1000	1000	1000	1000
IL valve opened from low PRZ level	1030	1030	1030	1053
Pressurizer heaters switched off	1040	1040	1040	1053
Primary pressure peak due to flow stagnation (maximum value)	1480	1478	1460	1500
Recirculation phase ended	1570	1620	1520	1800
Break flow two-phase	5110	2900	4770	-
CMT empty	5220	5760	4680	6350
Core heat-up begins	6865	6930	5720	-

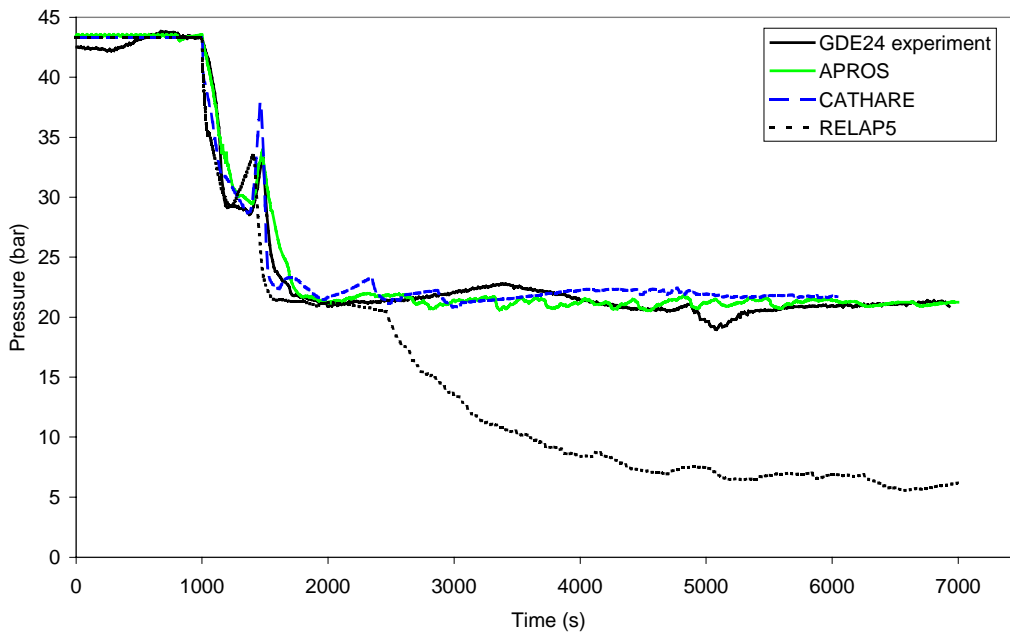


Figure 22. Pressurizer pressure in the simulations of the GDE-24 experiment.

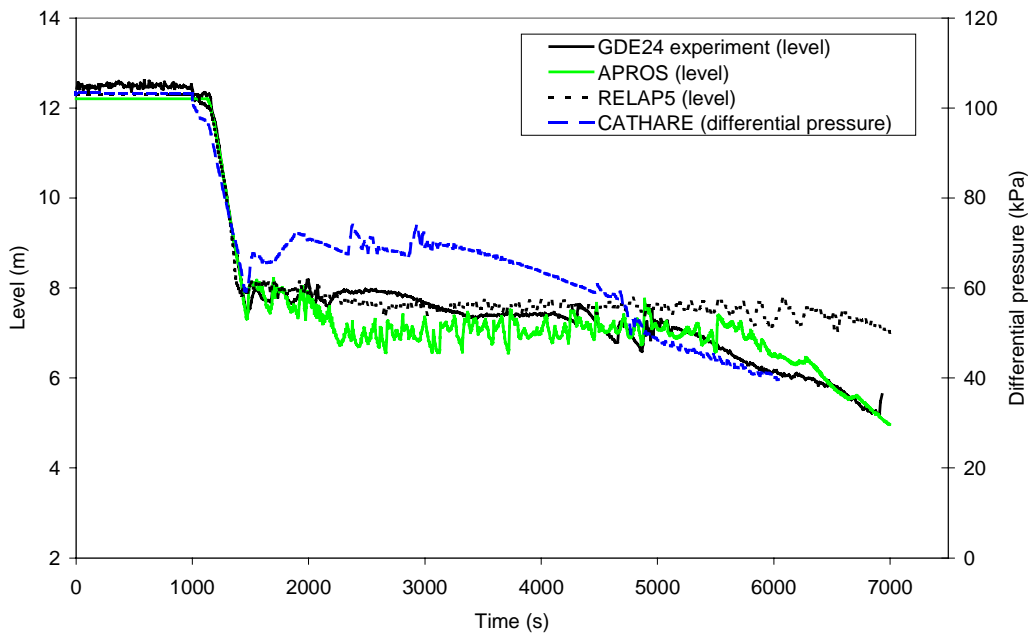


Figure 23. Core water level in the simulation of the GDE-24 experiment.

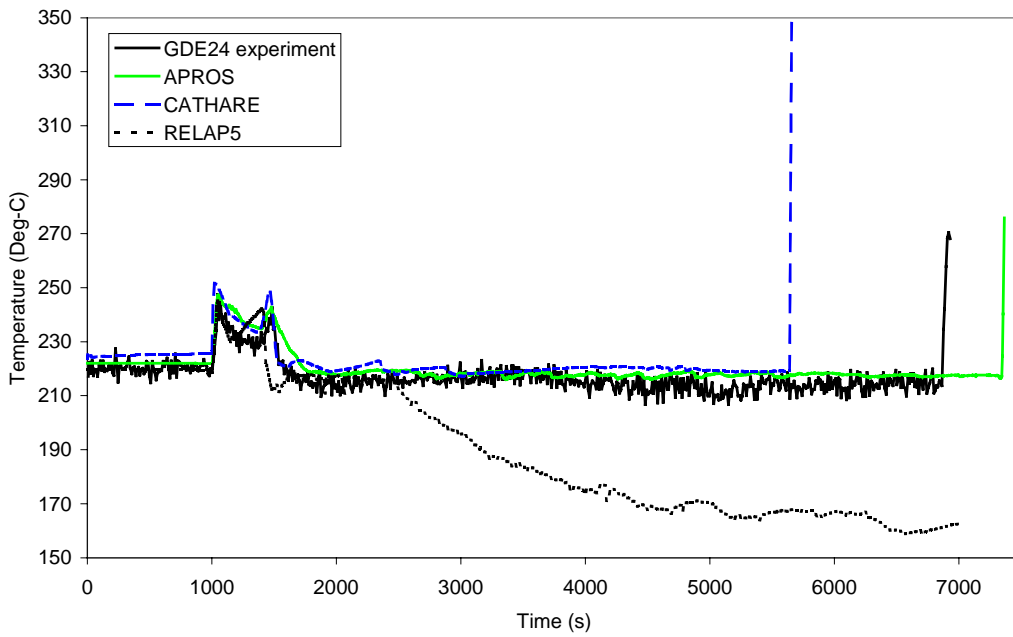


Figure 24. Heater rod cladding temperature at 2010 mm from the core bottom in the simulation of the GDE-24 experiment.

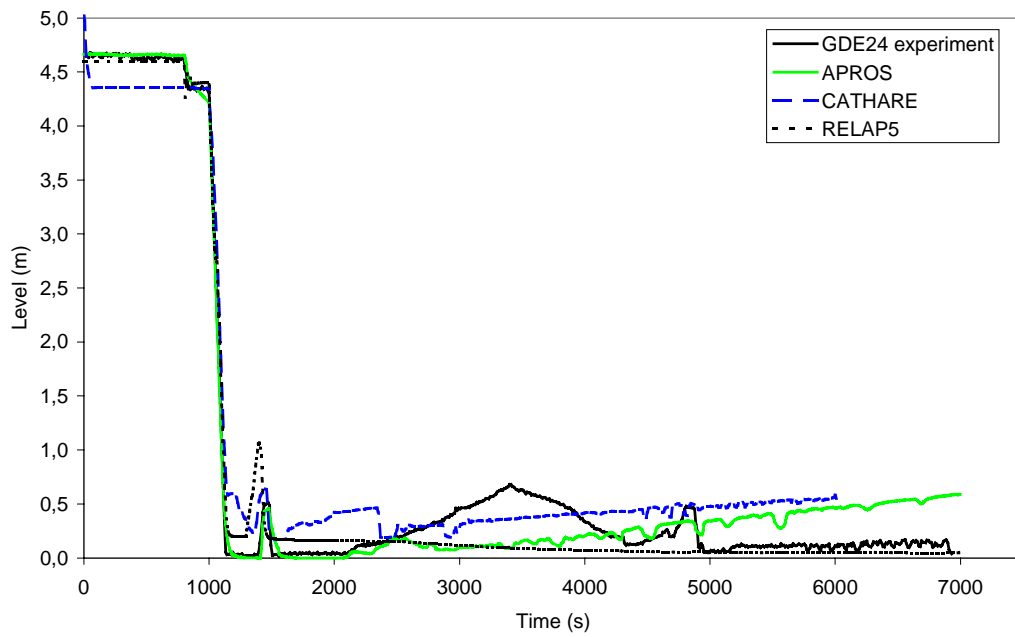


Figure 25. Pressurizer water level in the simulation of the GDE-24 experiment.

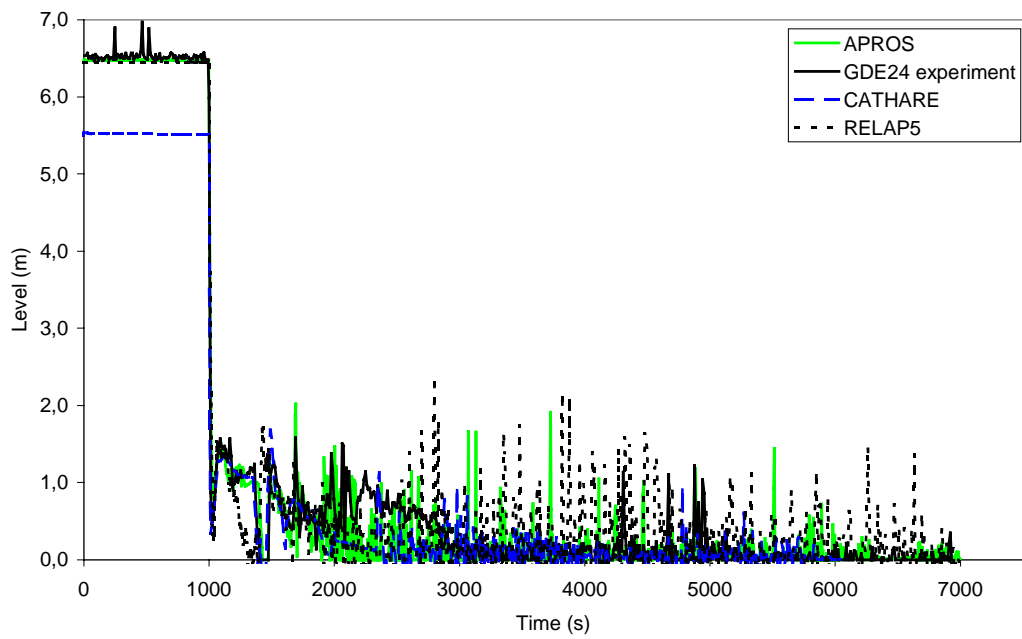


Figure 26. Downcomer mass flow rate in the simulation of the GDE-24 experiment.

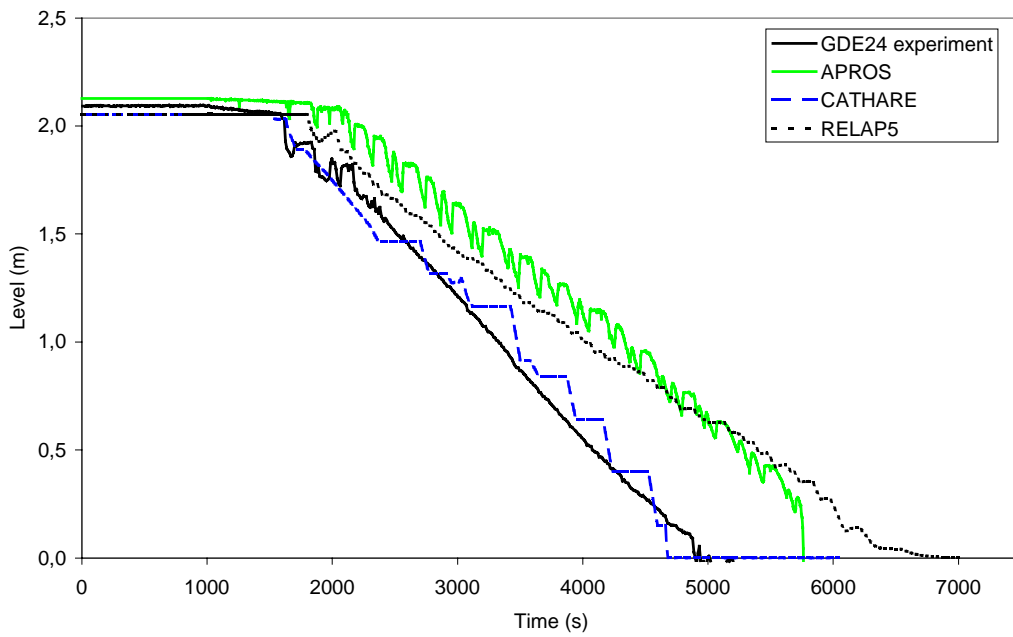


Figure 27. CMT water level in the simulation of the GDE-24 experiment.

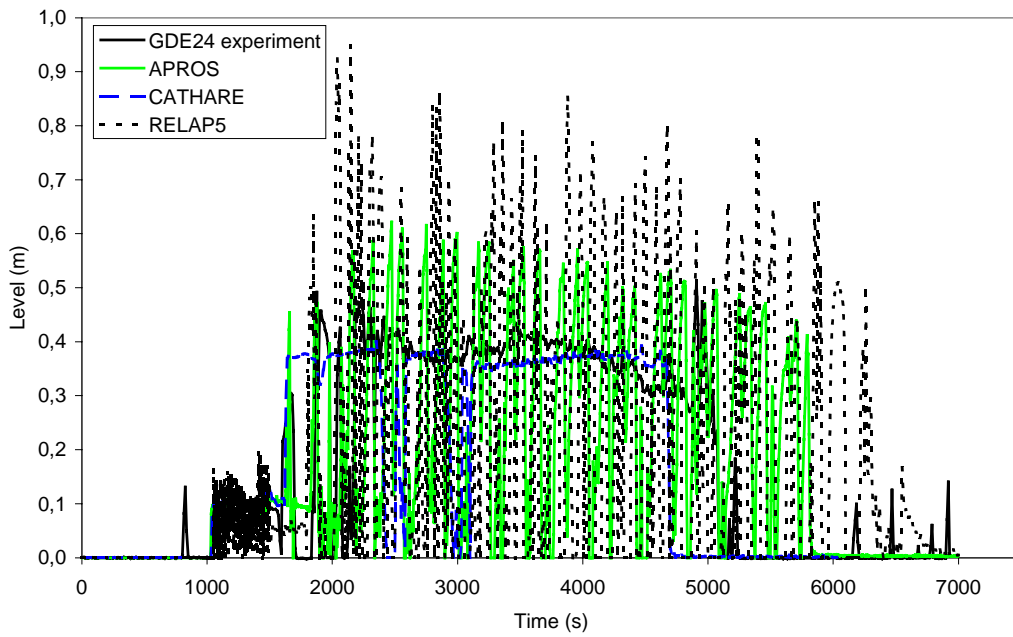


Figure 28. CMT injection line mass flow rate in the simulation of the GDE-24 experiment.

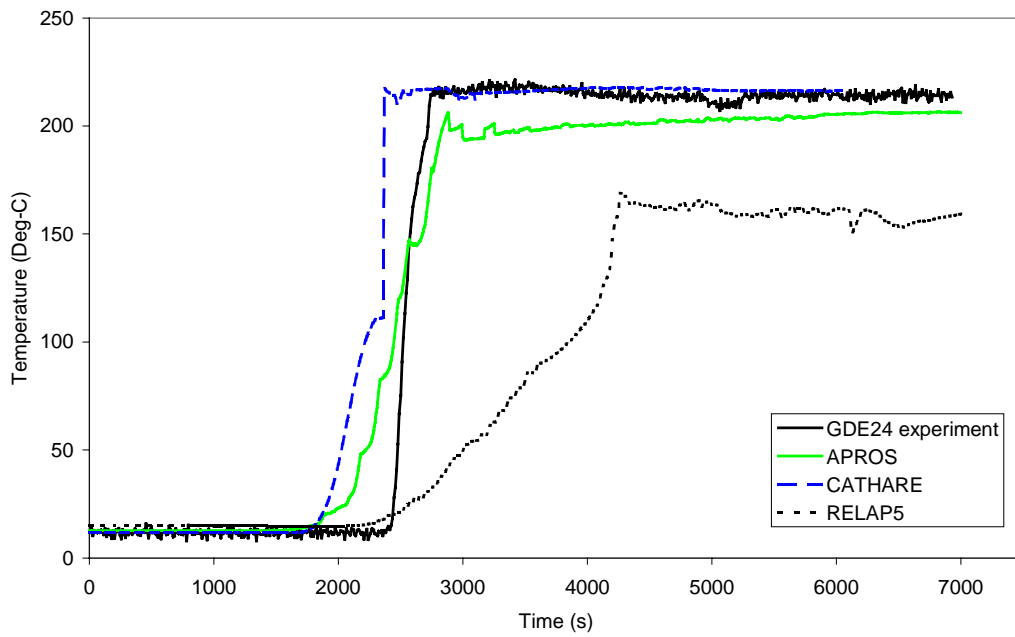


Figure 29. Water temperature at 1405 mm from the tank bottom in the simulation of the GDE-24 experiment.

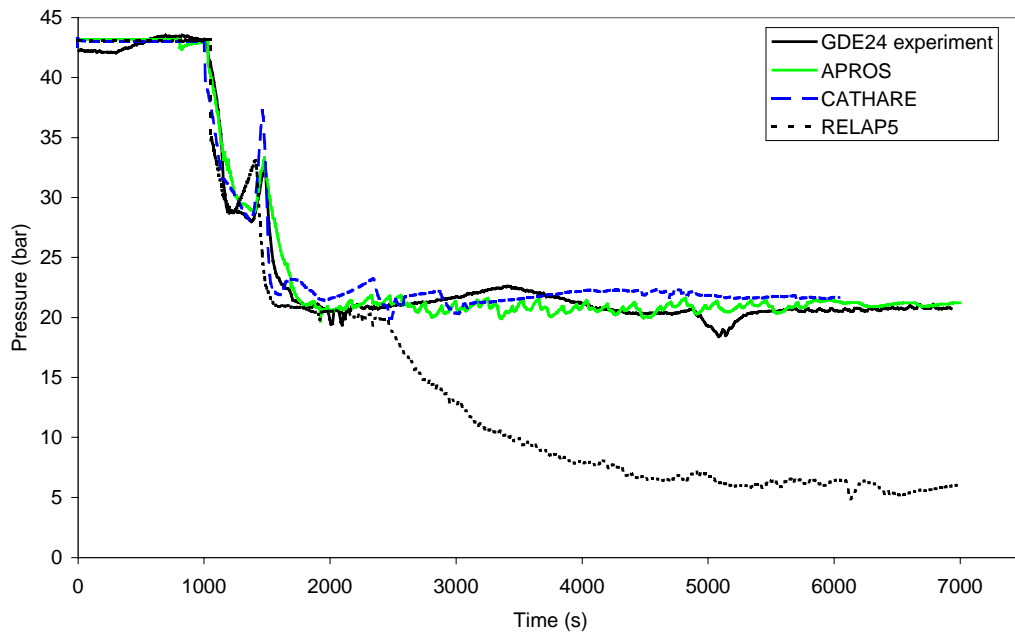


Figure 30. CMT pressure in the simulation of the GDE-24 experiment.

4.3.2 GDE-34

Experiment description

The objective of GDE-34 experiment was to investigate the PSIS behavior when the CMT is initially full of hot water. The CMT may become full of hot water during normal operation of the plant, if the IL check valve leaks. The break size was 3.5 mm in diameter. The break was located in the cold leg close to the downcomer. Figure 31 through Figure 39 presents the main results of the GDE-34 experiment. Table 13 summarizes the main events in the GDE-34 experiment.

The primary pressure dropped rapidly to the hot leg saturation pressure after the operators opened the break. The primary flow stagnated when the water level in the upper plenum reached the hot leg elevation. The primary flow resumed after the hot leg loop seals opened. Since the CMT was initially full of hot water, there was very little condensation in the CMT during the experiment. The hot leg water temperature followed the saturation temperature. The fuel rod cladding temperature rose at the end of the experiment, when the CMT became empty and the core water level dropped so much that the top of the core uncovered.

The first flow peak in the PBL flow measurement occurred when the operators filled the PBL with hot water slightly before the break opening. Since there was no density difference between the PBL and the IL, there was no recirculation flow through the PSIS. The injection phase of CMT operation started, however, when the water level in the Loop 2 cold leg dropped below the PBL connection position. The CMT became empty faster than in the GDE-31 experiment with cold water in the CMT.

Water level in the upper plenum remained close to the hot leg connections as long as there was water in the CMT. When the injection from the CMT ended, the upper plenum water level started to drop. Core heat-up took place when the level reached about 4.6 meters. The downcomer remained full of liquid until about 4000 seconds.

The water level in the pressurizer dropped slightly when the operators drained water out from the PBL. The pressurizer emptied when the operators opened the break. During the flow stagnation, water flowed to the pressurizer but the pressurizer emptied again after the loop seals opened. After about 2500 seconds, water started to fill the pressurizer. Some water stayed in the pressurizer until the end of the experiment.

Code calculation results

All codes calculated the primary pressure behavior well, although the pressure peak occurred too early in the RELAP5 calculation and the pressure dropped too slowly in the APROS simulation. The core water level dropped too fast in the calculations and the core heated up too early. The pressurizer level behavior and

the break flow in the CATHARE calculation did not differ substantially from the measured values. One reason for the early core heat-up in the CATHARE calculation was the incorrect coolant distribution in the primary circuit. The pressurizer water level behavior was well predicted in the CATHARE and RELAP5 calculations, but too much water accumulated in the pressurizer at the end of the transient in the APROS calculation. The codes calculated the downcomer flow and the CMT emptying well. All the codes predicted recirculation flow, which did not occur in the experiment. The recirculation flow oscillated and stopped periodically in the RELAP5 calculation, but did not stop completely. The CMT injection flow was oscillating in the APROS and RELAP5 calculation, but the injection rate average value was close to the measured flow. The CMT water temperature behavior was nicely followed in the code calculations, although numerical diffusion smoothed the temperature profile. Condensation in the CMT led to oscillations in the CMT pressure in the APROS calculation, but the oscillations were smaller than in the GDE-24 calculation.

Table 13. Timing of main events in the GDE-34 experiment and code calculations.

EVENT	TIME (s)			
	EXPERIMENT	APROS	CATHARE	RELAP5
PBL filled with hot water	820-840	825-875	1000	-
Blowdown initiated	1000	1000	1000	1000
Pumps switched off	1000	1000	1000	1000
Pressurizer heaters switched off	1030	1040	1030	1032
IL valve opened from low PRZ level	1040	1040	1040	1043
Primary pressure peak due to flow stagnation (maximum value)	1474	1499	1460	1394
Recirculation flow through the PSIS	none	1040-1650	1040	-
CMT Injection phase began	1480	1860	1790	1720
CMT empty	1570	3750	3620	3720
Break flow two-phase	5110	4010	4285	-
Core heat-up begins	5220	4700	4455	4560

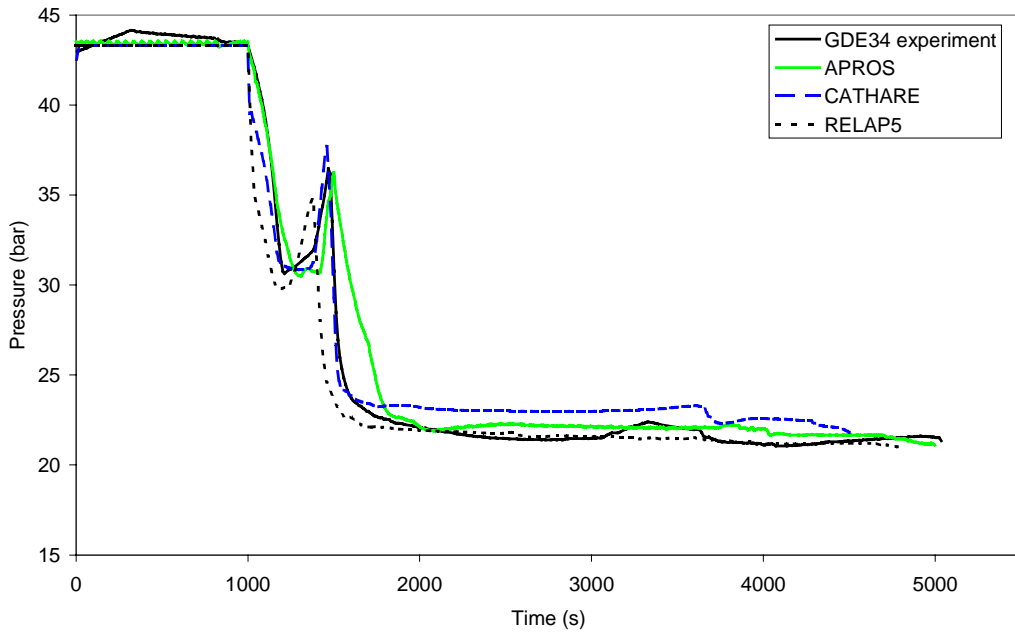


Figure 31. Pressurizer pressure in the simulation of the GDE-34 experiment.

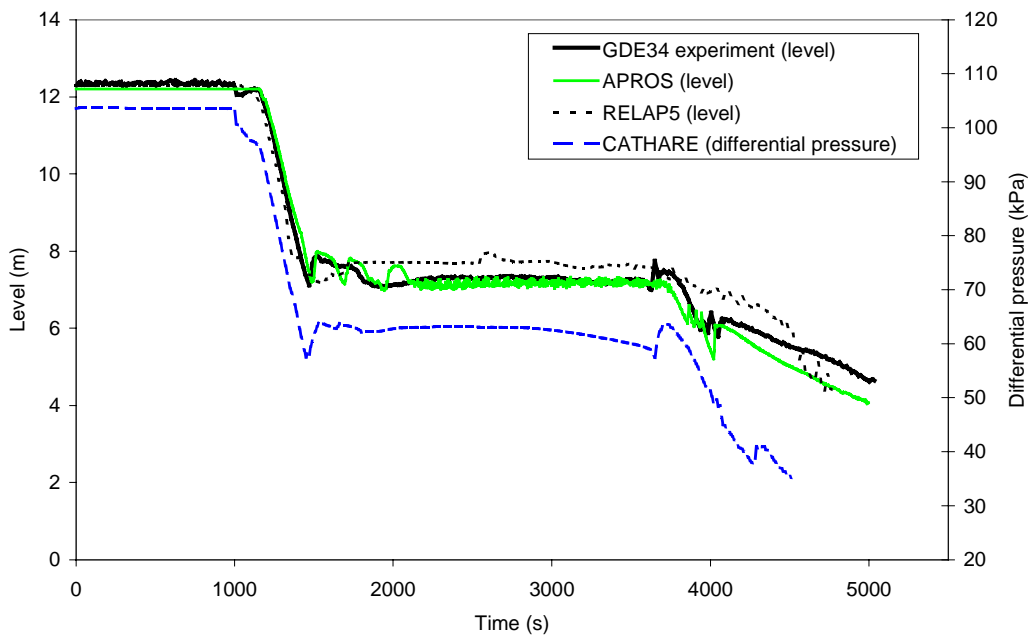


Figure 32. Core water level in the simulation of the GDE-34 experiment.

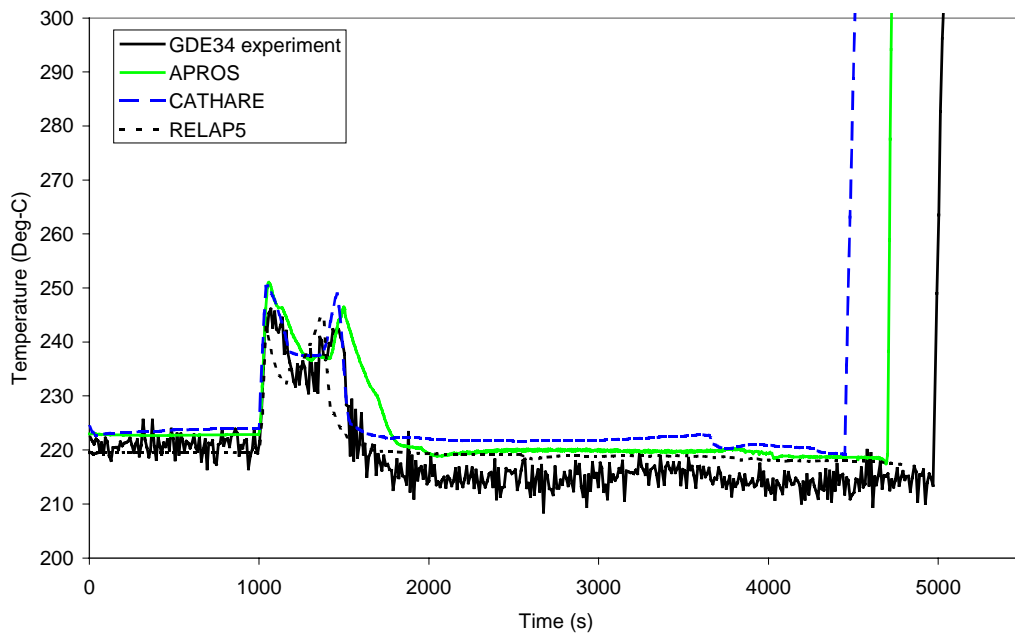


Figure 33. Heater rod cladding temperature at 2010 mm from the core bottom in the simulation of the GDE-34 experiment.

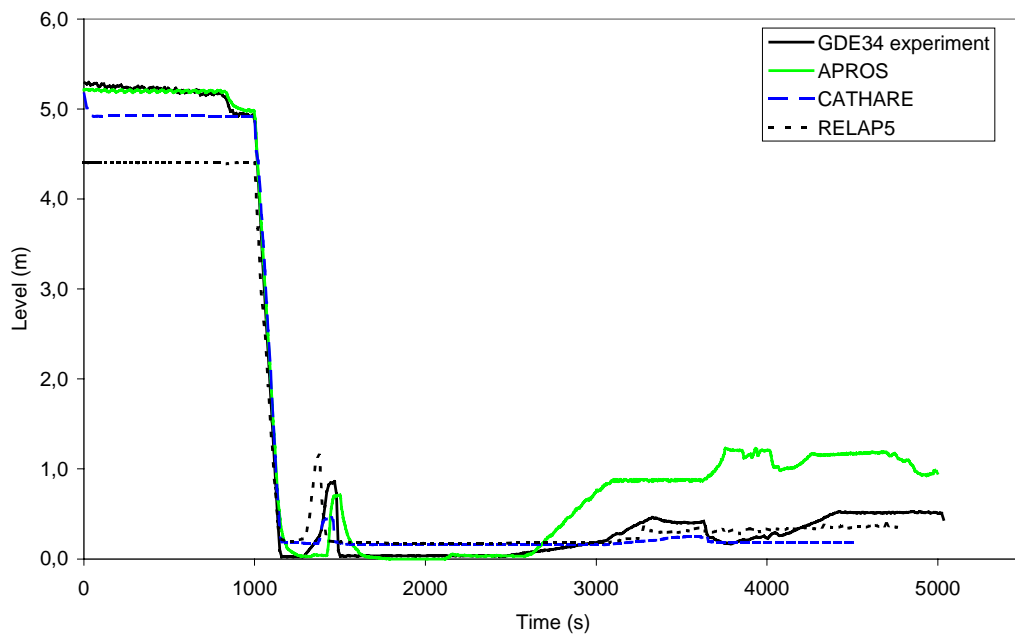


Figure 34. Pressurizer water level in the simulation of the GDE-34 experiment.

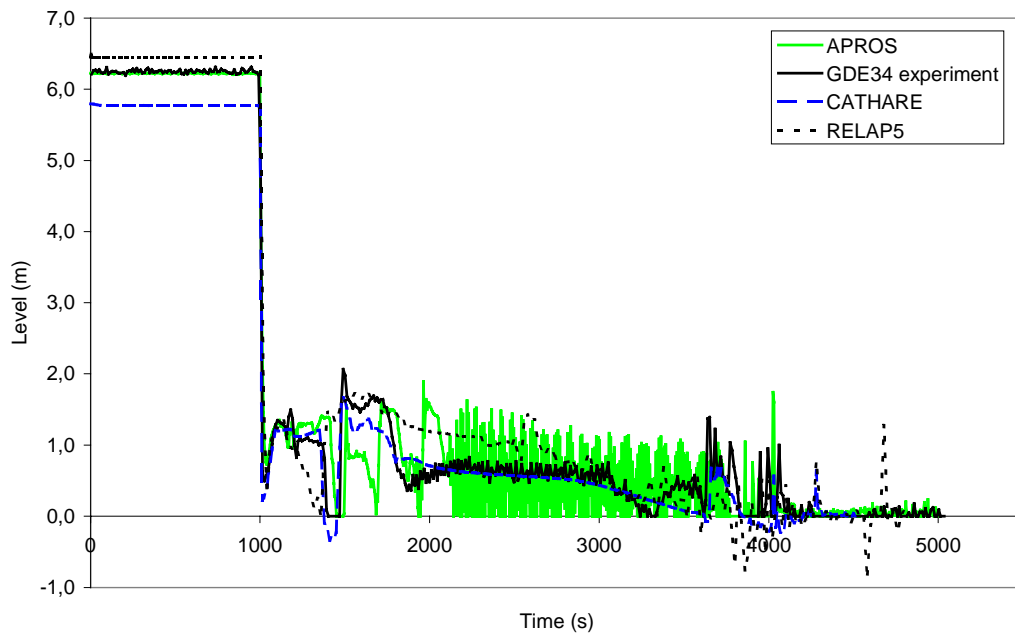


Figure 35. Downcomer mass flow rate in the simulation of the GDE-34 experiment.

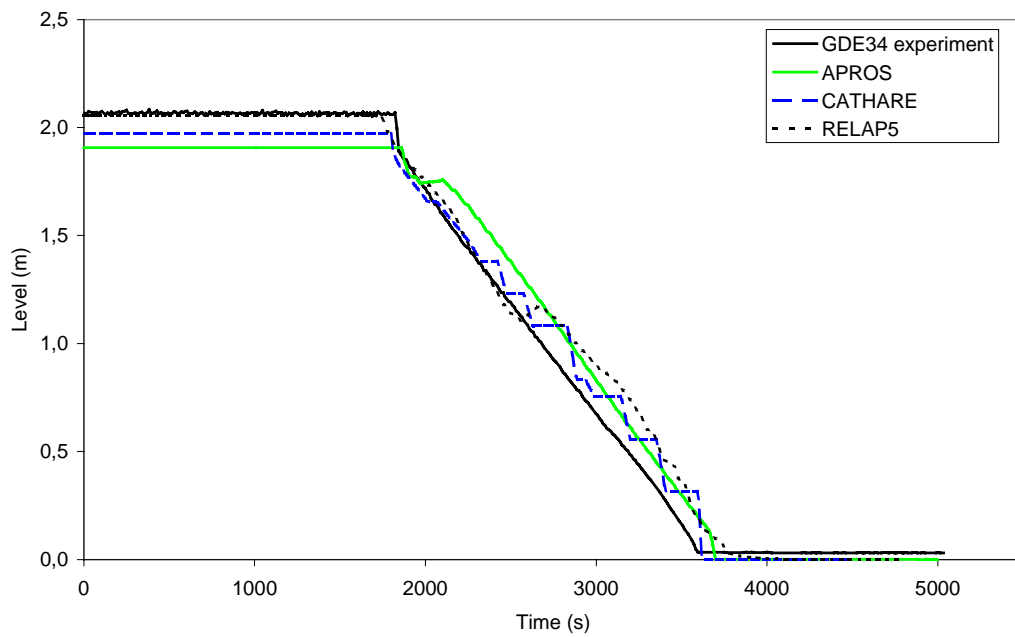


Figure 36. CMT water level in the simulation of the GDE-34 experiment.

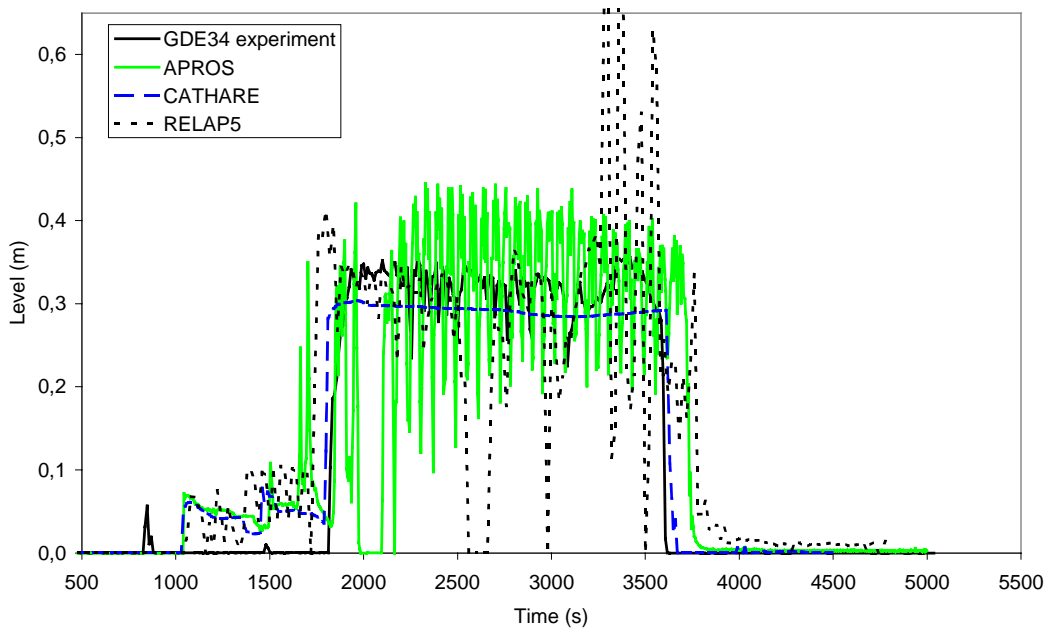


Figure 37. CMT injection line mass flow rate in the simulation of the GDE-34 experiment.

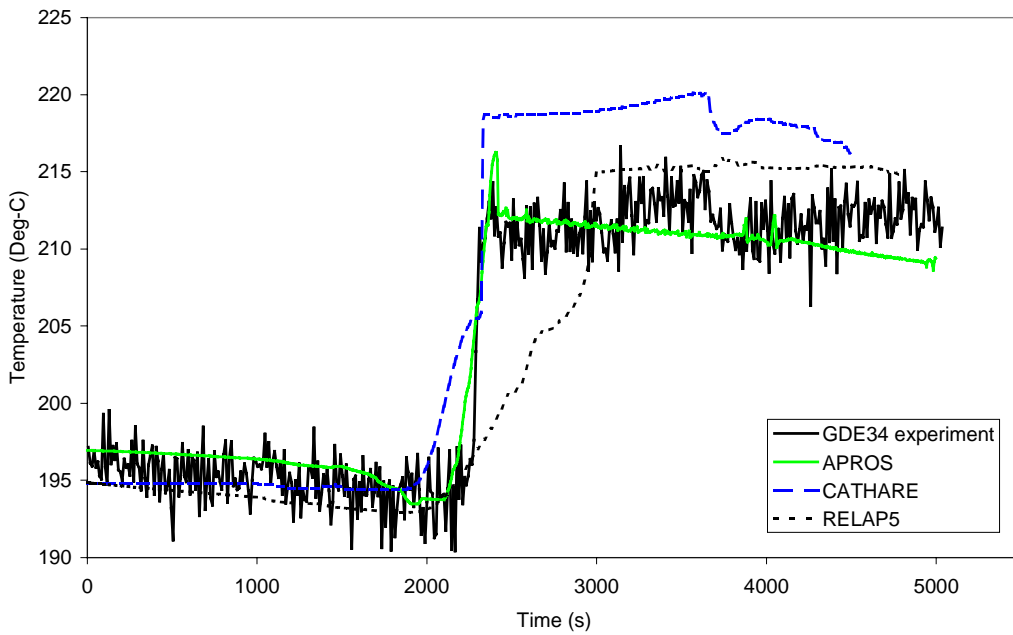


Figure 38. Water temperature at 1405 mm from the tank bottom in the simulation of the GDE-34 experiment.

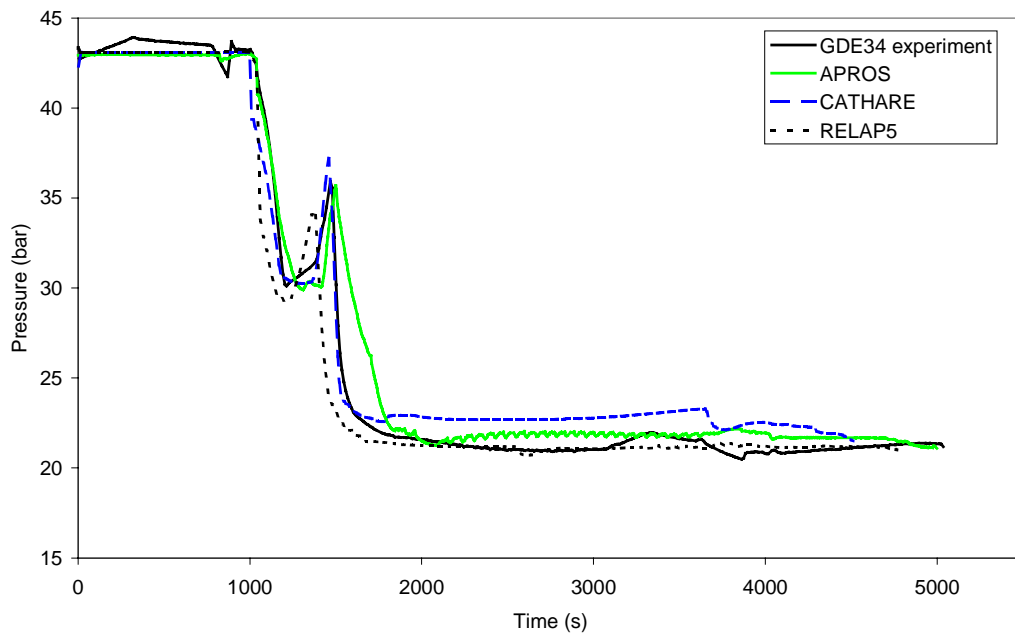


Figure 39. CMT pressure in the simulation of the GDE-34 experiment.

4.3.3 GDE-43

Experiment description

The objective of the GDE-43 experiment was to investigate the PSIS behavior in a situation, when the break size is small and, consequently, CMT recirculation phase is long. If the CMT recirculation phase is long, the whole PSIS may become full of hot water before the CMT begins to inject water, and the driving force for injection disappears. This may have effects on the beginning of safety injection from the CMT. In the GDE-43 experiment, the break was located in the Loop 2 cold leg close to the downcomer. The break size was 1.0 mm in diameter. Figure 40 through Figure 48 present the main results of the GDE-43 experiment. Table 14 summarizes the main events in the GDE-43 experiment.

The primary pressure started to drop slowly after the operators opened the break. The primary flow stagnated several times, which was the reason for the pressure peaks after 6500 seconds. During the last two pressure peaks, the operators had to open a drain valve in the upper plenum four times to keep the primary pressure below the maximum operation pressure of the loop. The water temperature in the upper plenum followed the hot leg saturation temperature. The core inlet temperature dropped during the flow stagnation period, when the heat losses cooled the loop. The temperature also dropped when the cold water from the CMT flowed to the downcomer and the lower plenum. The filling of the PBL with hot water slightly before the break opening was the reason for the first flow peak in the PBL flow measurement. When the operators opened the IL valve, the flow through the PBL was single-phase liquid. The PBL flow rate slowly decreased as

hot water filled the CMT during the recirculation phase. The recirculation flow stopped completely at 9800 seconds when the whole CMT and IL became full of hot water, and the driving force for CMT flow disappeared. The CMT flow remained stagnated for about 2800 seconds. The CMT started to inject water at about 11 600 seconds, when the water level in the cold leg dropped below the PBL connection.

The operators kept the water level in the steam generator secondary side above the horizontal heat exchange tubes during the whole experiment. Water level in the upper plenum dropped to the hot leg elevation at about 6500 s and remained there until the end of the experiment. The downcomer remained full of water throughout the whole experiment. The pressurizer level dropped after the opening of the break and the pressurizer became empty at 2980 s. The pressurizer level started to rise again and the level reached 4.4 m during the primary flow stagnation period. The pressurizer became empty again when the primary flow resumed. The pressurizer level was rising slightly during the last part of the experiment. The operators terminated the experiment at 15 000 seconds before the core started to heat up.

Code calculation results

The first pressure peak occurred too early in the APROS and CATHARE calculations and too late in the RELAP5 simulation. In the APROS calculation, one additional pressure peak was observed after the pressure had already started to drop in the experiment. The core water level dropped too fast in the APROS and CATHARE simulations in the early phase of the transient and the codes did not predict core water level lowering during the PSIS flow stagnation. The core water level was too high in the RELAP5 simulation in the early part of the transient, which was the reason for the delayed pressure peaks. Too much water accumulated in the pressurizer in the all calculations during the primary stagnation period. At the end of the transient, too much water accumulated in the pressurizer in the APROS and CATHARE simulations but too little in the RELAP5 calculation. The accumulation of water in the pressurizer partly explains the fact that the flow stagnation did not occur in the APROS and CATHARE calculations. The codes simulated the general trend of the downcomer flow behavior well. The CMT started to empty too early in the APROS and CATHARE calculations. This happened since too much water flowed into the pressurizer and the steam begun to flow to the cold legs too early. The recirculation flow through the PSIS decreased as the hot water filled the CMT in the APROS and CATHARE calculations, but the flow did not stop completely. The calculated recirculation flow at the end of the recirculation phase was about 50% of the initial value in CATHARE and about 75% of the initial value in the APROS calculation. The recirculation flow stagnated in the RELAP5 calculation and the stagnation lasted from 8560 to about 12 700 seconds. The core water level dropped at the end of the flow stagnation period in the RELAP5 calculation, but the heater rod temperatures did not start to rise. The affects of numerical diffusion were clear in the APROS and CATHARE calculation of CMT water temperature. The temperature rise was sharper in the

RELAP5 simulation. The CMT pressure did not oscillate in the APROS simulation, since the tank was full of hot water when steam began to flow into it. All the codes calculated the general CMT pressure behavior well.

Table 14. Timing of main events in the GDE-43 experiment code calculations.

EVENT	TIME (s)			
	EXPERIMENT	APROS	CATHARE	RELAP5
PBL filled with hot water	835-875	835-875	1000	
Blowdown initiated	1000	1000	1000	1000
Pumps switched off	1000	1000	1000	1000
Pressurizer heaters switched off	1565	1565	1565	1584
IL valve opened from low PRZ level	1565	1565	1565	1584
Primary pressure peaks due to flow stagnation (maximum value)				
first	6780	6610	6315	7719
second	7000	6830	6560	8000
third	7220	7070	6780- 7000	8315
fourth	7450	7390	7200	8631
fifth	7670	7520	7435- 7650	8982
sixth	7910	7696	7880	9298
Upper plenum relief valve opened				
first	7670	7520	7200	-
second (valve opened three times)	7910-7930	7700, 7940	7435- 7880	-
Recirculation flow stagnation	9830-11640	none	none	8561 - 12702
CMT Injection phase began	11640	10000	11335	12702

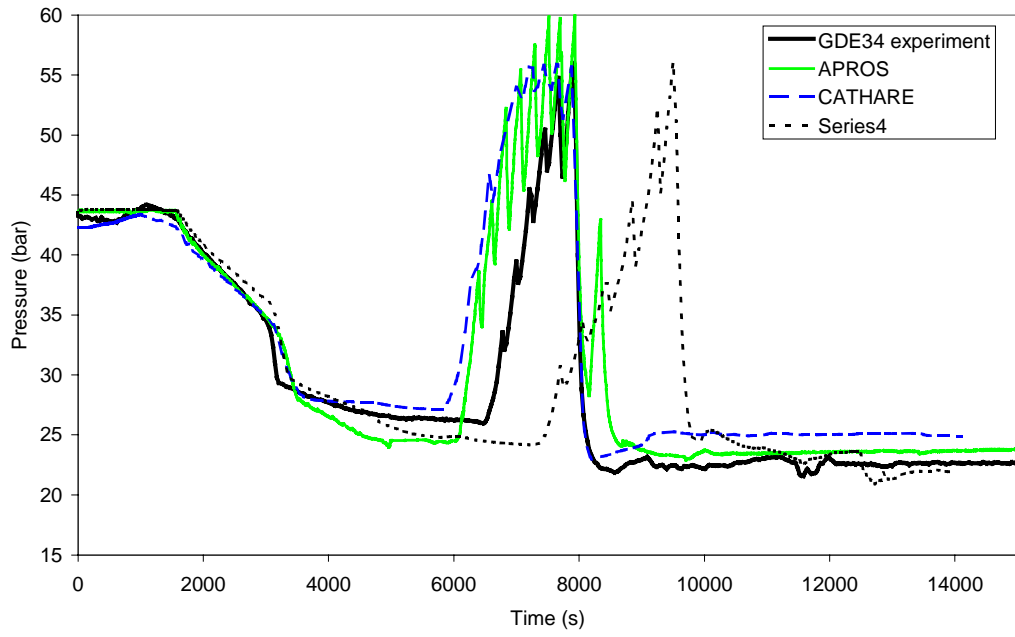


Figure 40. Pressurizer pressure in the simulation of the GDE-43 experiment.

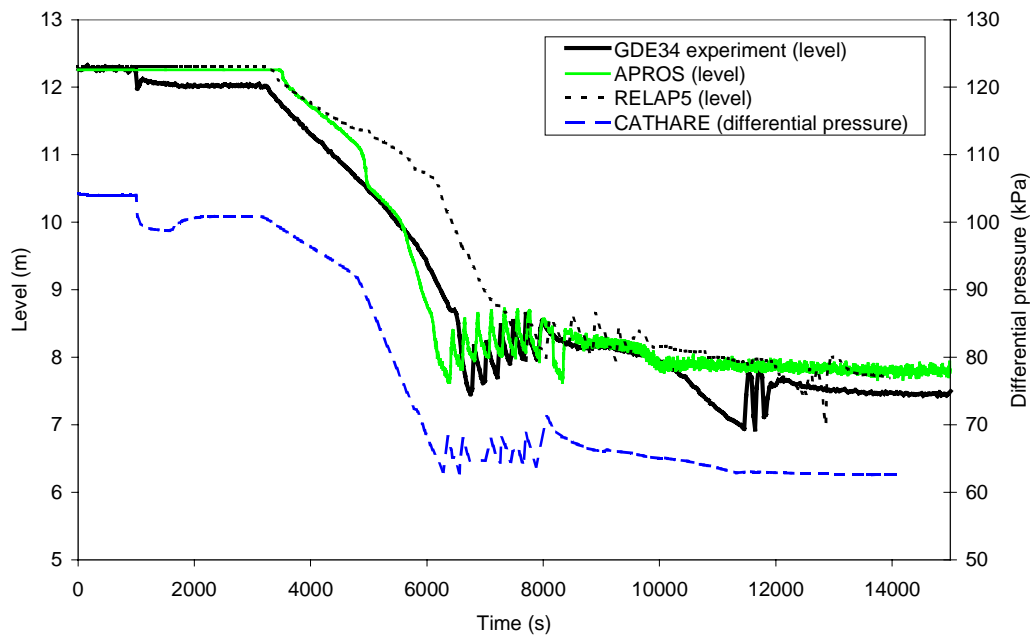


Figure 41. Core water level in the simulation of the GDE-43 experiment.

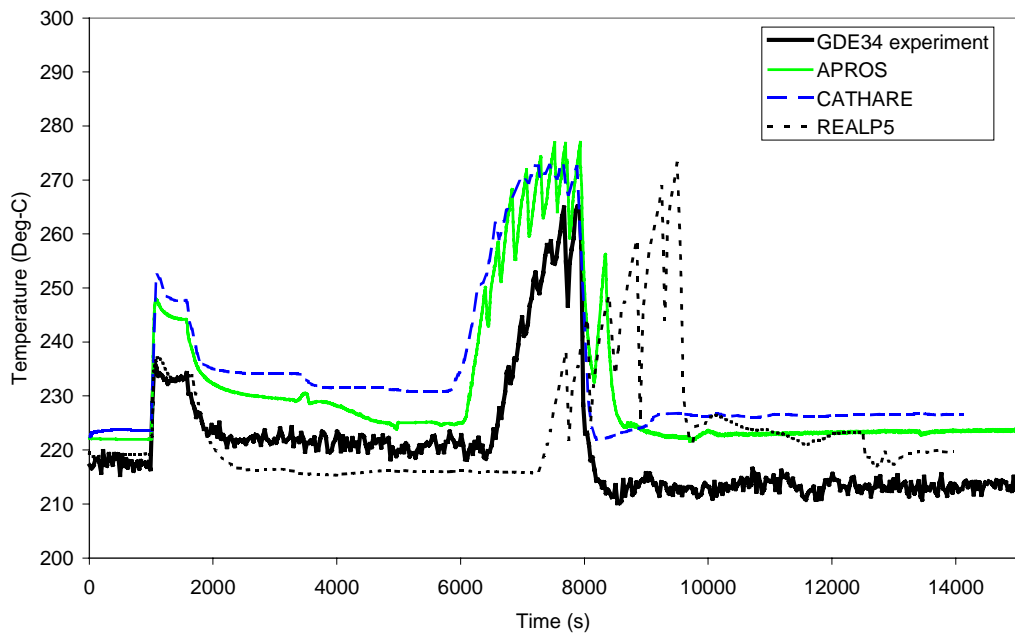


Figure 42. Heater rod cladding temperature at 2010 mm from the core bottom in the simulation of the GDE-43 experiment.

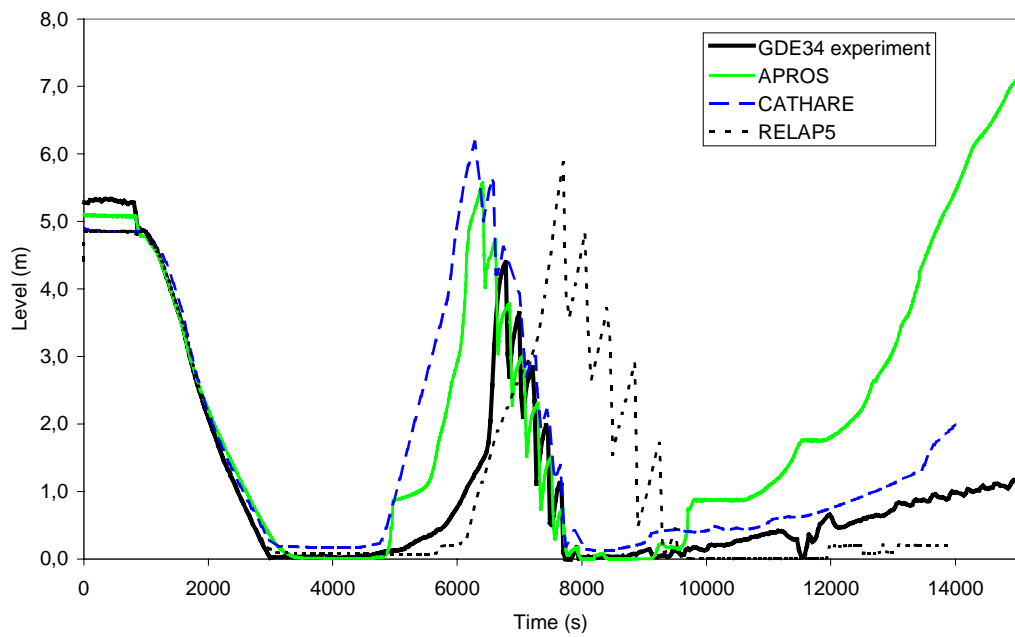


Figure 43. Pressurizer water level in the simulation of the GDE-43 experiment.

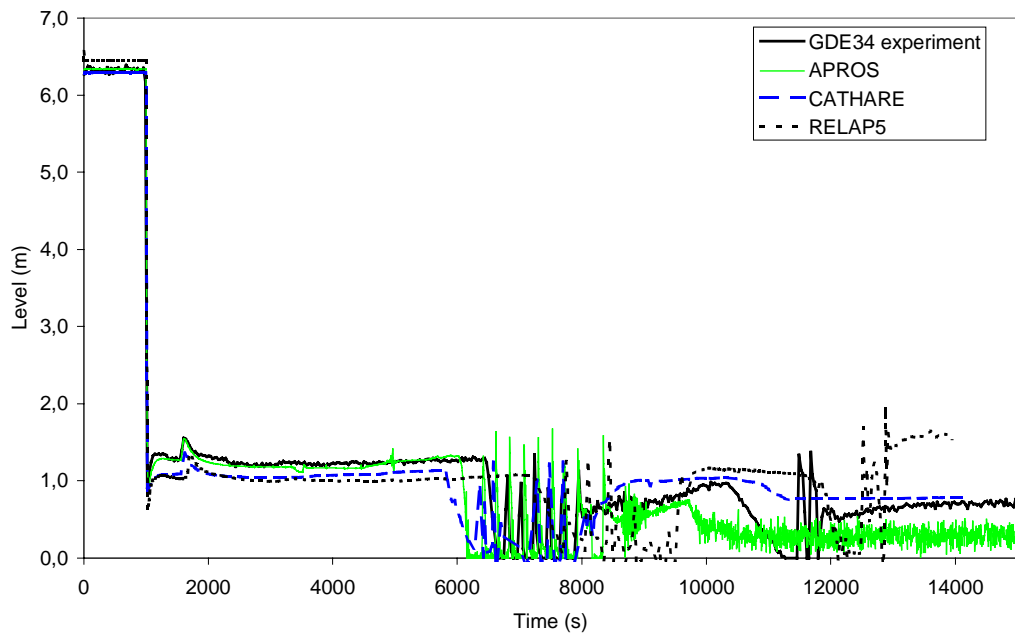


Figure 44. Downcomer mass flow rate in the simulation of the GDE-43 experiment.

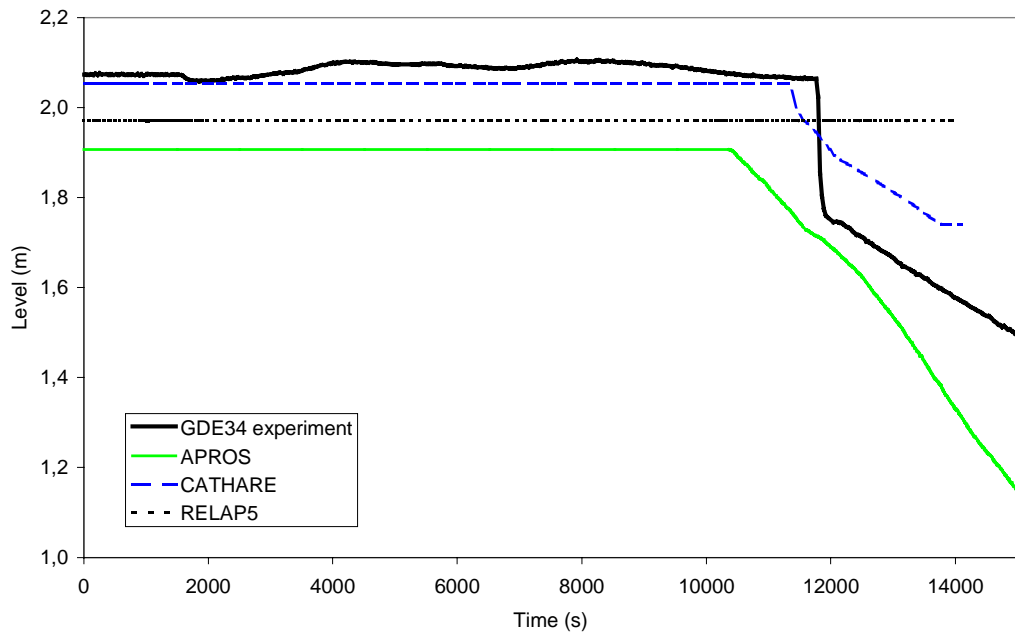


Figure 45. CMT water level in the simulation of the GDE-43 experiment.

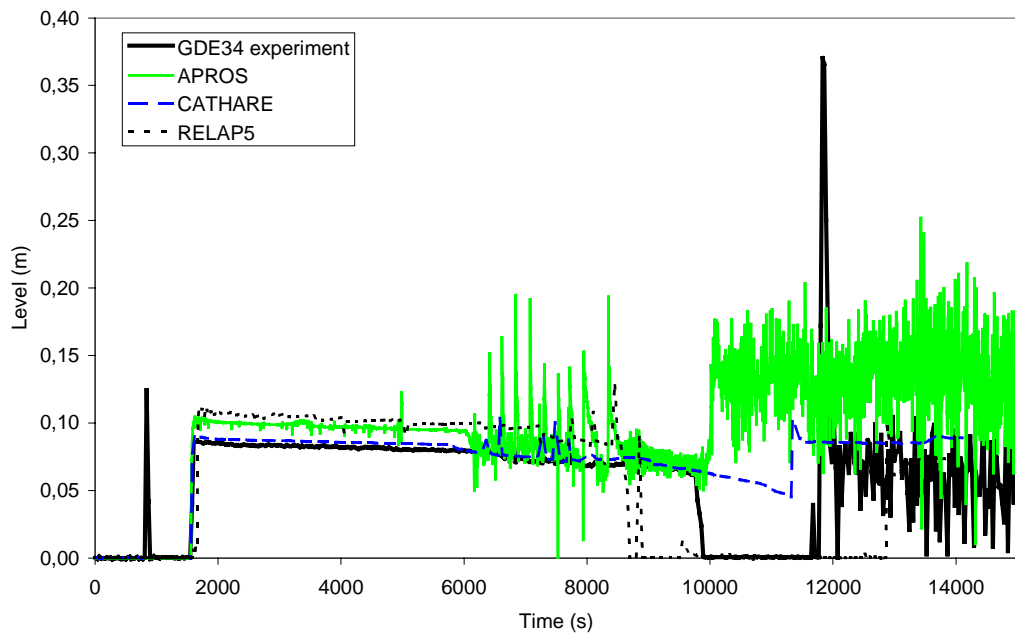


Figure 46. CMT injection line mass flow rate in the simulation of the GDE-43 experiment.

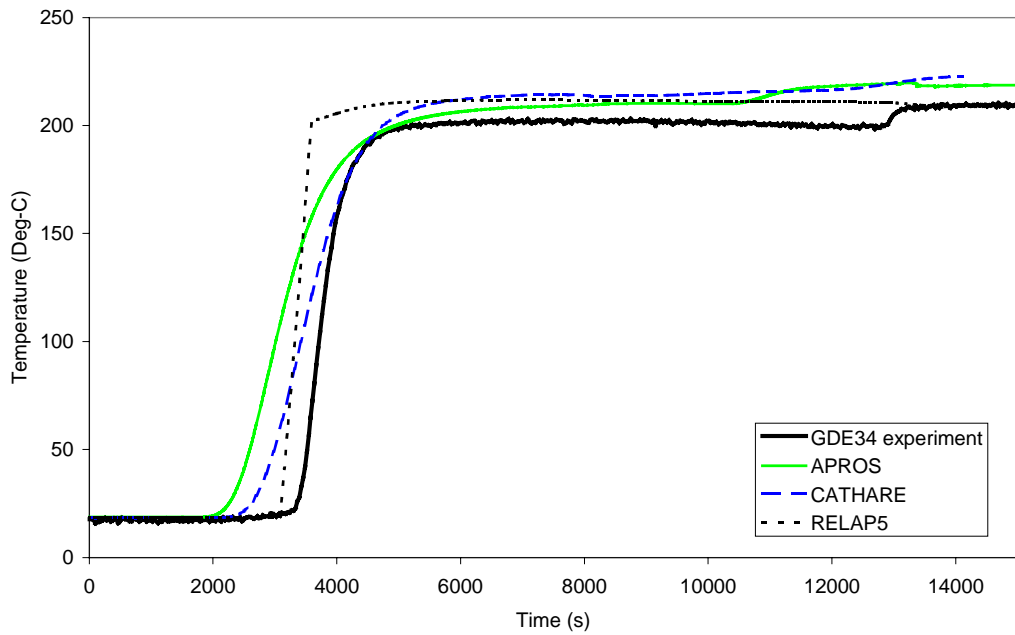


Figure 47. Water temperature at 1405 mm from the tank bottom in the simulation of the GDE-43 experiment.

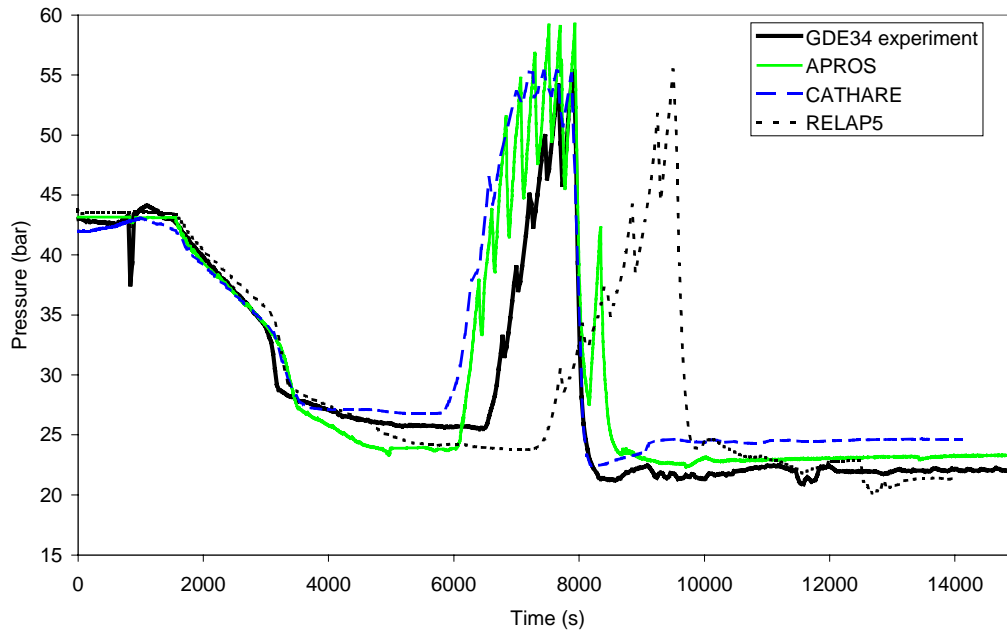


Figure 48. CMT pressure in the simulation of the GDE-43 experiment.

4.4 CONCLUSIONS FROM THE CALCULATIONS

4.4.1 APROS

Conclusions

From the APROS calculation results, the following conclusions can be drawn:

- 1) The code was able to predict the main transients in the primary side.
- 2) The prediction of the time for core heat-up was within the measurement uncertainties i.e. within the difference observed between the two repeated experiments.
- 3) The injection flow oscillated due to condensation in the CMT. The flow was more accurately predicted when the CMT was initially filled with hot water.
- 4) The heat losses became more important in the simulations of long transients. Especially, the heat losses from the pressurizer were important for the distribution of coolant in a long transient calculation.
- 5) Numerical diffusion led to smoothing of temperature profile in the CMT and to too high a condensation rate in the tank. Hence, it was the main reason for problems in the CMT calculation.

4.4.2 CATHARE

The CATHARE2 V1.3U code was fully able to calculate the overall scenario measured in the PACTEL facility. Discrepancies between measured and

calculated trends are mostly due to well known reasons also resulting from the analysis of other integral loop experiments. Three main sources of discrepancies can be identified:

- the distribution of pressure drops plays a role in the prediction of CMT related flowrate;
- the underestimation of heat losses to the environment (the right values of heat losses²⁴, supplied in the communication, were not included in the utilized input deck specifically considering their small effect upon the main phenomenon object of the investigation, e.g. the CMT performance); the consequence of this is the early prediction of the dryout occurrence in tests GDE-24 and GDE-34 [47], [48] and [49].
- the behavior of the secondary sides of the steam generators (mainly in test GDE-43, ref. [50]): the control system adopted in the experiment was not fully simulated.

The only code limitation identified is of general (and well known) type: during the draining period of the CMT, owing to the donor cell principle, hot liquid can move downstream in the cold liquid region. The result is the prediction of a much smoother fluid temperature gradient inside the CMT than measured in the experiment. However the range of parameters involved is not such as to cause important discrepancies between measured and calculated trends. The same can be said regarding the misprediction of the CMT loop behavior: even if a recirculation phase is poorly predicted by the code (tests GDE-34 and GDE-43), the overall prediction is quite satisfactory.

All the above conclusions are applicable if a "reasonable" noding scheme is considered. 43 nodes for the CMT were used (i.e. average node length equal to 0.05 m). In some cases, the "slice" nodalization concept has also been adopted: nodes at the same elevation in different parts of the loop have also the same height (this led to having 256 nodes for the CMT loop). In some of the sensitivity calculations, the number of meshes in the non-horizontal parts of the PBL has been doubled: the results are slightly improved, mainly concerning the draining flowrate, but the recirculation phase is not prevented.

Finally, the situation in the CMT does not appear ideal for the assessment of the fluid-to-wall condensation heat transfer coefficient; only a very rough assessment can be made considering that the heat transfer is limited by the heat losses to the environment (not by the condensation).

4.4.3 RELAP5

GDE-24 experiment

The GDE-24 experiment included a 3.5 mm cold leg break. The main objective was to investigate CMT behavior and in particular the effects of thermal stratification and condensation in the CMT.

Results from calculations representing the full transient are shown in this report, Figure 22 through Figure 29. The main features, however, are evident from the pressure response and the injection flow.

In the reference calculation there was a significant fall of pressure which occurred as the core make-up tank started to empty. In a sensitivity calculation the rate of condensation in the core make-up tank was artificially reduced and it was found that the results followed the experimental data almost precisely. This highlighted some inadequacy in the wall condensation modeling in the RELAP5 code.

A study of how the code calculated the heat transfer coefficients revealed a deficiency in the model, the principal feature being that the thickness of the condensation film on the wall is not modeled realistically.

The injection flow from the CMT is shown in Figure 28. It is readily apparent that the calculated flow is extremely unsteady. The calculation with the reduced condensation reduced some of this unsteadiness, principally at the start and the end of the injection period, but it did not remove the problem altogether.

Stand-alone modeling of the CMT indicated:

- that replacing the mesh in the CMT wall, over a practical range of sizes, produced little benefit. The implication is that it may be difficult to get the resolution necessary using a system code like RELAP5;
- flow oscillations could be reduced by refining the volumetric (vertical) mesh, but it was not possible to eliminate them altogether. Again this is a limitation of the approach inherent in system codes;
- the results were not sensitive to the noding refinement in the PBL. This is comforting because of the practical limitations of running a complete rig model with fine noding in the PBL.

The implication of the GDE-24 analysis was that, apart from the wall condensation modeling issue, the modeling in RELAP5 was broadly adequate for this experiment.

GDE-34 experiment

The second test analyzed, GDE-34, was similar to GDE-24 but with a smaller CMT. The CMT was initially full of hot water. The GDE-34 test represented the conditions that would prevail if a check valve in the pressure balance line had been leaking. The objective was to investigate the PSIS performance when the driving force for starting the recirculation was small.

Two calculations were performed each representing the full transient. In the reference calculation there was a significant disturbance to the emptying of the core make-up tank due to condensation being calculated. In a sensitivity calculation the rate of condensation in the core make-up tank was again artificially

reduced (as for the previous test) and it was found that the results gave an improved agreement with the experiment.

Stand-alone modeling of the CMT indicated support for the conclusions drawn from the GDE-24 analysis performed previously.

In addition:

- an alternative approach to the calculation of the wall heat transfer for condensation was tried making use of an input table in the input deck relating the heat transfer coefficient to the wall temperature. The heat transfer coefficients in the table were calculated from the average value obtained from the Nusselt theory [51]. Despite being only an approximate model, this showed improved steadiness in the injection flow and could provide a possible resolution to the condensation problem if implemented in the code;
- a more detailed study of the conditions around the time of emptying of a cell revealed that the code was calculating the vapor to become superheated. This is not physically realistic and is the result of a code error in a condensation routine. A corrected version has been supplied by the code developer but has not been employed in the analysis described in this report.

The implication remained that, apart from the wall condensation modeling issue, the modeling in RELAP5 was broadly adequate for this experiment as well.

GDE-43 experiment

The test conditions for this experiment were a very small break (0.13%), the PSIS geometry was as for GDE-34. The steam generator tubes were kept covered. The objective of this test was to focus on a long natural recirculation phase when the driving force for the flow slowly disappears. In this test, this led to a period of about 13 000s when the CMT injection ceased.

As previously, a reference calculation and a number of sensitivity calculations were carried out.

These included a number of single parameter changes. The calculations investigated the effects of the thermal stratification model in the CMT, the number of nodes in the pressurizer, the pressurizer heater modeling, and the heat losses from pressurizer.

The conclusions from the analysis of this experiment were:

- RELAP5/MOD3.2.1.2 predicted the CMT flow behavior with good accuracy.
- the injection flow rate was well predicted using the results of pressure loss tests in the CMT lines. A period when the recirculation ceased was also predicted, but only when the thermal stratification model was employed in the CMT and associated pipework;

- the overall course of the transient was followed by the calculation, although the secondary side pressure was under-predicted. The behavior of the pressurizer was particularly sensitive to the imposed heat losses;
- the CMT flow and its cessation were observed to be insensitive to the wide variations which occurred in different calculations.

Overall conclusions

The code was successful in calculating all three tests chosen for analysis. No code failures were encountered. The mass errors were small. From the analysis of tests GDE-24 and GDE-34 it is clear that the modeling of wall condensation in the RELAP5 code requires improvement for this application. The principal deficiency was shown to lie in the unrealistic modeling of the thickness of the condensate film on the wall. Some benefits could be obtained from reducing mesh sizes but, within practical limitations, it was not possible to achieve a complete resolution this way. An alternative model, not included in the code but applied as a revised boundary condition, successfully demonstrated a possible approach to overcoming the problem for this specific application.

A further observation of this work was some unphysical superheating of vapor in a cell just becoming empty. The correction was not included in the calculations of the project.

The analysis of test GDE-43 successfully reproduced the following CMT parameters:

- (a) the single phase recirculation flow rate,
- (b) the cessation of this flow when the circuit was full of hot water during the recirculation phase of the experiment.

The agreement of these features with the experiment was good provided the thermal stratification model was invoked in the code. The overall course of the transient was generally well reproduced but a particular sensitivity to heat losses in the pressurizer was observed. The failure to predict the secondary side pressure correctly was not significant for these tests.

Overall it is concluded that, subject to the particular issue of the condensation modeling noted above, the RELAP5 code is broadly suitable for the analysis of Passive Injection Systems of the type investigated here.

5. CONCLUSIONS

The purpose of the PACTEL experiments was to investigate phenomena in the PSIS during SBLOCAs. The investigated PSIS worked as planned in all experiments provided the CMT was equipped with a flow distributor (sparger). The main source of disturbances for the investigated PSIS is condensation, which could occur in the CMT when steam or two-phase mixture begins to flow to the tank. It also occurs in the PSIS pipelines if countercurrent flow of steam and cold water occurs or in the cold leg near the ECC water injection position. In the current experiment series, condensation did not cause problems for PSIS behavior as long as the sparger was used.

The computer simulations reproduced the measured transient behavior with good accuracy in all three simulation cases, except for one RELAP5 case. The reason for deficiencies of the RELAP5 calculations are well known. However, the simulations of the selected experiments included some problems in calculating the thermal stratification sufficiently and the condensation in the CMT. Also in the calculation of the PSIS flow when the driving force for the flow is small. The adopted donor cell principle of the codes is the reason for the problems in calculating thermal stratification in the CMT. Acceptable results were obtained only when the CMT was modeled with short nodes or when the condensation rate in the CMT was artificially reduced. The RELAP5 code already includes a thermal stratification model.

6. RECOMMENDATIONS

Based on the PACTEL experience, the following recommendations can be made for the designer of PSISs with CMT:

- The use of sparger in the CMT is of great importance since it largely reduces possibilities for condensation problems in the tank.
- The use of a tall CMT with a small diameter leads to a thicker hot liquid layer in the CMT, which protects the system against possible harmful condensation.
- A pressure balancing line connection to the cold leg leads to a thicker hot liquid layer in the CMT than in the case of PBL connection to the pressurizer. Connecting the PBL to pressurizer also leads to the accumulation of more water in the pressurizer at the end of the transient, and leads to earlier core heat-up. So, PBL connection to the cold leg can be recommended.

The PACTEL experiments concentrated on SBLOCA transients and covered only a part of the possible transients in a APWR plant. For the designers of further experimental work, the following recommendations can be made:

- Investigation of PSIS behavior in large break LOCAs would be of great importance. The LBLOCAs may show strong condensation in the CMT, since there will be practically no recirculation phase in LBLOCA's.

For the computer code developers and users, the following recommendations can be made:

- The code developers should consider more accurate modeling of the thermal stratification. The heat transfer from a vertically moving hot water layer to a wall also needs more precise modeling. It should be mentioned that although these phenomena were not completely correctly calculated, the overall behavior of the PSIS was predicted accurately.
- The code calculations indicated the condensation modeling of the current computer codes is inadequate for describing condensation in a large vessel, like the CMT. Especially, description of the liquid film behavior should be improved.
- The use of McAdams natural convection correlation to calculate heat transfer from the hot liquid layer to the CMT walls seems appropriate.
- Special attention should be paid to the noding of the CMT and the pressure drops in the PSIS lines.

For the experimental team, the following recommendations can be made from the code simulations:

- To improve the secondary side modeling it would be necessary to have some additional test data from the pressure and level controller behavior.

- The distribution of heat losses and pressure drops of the PACTEL facility should be evaluated more accurately with measured data.
- The curve of fluid volume vs. height of the PACTEL facility should be compared with the experimental value.

For the users of the experimental data it can be recommended:

- The data gathered can be used for following purposes: (1) for the design of PSIS's with CMT, (2) to improve thermal-hydraulic code models for thermal stratification or condensation and (3) to improve the capabilities of thermal-hydraulic or CFD codes.
- The scope of the experimental programme does not permit making recommendations to be made about the use of the investigated PSIS in existing plants as a substitute of the HPSIS.

REFERENCES

- [1] Tuunanen, J., Kouhia, J., Purhonen, H., Puustinen, M. & Riikonen, V. General Description of the PACTEL Experiment Facility. Espoo: VTT Energy, 1998. 35 p. + app. 74 p. (VTT Tiedotteita - Meddelanden - Research Notes : 1929) ISBN 951-38-5338-1; 951-38-5339-X.
- [2] Hänninen, M., et. al. APROS Code for the Analyses of Nuclear Power Plant Thermal-hydraulic Transients. Proc. of ANS Winter Meeting, Chicago, IL, November 15-20, 1992.
- [3] Farvaque, M. User's Manual of CATHARE 2 V1.3E. STR/LML/EM/91-61. November 1992.
- [4] The RELAP5 Code Development Team. RELAP5/MOD3 Code Manual vols I - VII. INEL: June 1995.
- [5] Tower, S. N., Schultz, T. L. & Vijuk, R. P. Passive and Simplified System Features for the Advanced Westinghouse 600 MWe PWR. Nuclear Engineering and Design, 1988. Vol. 109, pp. 147-154.
- [6] Tuunanen, J., Lillington, J., D'Auria, F. & Kalli, H. Review of Experimental Work and Code Application on the Simulation of Passive Safety Injection Systems. Espoo: VTT Energy, 1996. (Technical Report, PAHKO 3/96)
- [7] Wright, R.F., Hundal, R., Hochreiter, L. E., Friend, M. T. & Ogrins, M. Analysis and Evaluation of the AP600 SPES-2 Integral System Tests. ASME-JSME 4th Int. Conference on Nuclear Engineering Meeting Proceedings, New Orleans, LA, 10 -14 March 1996.
- [8] Shotkin, L. M. & Kukita, Y. Implications of the ROSA/AP600 High- and Intermediate-pressure Test Results. Nuclear Technology. Vol 119, September 1997.
- [9] Hochreiter, L. E. et al. Description of the OSU APEX Test Facility to Assess AP600 Passive Safety. ANS Winter Meeting, San Francisco, CA, October 1995.
- [10] Tuunanen, J. Minutes of the Third Meeting of the APSI Project. 19.12.1996.
- [11] Vihavainen, J. TRAVEL REPORT. ICONE-6, International Conference on Nuclear Engineering. July 1998.
- [12] *Addendum to the report* "Tuunanen, J., Lillington, J., D'Auria, F. & Kalli, H. Review of Experimental Work and Code Application on the Simulation of Passive Safety Injection Systems". November 15, 1998.
- [13] Tuunanen, J. Quick Look Report. Passive Safety Injection Experiments GDE-21, GDE-22, GDE-23, GDE-24 and GDE-25. Espoo: VTT Energy, 1996. (Technical Report, PAHKO 2/96.)
- [14] Tuunanen, J. Experimental Data Report. Passive Safety Injection Experiments GDE-21, GDE-22, GDE-23, GDE-24 and GDE-25. Espoo: VTT Energy, 1996. (Technical Report, PAHKO 4/96.)
- [15] Tuunanen, J. & Puustinen, M. Quick Look Report. Passive Safety Injection Experiments GDE-31, GDE-32, GDE-33, GDE-34 and GDE-35. Espoo: VTT Energy, 1997. (Technical Report, PAHKO 2/97.)

-
- [16] Tuunanen, J. & Puustinen, M. Experimental Data Report. Passive Safety Injection Experiments GDE-31, GDE-32, GDE-33, GDE-34 and GDE-35. Espoo: VTT Energy, 1997. (Technical Report. PAHKO 3/97.)
- [17] Tuunanen, J. & Puustinen, M. Quick Look Report. Passive Safety Injection Experiments GDE-41, GDE-42, GDE-43, GDE-44 and GDE-45. Espoo: VTT Energy, 1997. (Technical Report, PAHKO 7/97.)
- [18] Tuunanen, J. & Puustinen, M. Experimental Data Report. Passive Safety Injection Experiments GDE-41, GDE-42, GDE-43, GDE-44 and GDE-45. Espoo: VTT Energy, 1998. (Technical Report, PAHKO 2/98.)
- [19] Tuunanen, J., Munther, R., Vihavainen, J. PACTEL Experiments for Investigation of Passive Safety Injection Systems of Advanced Light Water Reactors. Proceedings of the 4th International Conference on Nuclear Engineering (ICONE-4). New Orleans, LA, March 10-14, 1996.
- [20] Chang, Soon Heung., No, Hee Cheon., Baek, Won-pil., Lee, Sang-il & Lee, Seong-Wook. Korea Looks Beyond the Next Generation. Nuclear Engineering International. February 1997.
- [21] Cunningham, J. P., Haberstroh, R. C., Hochreiter, L., E. & Wright, R. F. Analysis of the AP600 Core Makeup Tank Tests. ASME-JSME 4th International Conference on Nuclear Engineering, New Orleans, LA, March 10-14, 1996. (not in the Proceedings).
- [22] Hassinen, M. Estimation of the Heat Transfer Coefficient to the CMT Wall in Passive Safety Injection Experiments GDE-31 through GDE-45 (in Finnish). Espoo: VTT Energy, 1998. (Technical Report, PAHKO 5/98.)
- [23] Lomperski, S. W. & Kouhia, J. Estimation of PACTEL Heat Losses. VTT Energy. January 1992.
- [24] Raussi P., Kouhia J. Heat Loss Analysis of the PACTEL Thermalhydraulic Test Facility Modelling WWER-440 Reactors. VTT Energy
- [25] R. Scott Semken. *Quick Look Report. Pressure Drop Measurements of the Passive Safety Injection System Lines of PACTEL.* VTT Energy. Technical Report. PAHKO 6/96. 27.8.1996.
- [26] R. Scott Semken. *Quick Look Report. Pressure Drop Measurements of the Passive Safety Injection System Lines of PACTEL for GDE-31 through GDE-35.* VTT Energy. Technical Report. PAHKO 8/96. 18.11.1996.
- [27] Semken, R. S. Quick Look Report. Pressure Drop Measurements of the Passive Safety Injection System Lines of PACTEL. Passive Safety Injection Experiments GDE-41 through GDE-45. Espoo: VTT Energy, 1997. (Technical Report, PAHKO 8/97.)
- [28] Purhonen, H. Quick Look Report. Pressure Drop Measurements of PACTEL (under preparation). Espoo: VTT Energy. (Technical Report. PAHKO 7/98.)
- [29] Bernard, M. & D'Auria F. Validation of CATHARE on the Basis of LOBI Experiments. Seminar on the Commission Contribution to Reactor Safety Research, Varese (I), Nov. 20-24, 1989
- [30] D'Auria, F. & Galassi, G. M. The Application of CATHARE 1 v1.3 to LOBI Small Break LOCA Experiments and a Comparison with RELAP5/MOD2 - Final Report - CEC Report EUR 12404 EN, Luxembourg (L), 1989

-
- [31] Ambrosini, W., D'Auria, F. & Galassi, G. M. Application of the Cathare-2 Code to Integral and Separate Effect Tests. CATHARE and BETHSY 4th International Seminar, Grenoble (F), March 18-20 1991.
- [32] Belsito, S., D'Auria, F., Ingegneri, M., Chojnacki, E. & Gonzales, R. Post-test Analysis of Counterpart Tests in LOBI, SPES, BETHSY and LSTF facilities performed with CATHARE2 code. 3rd Regional Meet. Nuclear Energy in Central Europe, Portoroz (SLO), Sept. 16-19, 1996.
- [33] Ambrosini, W., Belsito, S., D'Auria, F. & Frogheri, M. OECD/CSNI ISP 33: Post-test Analysis of the PACTEL Natural Circulation Experiment Performed by CATHARE 2 v1.3E Code. University of Pisa Report, DCMN - NT 208(93), Pisa (I), May 1993 OECD CSNI Final Workshop on ISP 33 - Lappeenranta (SF), May 17-20, 1993.
- [34] Kalli, H., Miettinen, A., Purhonen, H., D'Auria, F., Frogheri, M. & Leonardi, M. Quantitative Code Accuracy Evaluation of ISP-33. 7th Int. Top. Meet. on Nuclear Reactor Thermal-hydraulics, Saratoga Springs, NY, (USA), Sept. 10-15 1995.
- [35] Bestion D. Dossier descriptif Cathare M1.4 - Description General des lois Physiques du Module de Base. SETH/LEML-EM/89-190, June 1990.
- [36] Vihavainen, J. Analysis of Passive Safety Injection Experiment GDE-24 with APROS 4.02 Code. Espoo: VTT Energy, 1997. (Technical Report, PAHKO 9/96.)
- [37] Vihavainen, J. Analysis of Passive Safety Injection Experiment GDE-34 with APROS 4.02 Code. Espoo: VTT Energy, 1997. (Technical Report. PAHKO 4/97.)
- [38] Vihavainen, J. Analysis of Passive Safety Injection Experiment GDE-43 with APROS 4.02 Code. Espoo: VTT Energy, 1998. (Technical Report. PAHKO 4/98.)
- [39] Kadri D. Dictionary of Operators and Directives of CATHARE 2 v1.3E. Seth/LEML/EM/90-224, Nov. 1990.
- [40] Bonuccelli, M., D'Auria, F., Debrecin, N. & Galassi, G. M. A Methodology for the Qualification of Thermalhydraulic Codes Nodalizations. 8th Meet. of OECD-CSNI Task Group on Thermalhydraulic System Behaviour Paris (F), June 30 July 2, 1992 6th Int. Top. Meet. on Nuclear Reactor Thermal-hydraulics, Grenoble (F), Oct. 5-8, 1993.
- [41] D'Auria, F., Leonardi, M. & Pochard R. Methodology for the Evaluation of Thermalhydraulic Codes Accuracy. Int. Conf. on New Trends in Nuclear System Thermohydraulics - Pisa (I) May 30 - June 2, 1994.
- [42] Kimber, G. R., Further Analysis of PACTEL Test GDE-24 with RELAP5/MOD3.2.1.2. AEA Technology Report, January 1997.
- [43] Kimber, G. R. & Allen, E. J. Analysis of PACTEL Test GDE-34 with RELAP5/MOD3.2.1.2. AEA Technology Report 2692, December 1997.
- [44] Kimber, G. R. Analyses of PACTEL test GDE-43 with RELAP5/MOD3.2.1.2. AEA Technology Report AEAT-4320, October 1998.
- [45] Tompot, R. W. RELAP5/MOD3.2.2(Beta) Development: Fall 1998 RELAP5 User meeting. Chicago Sept 1998 (Organised by Scientech Inc).

-
- [46] Hyvarinen, J. Heat Transfer Characteristics of Horizontal Steam Generators under Natural Circulation Conditions. Nuclear Engineering and Design, 1996. Vol. 166 pp. 191-223.
- [47] D'Auria, F., Frogheri, M. & Galassi, G. M. Application of the CATHARE" V1.3U Code to the Analysis of the PACTEL GDE-24 Experiment Relevant to the Innovative Reactors. University of Pisa Report, DCMN - NT 301(96), Pisa (I), December 1996.
- [48] D'Auria, F. & Galassi, G. M. *Addendum to the report "Application of the CATHARE" V1.3U Code to the Analysis of the PACTEL GE24 Experiment Relevant to the Innovative Reactors"*. University of Pisa Report, DCMN - NT 306(97), Pisa (I), February 1997.
- [49] D'Auria, F., Galassi, G. M. & Ingegneri, M. Application of the CATHARE" V1.3U Code to the Analysis of the PACTEL GDE-34 Experiment Relevant to the Innovative Reactors. University of Pisa Report, DCMN - NT 311(97), Pisa (I), June 1997.
- [50] D'Auria, F. & Galassi, G. M.. Application of the CATHARE" V1.3U Code to the Analysis of the PACTEL GDE-43 Experiment Relevant to the Innovative Reactors. University of Pisa Report, DCMN - NT 337(98), Pisa (I), April 1998.
- [51] Rogers, G. F. C. & Mayhew, Y. R., Engineering Thermodynamics, Work, and Heat Transfer. 4th ed. Longmans Scientific and Technical Publications, 1992.

Appendix 1 List of documents and publications prepared in the European Commission 4th Framework Programme project “Assessment of Passive Safety Injection Systems of ALWR’s (APSI)”

Document type	Deliverable	Date
MINUTES		
Kick-off meeting	-	07.02.1996
2 nd project group meeting		24.06.1996
3 rd project group meeting	-	19.12.1996
4 th project group meeting	-	23.04.1997
5 th project group meeting	-	30.06.1997
6 th project group meeting	-	02.02.1998
7 th project group meeting	-	04.08.1998
Final meeting	-	19.11.1998
PROGRESS REPORTS		
Progress report (1 st reporting period)	-	28.06.1996
1 st year progress report	-	31.01.1997
Progress report (3 rd reporting period)	-	30.06.1997
2 nd year progress report	-	28.01.1998
Progress report (5 th reporting period)	-	04.08.1998
WORK PACKAGE 1		
Summary report	D1	28.06.1996
Appendix to the summary report		12.11.1998
WORK PACKAGE 2		
Test specification report (1 st series)	D2	16.02.1996
Test data (1 st test series)	D3	
-1 st set of data		18.06.1996
Quick-Look report (1 st test series)	D4	28.06.1996
Quick Look Report.	-	27.08.1996
<i>Pressure drop measurements of the PSIS lines of PACTEL</i>		
Experiment Data Report (1 st series)	D11	07.10.1996
Test specification report (2 nd series)	D12	31.10.1996
Quick Look Report.	-	18.11.1996
<i>Pressure drop measurements of the PSIS lines of PACTEL for GDE-31 through GDE-35.</i>		
Quick-Look report (2 nd test series)	D14	14.02.1997
Test data (2 nd test series)	D13	16.04.1997
Experiment Data Report (2 nd series)	D15	16.05.1997
Test specification report (3 rd series)	D19	16.09.1997
Quick-Look report (3 rd test series)	D21	07.11.1997
Quick Look Report.	-	07.11.1997
<i>Pressure drop measurements of the PSIS lines of PACTEL for GDE-41 through GDE-45.</i>		
Test data (3 rd test series)	D20	15.01.1998
Experiment Data Report (3 rd series)	D22	16.03.1998
General Description of the PACTEL Facility	-	25.11.1998
<i>Description of the PACTEL test facility geometry and instrumentation</i>		
WORK PACKAGE 3		
Input data file for APROS code	D5	01.08.1996
Input data file for CATHARE code	D6	18.06.1996
Input data file for RELAP5 code	D7	01.08.1996
Code analyses reports ; <i>GDE-24 experiment</i>	APROS	D8
	CATHARE	D9
	RELAP5	D10
Code analyses reports ; <i>GDE-34 experiment</i>	APROS	D16
	CATHARE	D17
	RELAP5	D18
Code analyses reports ; <i>GDE-43 experiment</i>	APROS	D23
	CATHARE	D24
	RELAP5	D25
		11/98 (draft)
WORK PACKAGE 4		
Final report (large)	-	28.01.1999
Final report (commission report)	D26	11.01.1999

Appendix 1 List of documents and publications prepared in the European Commission 4th Framework Programme project “Assessment of Passive Safety Injection Systems of ALWR’s (APSI)”

PUBLICATIONS

Tuunanen, J., *Experimental Program on PACTEL for the Investigation of Passive Safety Injection Systems of ALWRs*. Jahrestagung Kerntechnik '96. Mannheim, Rosengarten, 21.-23. Mai 1996.

Tuunanen J., Vihavainen, J., *PACTEL Experiment Programme for the Investigation of Passive Safety Injection Systems of Advanced Light Water Reactors*. Proceedings of the POST_SMiRT 14 Seminar "Passive Safety Features in Nuclear Installations". Pisa. Italy. August 25-27, 1997.

Tuunanen, J. P., Lillington. J. N., D'Auria, F., Vihavainen, J. *Assessment of Passive Safety Injection Systems of Advanced Light Water Reactors*. Proceedings of the EC FISA-97 symposium. Luxembourg, 17-19 November 1997. pp.521-530.

Tuunanen, J., Riikonen, V., Kouhia, J and Vihavainen, J. *Analyses of PACTEL Passive Safety Injection Experiments GDE-21 through GDE-25*. Nucl. Eng. Des. 180 (1998) pp.67-91.

Tuunanen, J., Vihavainen, J. *Passive Safety Injection During SBLOCA from a Core Make-Up Tank with a Pressure Balancing Line to Pressurizer: Experiment in PACTEL and APROS Simulations*. 6th Int. Conference on Nuclear Engineering ICONE-6. San Diego. California. May 10-15, 1998.

G. R. Kimber and J. N. Lillington. *RELAP5 Analyses of PACTEL Passive Injection Tests*. IAEA Technical Committee Meeting on “Experimental Tests and Qualification of Analytical Methods to Address Thermohydraulic Phenomena in Advanced Water Cooled Reactors”. PSI, Villigen, Switzerland, 14-17 September, 1998.

D'Auria, F., Galassi G.M. *Experience Gained in the Application of RELAP5 and CATHARE Codes to Situation Relevant to the New Generation Reactors*. Proceedings of the POST_SMiRT 14 Seminar "Passive Safety Features in Nuclear Installations". Pisa. Italy. August 25-27, 1997. (Submitted for publication to Nucl. Eng. Des.).

D'Auria, F., Frogheri, M., Galassi G.M. *Natural Circulation Performance in Nuclear Power Plants*. IAEA Technical Committee Meeting on “Experimental Tests and Qualification of Analytical Methods to Address Thermohydraulic Phenomena in Advanced Water Cooled Reactors”. PSI, Villigen, Switzerland, 14-17 September, 1998.